WASM: Minerals, Energy and Chemical Engineering

Integrated Formation Evaluation Study in Cliff Head Field, Northern Perth Basin, Western Australia

Abdelrahman Aly Ahmed Elkhateeb

**This thesis is presented for the Degree
of
Doctor of Philosophy**

Curtin University

October 2021

Declaration

To the best of my knowledge and belief, this thesis contains no material previously published by any other person or any organisation, except where due acknowledgment has been made.

This thesis contains no material which has been accepted for the award of any other degrees or diplomas in any other institution but **Curtin University**.

Signature:

Date: 7th of October 2021

Copyright Statement

I have obtained permission from my supervisors, who are my co-authors in my publications, to use my own published journal and conference papers in my research.

Signature:

Date: 7th of October 2021

Acknowledgement

Table of Contents

List of Figures

List of Tables

Abstract

Within the very mature oil and gas industry that has been established for over a century, formation evaluation has been the key to undertake commitments that endure large costs. Petrophysics and reservoir characterisation have been the heart of the oil and gas business that give the light to pursue massive projects. The logging technology and formation evaluation techniques have gone through a significant revolutionary improvement for decades. In the last 30 years, the tools and the evaluation techniques, in addition to the software technology and digitalisation, have opened a new era for prospects' evaluation. The reservoir facies is considered one major step in the industry to unlock the reservoir complexity, understand the existing potential, and explore the best areas in any field. With the reservoir modelling advancements in the last two decades, petrophysical interpretation and parameterisation have become major inputs in geological reservoir assessment. Traditionally, prediction of flow capability for a reservoir rock, which is dependent on facies and permeability, was one of many challenges in the industry that necessitates sophisticated evaluation for effective reservoir description. Further, the water saturation in complicated facies embraces a lot of ambiguity that requires more than a simple log driven by Archie equation. Due to the reservoir heterogeneity and the clay distribution in the shaly sands, it is very challenging to resolve these parameters with high certainty, particularly in the light of conventional logs resolution. This research presents a resolution for the permeability and water saturation ambiguity in complex reservoirs by characterising the formation facies using core or well log data in a unique workflow.

A new technique was implemented to unlock the facies classification in complex reservoirs such as shaly sands and carbonates. A Permian shaly sand succession in Cliff Head Field, located offshore Perth Basin in Western Australia, has been chosen to run this research project and apply new technologies to resolve the petrophysical parameters. Integration between the conventional density log and the NMR free fluid index has been carried out, to generate a new reservoir electrofacies technique, named the Equivalent Flow Zone Indicator (EFZI). A number of different datasets have been integrated at a very detailed level including well logs, core thin sections, and rock capillary pressure measurements to establish a high quality geological lithofacies, with which the generated EFZI electrofacies could be correlated. To test the methodology, the reservoir permeability and the water saturation were calculated through two different new workflows, both are EFZI dependent, supported by the routine and the special core analyses. Nine reservoir electrofacies have been classified matched to four identified geological lithofacies. The reservoir permeability dependent on the EFZI have shown very heterogeneous reservoir rock that varies from few millidarcies up to an average of 740 mD, confirmed by the core permeability measurements under net confining stress. The water saturation has been calculated using three different methods, a conventional

interpretation using inversion petrophysical analysis, advanced method using the NMR variable T2 cutoff and the saturation height modeling dependent on the high resolution EFZI facies. The water saturation results have reflected the complex nature of the rock where an average reached up to 40% irreducible saturation was calculated. The modeling results have presented very high resolution outputs with high degree of accuracy that can be used for the cored and the uncored wells with high efficiency.

The workflows described allow independent methods for reservoir characterisation, regardless of the degree of the rock heterogeneity. The two most sophisticated parameters known to date in the petrophysical interpretation in complex reservoirs can be calculated with high accuracy through the presented workflows. A major outcome that would benefit the industry is the ability to distribute the calculations to any number of wells in the same field, with the availability or the lack of core measurements. Furthermore, the workflows used are applicable on real-time basis while drilling, with which a complete facies model would be available in much shorter time frame. The workflows are believed to provide significant value for prospects' evaluation and the calculated reservoir potential accuracy. The modeling can be applied in projects that tend to establish a solid base for large investments. Further it will contribute for projects of different nature, either frontier exploration or development where early analysing stages will turn into mature studies.

Chapter One: Overview

1.1. Introduction

Traditionally, prediction of facies and permeability for a reservoir rock was one of many challenges in the oil and gas industry that necessitates advanced and sophisticated evaluation for effective reservoir description. Due to the reservoir heterogeneity and the clay distribution in the rock structure, it is very challenging to resolve the effective pore volume, the reservoir facies and how the high permeability zones are distributed within the formation. Further, the saturation calculation in complex reservoirs remains a major challenge to the industry. In simple formations, a tendency towards simple saturation models such as Archie or Simandoux for clean and shaly reservoirs respectively is always preferable. These models were found to be working effectively in homogeneous formations within which the porosity and permeability are linked in the light of a simple facies scheme. Where the rocks show some degrees of heterogeneity, the well-logs are usually affected by different factors. This adversely results in a compromised or averaged logs' profiles that may affect the saturation calculations.

In this research, new techniques have been successfully tested on a shaly sand formation in The Perth Basin, located in Western Australia, to generate advanced facies classification for the interested reservoir section. Two different methods were established, one of which involves core measurements, while the second is purely based on the logging suite available for evaluation. The classified electrofacies have been used as the core base to establish permeability and saturation modeling that are accurate, efficient and of the least uncertainty. The reservoir characterisation was done through several integrated workflows that employed petrophysical logs, core thin sections, routine core measurements, special core measurements for Archie saturation parameters and rock capillary pressure.

One of the major offshore Western Australian fields, that has been producing for 15 years, was chosen to test the workflows in this research project, which is the Cliff Head Field. The interested reservoir section consists of three different sand packages of different characteristics, which constitute the Irwin River Coal Measures and the High Cliff Sandstone Formations, both proven to belong to the Early Permian age (Mory and Iasky, 1996; Mory and Haig, 2011). A total number of nine hydraulic flow units (HFU) have been identified in the studied reservoir sands supported by the core data. The unique Flow Zone Indicator Technique (FZI) has been followed to assess the accuracy of the method used for facies distribution (Amaefule, 1993).

The power of the new methodologies flourishes in the possibility to extend the complete evaluation to any number of wells encountered the same reservoir section. Further, the models can be applied in large field studies and on legacy data. Moreover, a high resolution permeability can be predicted in the absence of core measurements, and water saturation can be calculated in the lack of resistivity logs. A further possibility to complete the reservoir characterisation workflow on real time basis, extended to the uncored wells

is another major step forward that has been tested in various well trajectories, either vertical, deviated, or horizontal long boreholes.

1.2. Research Objectives

The objective of this research study is to establish an efficient approach to integrate very different datasets together to complete the reservoir characterisation. For decades, the permeability is known to be generated with very low accuracy using various mathematical models, upon which the calculations are known to be indicative rather than representing the correct reservoirs permeability. Similarly, the calculation of the water saturation using resistivity logs that are compromised in shaly reservoirs resulted in saturations of very high uncertainty. The research aims to the following:

- Explore new methods that can efficiently produce high-resolution facies classification in complex reservoirs.
- Establish new techniques to solve the two main uncertain petrophysical parameters, which are the permeability and the water saturation, dependent on the generated facies.
- Develop possible resolution to identify the NMR T2-Cutoff upon which the true irreducible water saturation can be estimated.
- Identify the best possible petrophysical analysis approach through which the output model reflects the true reservoir nature.

Cliff Head Field is found to contain the necessary datasets to run the methodologies mentioned. The reservoir section in the area is a typical example of a heterogenous shaly sand with high complexity.

1.3. Study Area

Perth Basin has experienced heavy drilling activity in the last five decades (Geoscience Australia, 2020). Three-quarters of the explored fields were located in the northern part of the basin. Cliff Head oil Field, discovered in 2001 by Roc Oil company towards the Eastern boundary of the old Exploration Permit WA-286-P (Roc Oil, 2002), currently resides in the Production License WA-31-L (Triangle Energy, 2021), is considered the first commercial offshore oil discovery in the Perth Basin (**Figure 1**). The field is located 10 kilometres offshore within 15-20 meters water depth, approximately 25 Km to the South-Southwest of Dongara, and 300 Km to the North of Perth (Roc Oil, 2014). The field had proven high estimated recoverable reserves of 20-30 MMbbls (Roc Oil, 2014) from the Early Permian Irwin River Coal Measures Formation (Mory et al., 2005). Since then, the field has been producing above the original forecast rates (Triangle Energy, 2021). Cliff Head Field encountered the North Perth Basin stratigraphy (Geoscience Australia,

2020), with sediments aged between Precambrian to Quaternary as shown in **Figure 2**. Three main interesting reservoir sections in Cliff Head which are the Dongara Sandstone, the Irwin River Coal Measures and the High Cliff Sandstone, all found hydrocarbons where encountered above the Free Water Level. The well logs identified a clear oil water contact at 1261 mSS that is proven to be the same as the Free Water Level (Roc Oil, 2003). The sands have shown a fining upwards sequence of sandstone reservoir of very good formation characteristics. Generally, the average porosity in the sand sequence ranges between 10 to 25% while the permeability varies from few millidarcies to 1 Darcy for the same porosity range.
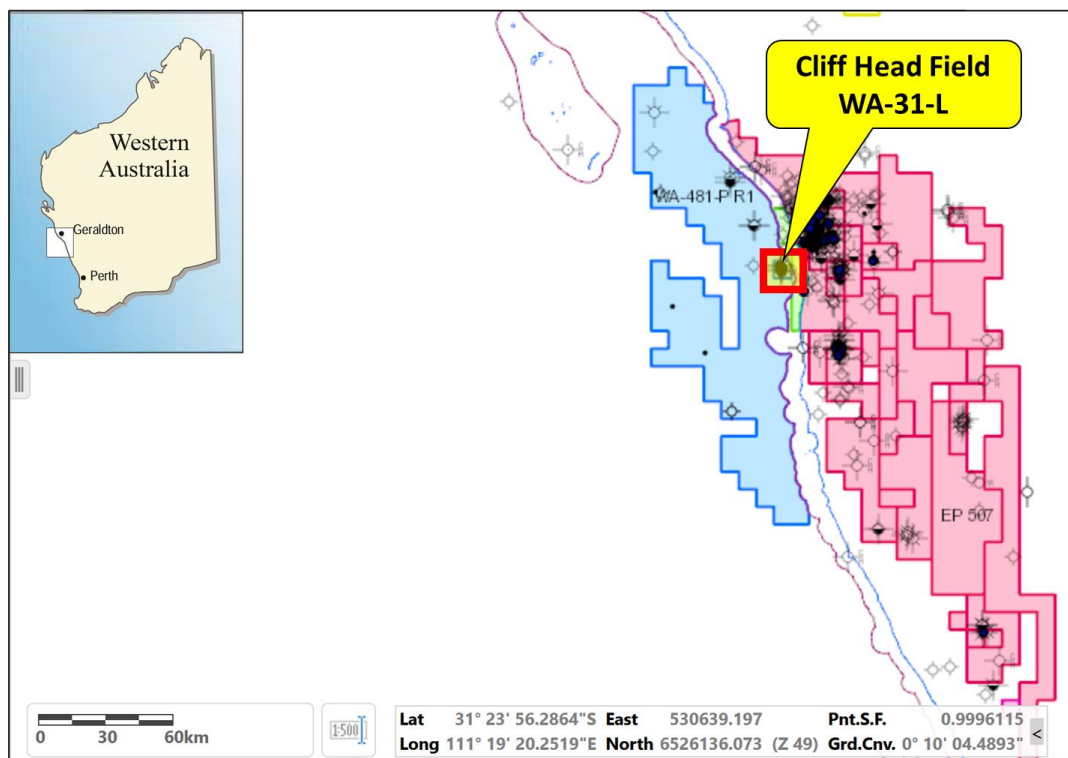
Figure 1: *Cliff Head Field location map, Offshore Perth Basin, Western Australia (After Dept. of Mines, Industry Regulations and Safety, Govt. of Western Australia)*

The dominant clay mineral in the clastic rocks is the authigenic kaolin, present mainly as dispersed clays within the pore spaces (Elkhateeb et al., 2019). A conducted well test resulted in production rates as high as 3019 barrels per day (Roc Oil, 2003) constantly with negligible water produced throughout the well testing operation.

Figure 3 shows a structure map for Cliff Head Field with the five wells used in this research study (Roc Oil, 2006). Two main segments can be identified clearly from the presented map, a small segment located in the Northwest of the field and another much larger segment extended in the Northwest – Southeast direction, which contains the main hydrocarbon volume. The segments are as follows:
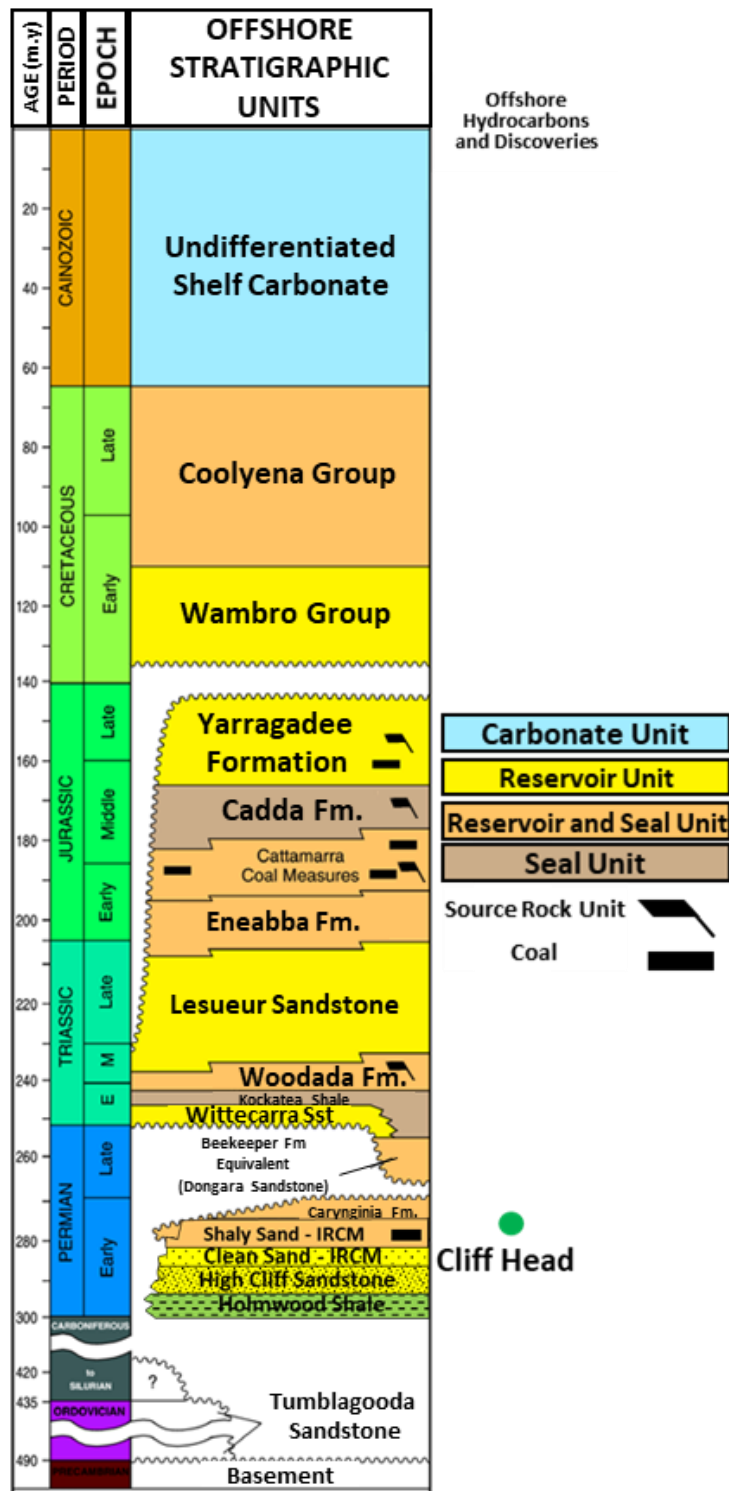
Figure 2: *Stratigraphic column of the Northern Perth Basin in the offshore areas; (Modified from Geoscience Australia, 2020)*
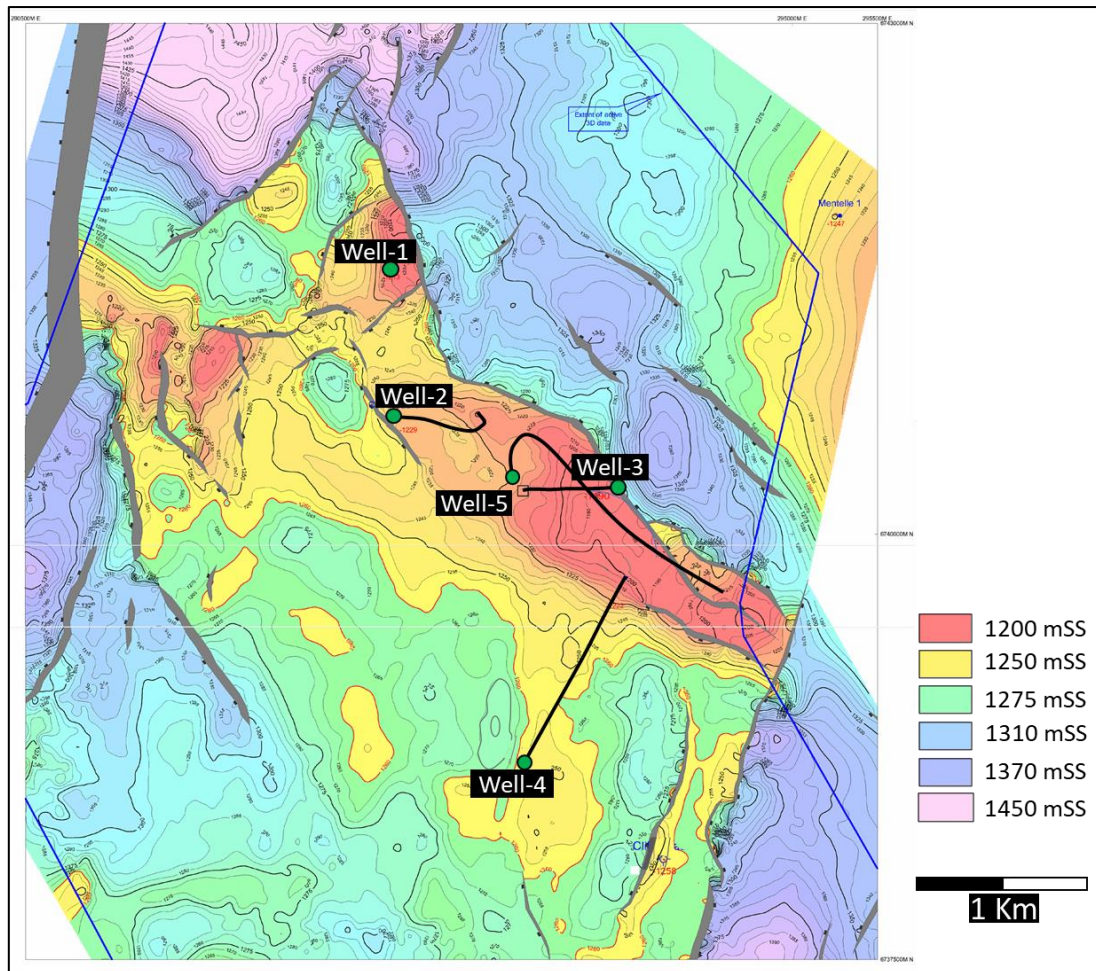
Figure 3: *Field structure map showing the two main segments in the Cliff Head area, (Modified after Roc Oil, 2006)*

1.3.1.   Northwest Segment

This segment lies to the Northwest of the field, with proven hydrocarbon produced through the conducted well test in Well-1. The area is bounded by 4 faults from all directions, which affected the Irwin River Coal Measures Formation sand sequence in this location. The drilled well-1 encountered a thinner shaly sand that belongs to the Dongara Sandstone, underlain by two clean sandstone sequences from the Irwin River Coal Measures and the High Cliff Sandstone (Rock Oil, 2006).

1.3.2.   Main Horst Segment

The Main Horst segment is the largest and the main producing segment in the area, bounded by two main faults running from the Northwest to the Southeast. Wells 2 through to Well-5 were drilled in this segment, with Well-3 encountered the thickest complete section in the field. This segment includes most of the hydrocarbon volume proven from the conventional and the advanced logs (Rock Oil, 2006). The lateral

variation in the reservoir facies is very complex and the reservoir quality varies significantly at the well locations.

1.4. Structure of the Thesis

The thesis consists of six chapters, including this overview chapter, in which three chapters are peer-reviewed publications, aiming to address the research objectives discussed earlier. Below is the detailed structure for the research:

Chapter 1: Introduces the research outlines and objectives with a brief description of Cliff Head field history and geology in addition to the structure of the thesis.

Chapter 2: A literature review for the deterministic and inversion petrophysical approaches used for the analysis and the background of the methodologies applied in the research. The chapter also discusses the hydraulic flow units (HFU) technique for facies classification and the saturation height modelling for quantitative saturation calculation at different reservoir heights in relation to the free water level.

Chapter 3: This chapter will include the paper published in 2019 in the Journal of Petroleum Science and Engineering. The paper explains a new method that unlocks the complexity of the electrofacies classification in heterogeneous reservoirs. The method is explained in detail and tested using core datasets proving effectiveness in modeling the permeability for such reservoirs with high accuracy.

Chapter-4: The chapter will present a new approach to predict the electrofacies from the well logs only. The prediction technique was published in 2019 in a peer reviewed publication and presented in the Australasian Exploration Geoscience Conference held in Perth. The modeling was tested using the reservoir repeat formation tester mobilities and verified against stressed core permeability measurements.

Chapter 5: This chapter will present a new methodology published in the Journal of Petroleum in 2021. The publication explains a new technique that integrates capillary pressure measurements with the core thin sections to establish a powerful lithofacies scheme. Furthermore, a complete workflow will be presented explaining an integrated evaluation using the conventional and the NMR logs with the capillary pressure data to generate high resolution saturation height modeling. The method will unlock the complexity of the water saturation calculation in complex reservoirs, which can be applied in either cored or uncored wells.

Chapter-6: This chapter will present the deterministic petrophysical analysis and will compare the results of each interpretation technique. It will further summarise the possible problems with the methodologies presented in the previous chapters that may lead to compromised results. Finally, a section for the research conclusions will be explained.

1.5. Data Used in the Research

The data used in Cliff Head Field reservoir analysis includes different types of data from different sources, between logs and core studies to well completion reports. The data was acquired across the Permian reservoir interval that includes the Dongara Sandstone, the Irwin River Coal Measures and the High Cliff Sandstone Formations. The Core Analyses acquired covered the clean and the shaly sands of the Irwin River Coal Measures Formation. **Table 1** lists the used datasets in the research project:

Table 1: List of the used datasets in Cliff Head Field reservoir study

Well	Logging/Data	Run	Date	Tools/Analyses Acquired
Well-1	**Wireline**	**1**	**19 Jan 2003**	**GR-Resistivity-Density-Neutron-Sonic**
		2	**19 Jan 2003**	**Spectroscopy-GR**
		3	**19 Jan 2003**	**CMR-GR**
	Testing	**1**	**24 – 27 Jan 2003**	**Well Testing**
	RCA	**1**	**May 2003**	**Porosity-Permeability-Grain Density (Conventional Core)**
	Report	**1**	**Dec 2003**	**Well Completion Report**
	SCAL	**1**	**April 2004**	**FRF-RI-Pc**
	Geological Studies	**1**	**July 2004**	**Petrography (Thin Sections)**
Well-2	**Wireline**	**1**	**11 Mar 2003**	**GR-Resistivity-Density-Neutron-Sonic**
		2	**11 Mar 2003**	**Spectroscopy-GR**
		4	**11 Mar 2003**	**Formation Tester-GR**
		6	**12 Mar 2003**	**CMR-GR**
	Report	**1**	**Feb 2004**	**Well Completion Report**
	Geological Studies	**1**	**July 2004**	**Petrography (Thin Sections) & Pc**
Well-3	**Wireline**	**1**	**9 Mar 2005**	**GR-Resistivity-Density-Neutron**
		2	**9 Mar 2005**	**Sonic-Resistivity**
		3	**9-Mar-2005**	**Formation Tester-GR**
	RCA	**1**	**Sep 2005**	**Porosity-Permeability-Grain Density (Conventional Core)**
	Geological Studies	**1**	**Oct 2005**	**Petrography (Thin Sections)**
	Report	**1**	**Feb 2006**	**Well Completion Report**
Well-4	**LWD**	**1**	**03 Jan 2002**	**GR-Resistivity-Density-Neutron**
Well-5	**LWD**	**1**	**13 Jul 2006**	**GR-Resistivity-Density-Neutron-Sonic**

1.6. Significance of The Research

The research will unlock the complexity of the facies analysis in complex reservoirs and provide solutions to overcome the ambiguity of two major petrophysical parameters, which are permeability and fluid saturation. The techniques applied have been tested on

a wide range of facies complexity and proven to provide very quantitative data that reflects the true nature of reservoirs. The techniques can be widely used in similar, or less complex, formations to characterise facies and effectively generate high-resolution permeability and saturation logs. The research will discuss the uncertainty of the results between the conventional and advanced approaches. Furthermore, the methods can be used to provide real-time analysis while drilling operation is ongoing, which can significantly benefit the industry in planning for the subsequent operations at a very early stage (e.g.: Perforation and well testing through sweat spots).

1.7. Publication Outlines

This thesis will be hybrid organized based on the outcome of 3 peer-reviewed publications, two of which are journal publications, and one is a conference paper as listed below, each of these publications correspond to a separate chapter. The last chapter (Chapter-6) includes non-published content.

Chapter-3:

Elkhateeb A., Rezaee R., and Kadkhodaie A., 2019, Prediction of high-resolution reservoir facies and permeability, an integrated approach in the Irwin River Coal Measures Formation, Perth Basin, Western Australia, Journal of Petroleum Science and Engineering, **181** (2019) 1-12. https://doi.org/10.1016/j.petrol.2019.106226

Chapter-4:

Elkhateeb A., Rezaee R., and Kadkhodaie A., 2019, Log Dependent Approach to Predict Reservoir Facies and Permeability in a Complicated Shaly Sand Reservoir, Presented in the Australasian Exploration Geoscience Conference, Perth, Western Australia, September 2 – 5, 2019, pp. 1-5, https://doi.org/10.1080/22020586.2019.12072924

Chapter-5:

Elkhateeb A., Rezaee R., and Kadkhodaie A., 2021, A New Integrated Approach to Resolve the Saturation Profile Using High-Resolution Facies in Heterogeneous Reservoirs, *Journal of Petroleum*, 2021. https://doi.org/10.1016/j.petlm.2021.06.004

Chapter 2: Literature Review

This chapter discusses the literature review for the research methodologies starting with the deterministic and the mineralogical evaluation, through to the saturation height modeling. With the current revolution in the industry's technology, in shaly reservoirs some parameters are easier to calculate compared to the others such as the shale volume, whereas the water saturation and permeability still embrace huge uncertainty. The core analyses act as a considerable trusted solid reference in those formations to which the petrophysical logs are matched. This chapter will review the available methodologies to complete a quantitative formation evaluation for complicated reservoirs.

2.1. Deterministic Petrophysical Analysis

The standard petrophysical analysis is the core for log interpretation, known widely in the industry as the Deterministic Analysis approach (Darling, 2005 and Kennedy, 2015), where the properties are expressed in a series of equations, from shale volume through to the formation porosity and water saturation. The final outputs include a complete rock volume to show the formation lithology.

2.1.1.　Shale Volume Calculation

The first step in the simple petrophysics workflow is to estimate the shale or clay volume in the reservoir. If the reservoir is more shaly, in the availability of the gamma-ray and the two main porosity logs, the density and the neutron, the shale volume can be calculated using single and double indicators, which are the GR and a combination of the density and the neutron. Calculating the shale volume from two different methods allows more control on the considerable effect on the gamma-ray log in shaly reservoirs, hence more accuracy in the results. The shale volume is calculated from the GR log as per the following equation:

$$V_{sh} = \frac{GR_{Log} - GR_{Clean}}{GR_{Shale} - GR_{Clean}} \dots \dots \dots (1)$$

(**Bassiouni 1994**)

Where:

V_{sh}:　　Volume of shale (V/V)

GR_{Log}:　Gamma-ray log reading in the zone of interest (GAPI)

GR_{Clean}:　Gamma-ray log reading in clean formation (GAPI)

GR_{Shale}:　Gamma-ray log reading in 100% shale (GAPI)

The double indicator approach utilises a combination of two porosity logs, particularly the density and the neutron based on the crossplot. The calculation is done using the following equation:

$$V_{sh} = \frac{NPHI + \left[\dfrac{NPHI_{fl} - NPHI_{ma}}{\rho_{fl} - \rho_{ma}} * (\rho_{ma} - \rho_b)\right] - NPHI_{ma}}{NPHI_{sh} + \left[\dfrac{NPHI_{fl} - NPHI_{ma}}{\rho_{fl} - \rho_{ma}} * (\rho_{ma} - \rho_{sh})\right] - NPHI_{ma}} \dots \dots \dots (2)$$

(Schlumberger, 2019)

Where:

V_{sh}:   Volume of shale (V/V)

$NPHI$:   Neutron porosity log reading in the zone of interest (V/V)

$NPHI_{fl}$:   Neutron porosity log reading in 100% water (V/V)

$NPHI_{ma}$: Neutron porosity log reading in 100% matrix rock (V/V)

$NPHI_{sh}$:   Neutron porosity log reading in 100% shale (V/V)

ρ_b: Bulk density log reading in zone of interest (g/cc)

ρ_{ma}:   Bulk density log reading in 100% matrix rock (g/cc)

ρ_{sh}:   Bulk density log reading in 100% shale (g/cc)

ρ_{fl}:   Bulk density log reading in 100% water (g/cc)

On the density-neutron crossplot, the parameters can be picked based on the concept shown in **Figure 4**. There is a difference between the shale and the clay points on the plot. The points plotted above the sand line (Sd) to the shale point (Sh_o) represent a formation ranging from clean formation to laminar shales to shale at Sh_o point, at which a representation for the 100% shale. The points falling to the right of the Sd- Sh_o line, or Group-C, is more clay rich than silty shales, whereas those plotted to the left of the line are of more dispersed shales (Bowen, 2003). The Group-B points, which is considered as an extension for the clean quartz to the 100% shale line on the plot, are reflecting shales with varying silt content. As shales consist of variable amount of clay minerals, hence not 100% clay, then the far the point is located from the Sh_o points, the larger the silt matrix in the formation (Spooner, 2014). Silt Index (I_{silt}) can be identified in terms of V_{sh} and V_{cl} as $I_{silt} = (V_{sh} - V_{cl})/V_{sh}$ (Bowen, 2003). The shale point in such case is representing two main inputs in the density neutron equation for shale volume, which are the shale density and the shale neutron.

Following the calculation of the shale volume from both equations, an arithmetic average can be used to estimate a final shale volume to use for the subsequent analysis.

2.1.2.   Porosity Evaluation

The reservoir porosity is the second step in the basic petrophysics workflow after the shale volume calculation. The calculated shale volume is used to solve for the effective porosity. The porosity can be calculated from one of the three porosity tools, which are density, neutron and sonic. The following equation is used to calculate the formation porosity from the density log:
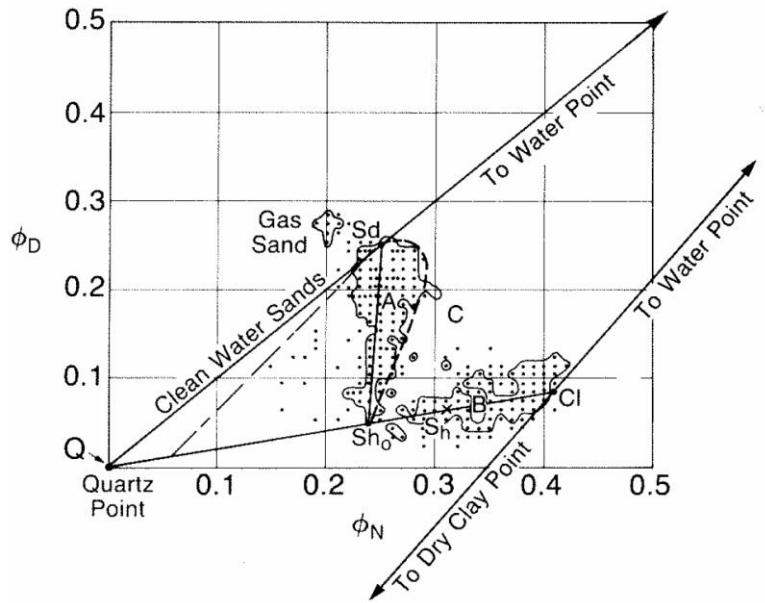
Figure 4: *Neutron-Density crossplot showing shale versus clay end points (After Bowen, 2003)*

$$\emptyset_{T\,Dens} = \frac{\rho_{ma} - \rho_b}{\rho_{ma} - \rho_{fl}} \dots\dots\dots (3)$$

(Schlumberger, 1989)

Where:

$\emptyset_{T\,Dens}$: The total density porosity (V/V)

ρ_{ma}:   Matrix density (g/cc)

ρ_b: Density log reading (g/cc)

ρ_{fl}:   Fluid density in the invaded zone (g/cc)

In shaly formation evaluation, a modified model is used that involves the estimated shale volume to solve for the effective porosity. The final effective porosity equation has the following form:

$$\emptyset_{eff\,Density} = \frac{\rho_{ma} - \rho_b - V_{sh} * (\rho_{ma} - \rho_{shale})}{\rho_{ma} - \rho_{fl}} \dots\dots\dots (4)$$

(Schlumberger, 1989)

Where:

$\emptyset_{eff\,Density}$: Effective density porosity (V/V)

V_{sh}:   Shale volume (V/V)

ρ_{shale}:   Wet shale density (g/cc)

This equation involves the density of the wet shale porosity, referred to as Sh_o point on the crossplot, picked from a nearby shale section. As the shale porosity will control the

variance between the total and the effective porosities, the error in the picked shale end points may result in considerable uncertainty for all subsequent results. The shale porosity, or the shale bound water, is calculated through the following equation:

$$\emptyset_{Sh} = \frac{\rho_{dry} - \rho_{wet\ shale}}{\rho_{dry} - \rho_{fl}} \dots \dots \dots (5)$$

(Schlumberger, 1989)

Where:

$\emptyset_{Sh}$:   Shale porosity, or the shale bound water (V/V)

ρ_{dry}:   Dry shale density (2.78 g/cc)

$\rho_{wet\ shale}$: Wet shale density (g/cc)

ρ_{fl}:   Fluid density (g/cc)

In the shaly sand formation, it is expected to have a considerable difference between the effective and the total porosity, opposite to what might be expected in carbonates where clays may not constitute or play any major role within the rock system. With the density porosity considered the most robust, it is likely to have the total density porosity aligns very well with the core measured porosity, particularly with the application of the effective stress on the core plugs (McPhee et al., 2015), indicating that the calculated total porosity should be correlated to the core porosity.

Similarly, the neutron log ($\emptyset_N$) is used as a porosity index with an assumption that the matrix has the same properties as a water-filled limestone (Bassiouni, 1994). The following equation expresses the neutron porosity:

$$\emptyset = f(\emptyset_N) \dots \dots \dots (6)$$

Diab and Donaldson (2004) confirmed that the modern neutron logs are recorded directly in apparent porosity units with required minor corrections for salinity, hole size and temperature. In the clean formations of pores filled with water or oil, the neutron log will reflect the amount of liquid filled porosity (Schlumberger, 1989). This is due to that the liquid hydrocarbons have hydrogen index closed to that of water. On the other hand, formation gas and/or shales will have a considerable effect on the neutron tools. To correct the shale effect on the neutron porosity, the following equation can be applied:

$$\emptyset_{N\ corrected} = \frac{\emptyset_N - V_{sh} * \emptyset_{sh}}{1 - V_{sh}} \dots \dots \dots (7)$$

(Diab and Donaldson, 2004)

The gas exhibits a lower hydrogen index that varies with temperature and pressure in the reservoir that significantly affects the neutron tool readings. Where gas is present

near the wellbore within the neutron tool's depth of investigation, the neutron log will read much lower porosities. Further, the density tools will experience a similar gas effect on the measurements due to the lower gas densities. Accordingly, the presence of gas zones can be identified from the combination of the density and the neutron logs, apart from any possible existing gas to oil, or gas to water, contacts. The total porosity in gas-bearing formations from the density and neutron is calculated through the following equation:

$$\emptyset_{T_{gas}} = \sqrt{\frac{\emptyset_{T_{Den}}^2 + \emptyset_N^2}{2}} \ldots \ldots \ldots (8)$$

$where$:

$\emptyset_{T_{gas}}$: The total porosity from the density and neutron in gas reservoirs (V/V)

$\emptyset_{T_{Den}}$: The total porosity from the density log (V/V)

$\emptyset_N$:   The neutron porosity (V/V)

There is a strong tendency towards the density porosity model as the preferred total porosity in the industry amongst industry experts, which will reflect both the primary and secondary porosities. With the fact that the neutron, reflecting both primary and secondary porosities as well (Schlumberger, 1979), requires up to 8 environmental corrections (Schlumberger, 2013), the density is a more robust measurement where the boreholes have not experienced high washouts or breakouts. However, this assumption only applies to relatively simple reservoir environments. "*In complex environments such as shaly sands, gas bearing formations and complex lithologies, the density log is combined with other logs for better evaluation*" (Bassiouni, 1994).

The third tool is the acoustic tool that provides a sonic slowness log from which the primary porosity can be calculated. The porosity can be calculated using the following equation:

$$\emptyset_S = \frac{\Delta T_{Log} - \Delta T_{matrix}}{\Delta T_{fl} - \Delta T_{matrix}} \ldots \ldots \ldots (9)$$

(Wyllie et al., 1956)

$where$:

$\emptyset_S$: Sonic porosity (V/V)

ΔT_{Log}: Sonic log reading (μs/ft)

ΔT_{fl}: Sonic slowness of the fluid (μs/ft)

ΔT_{matrix}: Sonic slowness of the formation matrix (μs/ft)

In the presence of shale in the reservoir, a modified model is applied that involves the shale volume to generate the effective porosity:

$$\emptyset_{S_{eff}} = \frac{\Delta T_{Log} - \Delta T_{matrix} - V_{sh}(\Delta T_{sh} - \Delta T_{matrix})}{\Delta T_{fl} - \Delta T_{matrix}} \dots\dots\dots (10)$$

The sonic log is affected by the presence of hydrocarbons whether it is oil or gas. Hilchie (1978) suggested correction factors of 0.9 and 0.7 for the presence of oil and gas respectively. Accordingly, the following equations are used in the presence of hydrocarbons:

For Oil:

$$\emptyset_{S_{corrected}} = \emptyset_S * 0.9 \dots\dots\dots (11)$$

For Gas:

$$\emptyset_{S_{corrected}} = \emptyset_S * 0.7 \dots\dots\dots (12)$$

However, Schlumberger (1989) indicated that in case of combining the sonic log with either density or neutron on crossplots, the gas will shift the log responses from density and neutron as a result of reduction of their values rather than an effect on the slowness log itself. Bassiouni (1994) did link the existence of gas anomaly in the sonic measurements to the compaction of the rock. Accordingly, the sonic log is not necessarily suitable for gas detection.

Between the three porosity tools, a generalised equation to calculate effective porosity can take the following form:

$$\emptyset_{eff} = \emptyset_{Total} - V_{sh}\emptyset_{sh} \dots\dots\dots (13)$$

(Schlumberger, 1989)

2.1.3.   Water Saturation

The calculation of the water saturation is the last step in the deterministic petrophysics workflow that comes after the porosity computation. Archie (1942) introduced a relationship between the formation resistivity factor (F) and the porosity ($\emptyset$) as per the following:

$$F = a * \emptyset^{-m} \dots\dots\dots (14)$$

$where$:
F: The formation factor
a: The tortuosity factor
m: The cementation factor

The Formation Factor is representing the relation between the resistivity of a 100% water saturated rock (R_o) to the formation water resistivity, whereas the water saturation is the ratio between the saturated rock to the true formation resistivity (R_T) as follows:

$$F = \frac{R_o}{R_W} \dots \dots \dots (15)$$

$$Sw^n = \left(\frac{1}{R_I}\right) = \frac{R_o}{R_T} = \frac{F * R_W}{R_T} \dots \dots \dots (16)$$

Where (n) represents the saturation exponent and (R_I) represents the formation resistivity index. Combining these equations provides the final form of the Archie equation (1942):

$$Sw^n = \frac{a * R_W}{\emptyset^m * R_T} \dots \dots \dots (17)$$

The water saturation involves several parameters that need to be calculated, including Archie parameters (m & n), and the water resistivity (R_W). In the petrophysical workflow, the applied value for both cementation factor and saturation exponent is equal to 2 (Bassiouni, 1994) and (Schlumberger, 1989). In case of existing core measurements for the formation resistivity factor and resistivity index, the values for Archie parameters are estimated based on these measurements. Cannon (2016) confirmed that using the default Archie parameters (m & n) is acceptable unless there is calibrated offset data in hand. This will allow a quick look evaluation with reasonable outputs from the log analysts.

Herrick and Kennedy (2009) confirmed that calculating water saturation from resistivity logs in shaly sands has been a problem. Archie equation was designed to calculate the water saturation in the clean reservoirs. Therefore, utilising the equation in shaly formations would overestimate the water saturation (Cannon, 2016). In the shaly sand formations, the equation is modified with the shale terms to provide more accurate water saturation calculation. A good model used for the shaly sands is the Simandoux model, in which two terms are modified to Archie model, the shale volume and the shale resistivity (Simandoux, 1963).

$$\frac{1}{R_T} = \frac{\emptyset^m * Sw^n}{a * R_W} + \frac{V_{shale} * Sw}{R_{shale}} \dots \dots \dots (18)$$

2.2.Mineralogical Analysis

The advanced petrophysical interpretation provides more accurate analysis upon the selection of valid mineral inputs in the evaluation. The mineralogical inversion, known as Multimineral Statistical Inversion Modeling (Darling, 2005), or Probabilistic Analysis (Kennedy, 2015) is one of the best approaches used in the industry to date. The methodology is designed to minimise the gross error in the calculations but does require accurate parameters selection (Barson et al, 2005), or in other words the correct mineralogy for a particular reservoir.

There is a continuous argument against the inversion approach as to whether the end results are more valid. Darling (2005) stated that in the presence of heavier minerals, the conventional approach using the deterministic equations is not reliable, even if the answer is reliable. Spooner (2018) discussed in detail the errors existing in the petrophysical deterministic model by the nature of the applied equations. The matrix densities used for the clays are those used for the dominant rock matrices, sandstone, limestone, and dolomite. This provides a wrong total porosity across the shale sections and the shaly formations, hence the subsequent calculated effective porosity and water saturation. In probabilistic modeling, the solver tends to work towards the best possible answer for reservoir evaluation, provided that the mineral inputs are correct and data is of normal quality.

In case the data quality is affected by existing bad hole conditions, large washouts, data gaps, or spiky logs, this will impact the evaluation regardless of the approach taken to run the petrophysical interpretation. Furthermore, whether the deterministic or the mineral inversion workflow is to be followed, the user needs to understand the basic standard quality check requirements to assess the outputs. In bad borehole conditions and if the data is not processed with extreme care, this may lead eventually to higher or lower net calculations than necessary.

2.2.1. Inversion Modelling

The manual picking for the parameters in the deterministic workflow is a matter of judgment from the users. The inversion modelling relies on the fact that the parameters are likely to be constant over the studied zone (Christensen et al., 2005). Different users tend to change the parameters for each reservoir to reach a certain output. This becomes a serious problem in the subsequent geological modeling as it may significantly affect the clay volume estimated, hence the formation porosity, between the wells. A result of such a wrong approach does not add a factor of uncertainty in the analysis, it rather overestimates or underestimates the results for certain areas, leading to wrong volumetric calculations. The quantitative evaluation through the inversion modeling, particularly in the presence of supporting core data, concentrates the users' efforts

towards picking the correct mineralogy for the reservoir in hand. Then models are driven to provide the most probable, or the highly likely, answer.

2.2.1.1.   Historical Background

The "Global" processing technique, introduced by Mayer and Sibbit (1980), was a major step forward in the history of log analysis. The methodology could be used for complex lithologies particularly as it generated an "Error" model using which the results could be identified as valid or inadequate. Before the Global method was introduced, the evaluation techniques were based on cross plots (e.g. Neutron and Density) using different Computer Processed Interpretations (CPIs) such as CORIBAND and SARABAND. In complex formations, the models were still valid to use, however, they became more difficult to control and did not make the best use of the available information. Therefore, the Global Method was introduced to provide a powerful technique for quality control of the interpreted results.

The principle of the method is that for each depth of any well, there are three sets of equations; The inputs, the reservoir parameters and the outputs. The inputs can be written as an array as follows:

$$a = (\rho_b, \emptyset_N, R_{xo}, R_T, GR, SP) \dots \dots \dots (19)$$

The set of the input parameters are the water resistivity (Rw), the Clay parameters, the mud characteristics..etc. The output set, or the Unknowns, can be written as follows:

$$x = (\emptyset, V_{cl}, Sw, S_{xo}, \rho_{ma}) \dots \dots \dots (20)$$

The relationship between inputs and outputs can be expressed by a set of tool response equations, one equation for each tool. For example, the density relationship may be expressed as:

$$\rho_b = \emptyset S_{xo}\rho_{mf} + \emptyset(1 - S_{xo})\rho_{hyd} + V_{cl}\rho_{cl} + (1 - \emptyset - V_{cl})\rho_{ma} \dots \dots \dots (21)$$

Using the arrays introduced, the tool response equations may be written as below:

$$a_1 = f_1(x) \dots \dots \dots (22)$$

$$a_2 = f_2(x) \dots \dots \dots (23)$$

Where (a) is the set of inputs at particular level or depth and (f) is the tool response function of the ith tool type.

The Global method is a maximum likelihood method, finding for a set of log responses the most probable log interpretation using all the logs and their responses (Mayer and Sibbit, 1980). This method was an extraordinary step in the well log interpretation. However, there was a problem in the complicated

formations where a particular mineral does not constitute a consistent volume in the rock matrix, or when it does not exist at all reservoir levels.

Quirein et al. (1986) developed a new technique that is widely used till date that assigns a probability to a certain model. This allowed the users to create several models and integrate them together using a probability assigned for each. The most powerful softwares in the market has been using the probability equation to generate a final "Combined" interpretation model, where it is referred to as the probabilistic interpretation. "*Multiple individual models, each of which corresponds to a particular formation type or petrophysical situation, can be computed in parallel*" (Quirein et al., 1986). This is greatly describing what the software would be capable of and what the user can do to reach the best answer for a studied reservoir. Accordingly, there should be no calcite where there is no calcareous sandstones, and vice versa. This has allowed a much better geological sense in the petrophysical interpretation with a direct link to geology and lithofacies and prevented log cosmetics. Nevertheless, where the logs are of bad quality, a valid quality control is required followed by careful interpretation to avoid wrong analysis.

2.2.1.2.   *Models and Combination*

The number of independent component volumes must be always less than or equal to the number of logging measurements plus 1. As stated earlier, the advent of the new tools in the market provided an increasing number of input logs to be used in the mineralogical modelling; thus, more minerals can be generated that describe the reservoir more quantitatively. The reasoning is to reflect a closer coherent model with subsurface geology. Quirein et al., (1986) presented the solution for the complicated lithology by defining several individual models.

Three methods can be used to combine individual models:

1. External probability functions
2. Assign probabilities based on the volumetrics in each of the models
3. Manually select the desired model

2.3. Nuclear Magnetic Resonance

The Nuclear Magnetic Resonance (NMR) tool is a porosity-independent lithology tool, with which the output porosity is not affected by the rock matrix. Freedman (2006) indicated that the NMR tools measure the relaxation rates of the hydrogen atoms in the pore spaces of earth formations by detecting the amplitude and decay rate of signals resulting from pulsed NMR spin-echo sequence (**Figure 5**). The initial amplitude of the spin-echo is proportional to the density of the hydrogen atoms, which is directly proportional to the total formation porosity due to the presence of hydrogen in water, oil

and gas. Therefore, the tool is considered a completely independent measurement for the formation porosity irrespective of the type of lithology. Add to this, the tool does provide multiple other outputs that play a crucial role in reservoir fluids characterisation. The porosity measured by the tool can be partitioned into groups to reflect fluid type, pore size and the mobility of that particular fluid. In petrophysics, the NMR tools are considered very valuable in complicated reservoir cases, where they can provide answers to questions beyond the capabilities of the conventional logging tools. In the last decade, the NMR has been considered a basic tool in the logging programs designed for carbonates and shaly sand reservoirs.
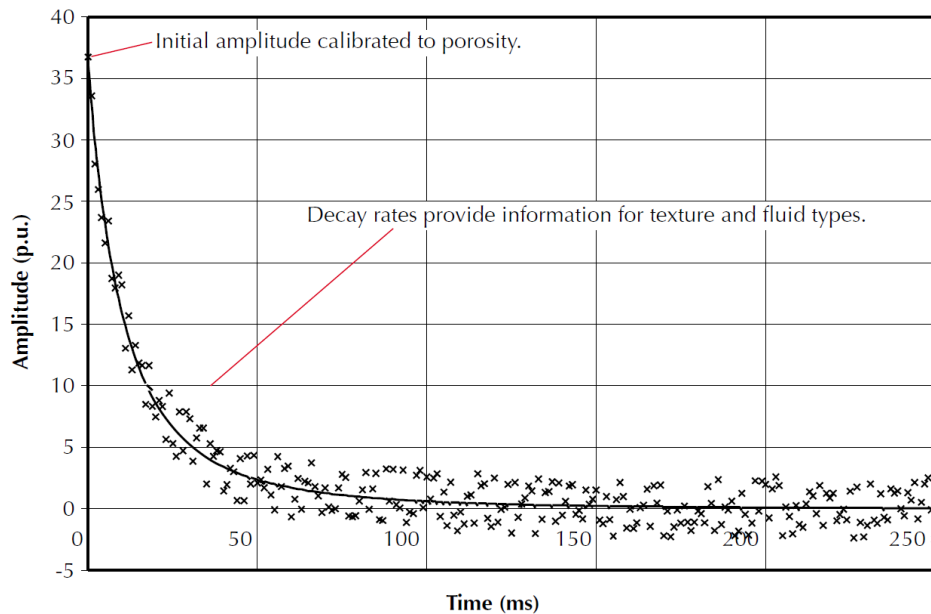
Figure 5: Spin echo train as a function of the hydrogen amount in the formation fluids (After Coates et al., 1999)

2.3.1.   The NMR Porosity Model

The Nuclear Magnetic Resonance log, regardless of the tool type or the vendor, provides a main output known as the T2-Distribution array, which is a result of the spin-echo train measured at each reservoir depth. This array is a direct indicator of the total porosity. As the initial amplitude directly indicates the total pore volume, the decay will include information about the small pores in the reservoir clays, reservoir fluids and pore size (Coates et al., 1999).

Three different types of fluids may be present in the pore volume of the reservoir, the clay bound water, the irreducible or capillary bound fluid, and the free fluids, including water, oil and gas. The NMR log needs to be interpreted to calculate the volume of each of these different fluids. **Figure 6** presents the NMR porosity model that can be analysed from any magnetic resonance tool. The total NMR porosity is considered a very good quality check log for the porosity calculated from the density and neutron logs, or through a combination of two of the three porosity tools.
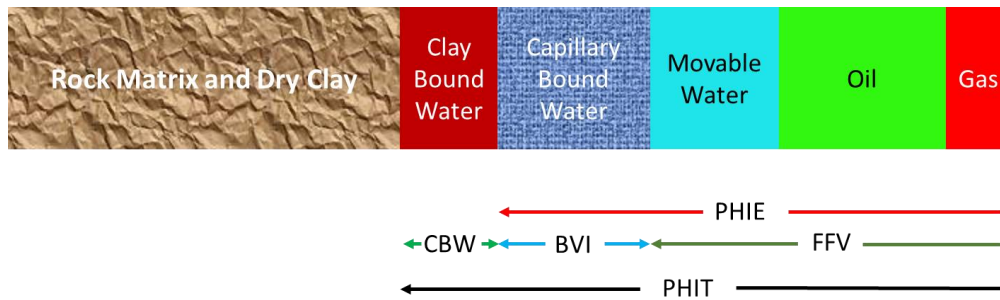
Figure 6: Nuclear magnetic resonance porosity model; PHIE: Effective porosity; CBW: Clay bound water; BVI: Bound volume irreducible; PHIT: Total porosity (Modified after Coates et al., 1999)

The NMR tools are known to provide measurements of very shallow depth of investigation between 2.5 inches (Minh and Sundararaman, 2011) to possibly 3.8 inches into the formation near the well bore (Baker Hughes, 2018). This certainly reflects a measurement that is very shallow within the flushed zone near the borehole wall. "*One major deficit for the NMR tools is the invasion effect. The tools have generally shallow depth of investigation and highly affected by the rugosity of the holes*" (Coates et al., 1999). Accordingly, a very high caution is required with the data quality in enlarged boreholes. A variance between the NMR porosity and the calculated porosity from the conventional pad tools would indicate a possible error in one of the parameters used in the calculation unless the tool measurements are affected by borehole irregularities.

The evaluation of the reservoir fluids depends mainly on two defined cutoffs. The free fluid cutoff, named T2 Cutoff, and the clay bound water cutoff. These two cutoffs classify the reservoir fluids into the mentioned three volumes. Then, the free fluid volume itself can be classified into volume filled with free hydrocarbons or free water depending mainly on the formation salinity, or fluids diffusivity (Romero, 2012). The total NMR porosity is representing the following volumes:

$$nmrPhiT = FFV + BVI + CBW \dots \dots \dots (24)$$

$Where$:
$nmrPhiT$: Total NMR porosity (V/V)
FFV: Free Fluid Volume (V/V)
BVI: Bulk Volume Irreducible (V/V)
CBW: Clay Bound Water (V/V)

2.3.2.   NMR Cutoffs and Interpretation

The interpretation workflow applies a series of equations that are simple in general as they coincide with the NMR porosity model.

Whereas the relaxation time log in the form of the T2 Distribution array will indicate the total porosity, the application of the free and clay cutoffs, shown as red and black

lines in **Figure 7** respectively, will define the total from the effective porosities. In clastic reservoir rocks, 33 milliseconds is an empirically used cutoff to partition the pore volume estimated from the NMR tool into bound and free fluid porosities (Freedman and Morriss, 1995). For Carbonates, a value of 92 milliseconds can be used (Coates et al., 1999).
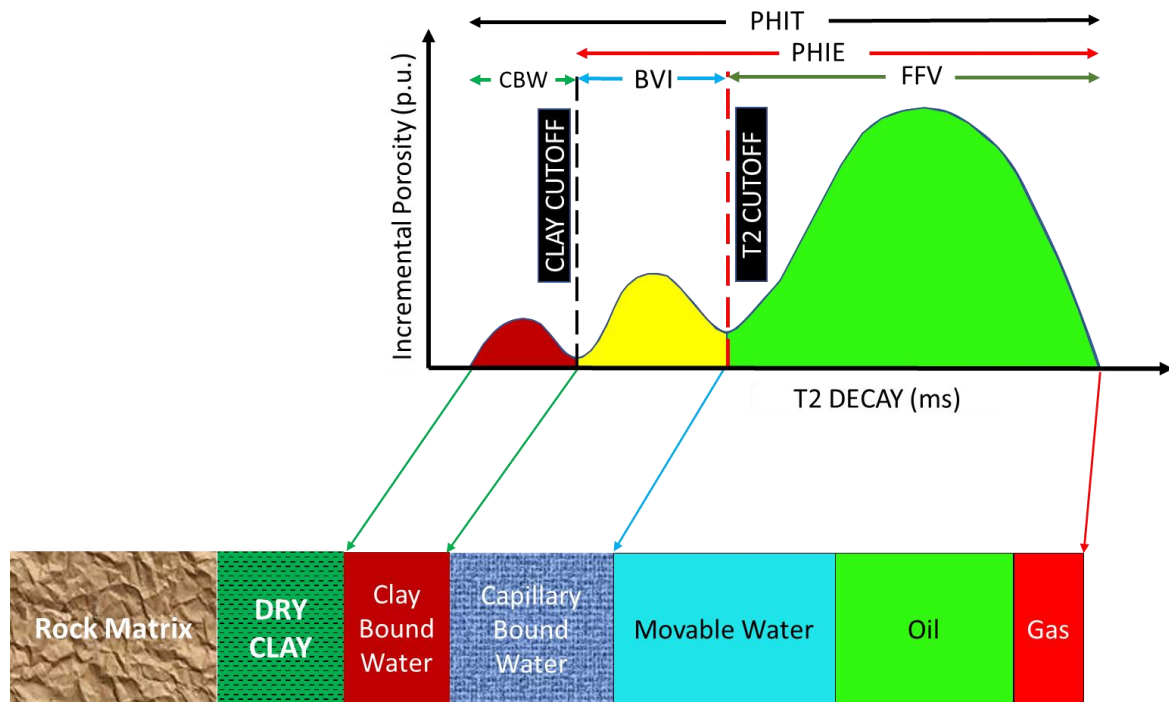
Figure 7*: T2-Distribution log portioned to clay water, capillary bound fluid and free fluid volumes (Modified after Coates et al., 1999)*

The difference between the total and effective porosities from the NMR log is the contribution of clay bound water within the total pore system as per the following equation.

$$nmrPhiE = nmrPhiT - CBW \dots \dots \dots (25)$$

The irreducible fluids or the capillary bound water accordingly is part of the effective porosity, but they will not contribute to the fluid flow by any means. In other words, the irreducible volume would be trapped in a larger pore size compared to clays bound water, and smaller pore size than the one associated with the fluid flow. The total irreducible volume ($nmrBFT$) and the bound volume (BVI) are calculated as per the following:

$$nmrBFT = CBW + BVI \dots \dots \dots (26)$$

$$nmrBFT = nmrPhiT - FFV \dots \dots \dots (27)$$

$$BVI = nmrPhiE - FFV \dots \dots \dots (28)$$

Where the free fluid volume (FFV) will represent the larger contribution for the effective porosity:

$$FFV = nmrPhiT - nmrBFT \dots \dots \dots (29)$$

As the irreducible volume can be estimated through the cutoffs, the irreducible water saturation can be calculated from the NMR logs, which plays a major role in assessing the true reservoir productivity.

$$Swi = 1 - \left(\frac{FFV}{nmrPhiE}\right) \dots \dots \dots (30)$$

The accuracy of the outputs from NMR log interpretation is mainly dependent on the chosen cutoffs. The best calibration for such cutoffs is done through core labs where they can measure both cutoffs on plug samples, similar to Archie parameters for the saturation. Coates et al., (1999) confirmed that it is more accurate to obtain the cutoff values by performing core measurements on samples from the exact logged intervals. In the absence of the core measurements, the standard cutoffs are the best choice to use for NMR interpretation.

2.4. Reservoir Permeability

The calculation of permeability is dependent on different empirical models of high uncertainty. Timur (1968) developed the first model to calculate the permeability by using the irreducible water saturation and the porosity as follows:

$$K_{Timur} = 0.136 \, \frac{\varphi^{4.4}}{Swi^2} \dots \dots \dots (31)$$

Later, Timur (1969) modified this equation to take the following form:

$$K_{Timur}^{\frac{1}{2}} = 100 * \frac{\varphi^{2.25}}{Swi} \dots \dots \dots (32)$$

These equations were established for relatively clean, consolidated sands of medium porosity. Coates and Dumanoir (1973) indicated that these relationships are essentially dependent on the calculated porosity, and they lose accuracy in fine-grained or shaly

formations. Coates et al., (1999) developed standard correlations to allow computing the NMR log permeability index. The Timur-Coates calculation is dependent on the T2 cut-off and uses the ratio of free water to bound water, which is usually preferred for clastics.

$$K = \left[\left(\frac{\varphi}{C}\right)^2 * \left(\frac{FFV}{BVI}\right)\right]^2 \dots\dots\dots (33)$$

Another model named The Mean T2, or SDR, usually preferred for carbonate rocks (Van Steen et al., 2012) depends on the logarithmic mean of the T2-Distribution log takes the following form:

$$K_{SDR} = a * T2LM^2 * \emptyset^4 \dots\dots\dots (34)$$

$where$:
$T2LM$: T2 Distribution Logarithmic Mean (ms)
$\emptyset$:   Effective porosity (V/V)

The Coates model depends on the T2-Cutoff value used in the NMR interpretation, usually provides a continuous permeability log through the NMR logged interval. Yet it is considered aa a permeability index rather than a true permeability as in most of the cases the T2 cutoff is not calibrated to core NMR measurement, or there is a considerable variance with the core permeability.

Another possible measurement out of which the permeability can be calculated is the repeat formation tester pressure acquisition. The tool acquires pressure at certain defined depths through the reservoir interested section. During the acquisition, a pressure drawdown is allowed with a little volume of formation fluids is allowed into the tool chamber. Then the pressure is acquired continuously to obtain a pressure build up trend. Accordingly, the mobility of reservoir interaction with the tool can be computed from the drawdown and the build-up data through the following equations (Schlumberger, 1989):

$$K_{DD} = 5660 * \left(\frac{q * \mu}{\Delta P}\right) \dots\dots\dots (35)$$

$$K_{BU} = \frac{8 * 10^4 * q * \mu * (\varphi\mu C_t)^{(1/2)}}{P_e - P_s} * f_s \dots\dots\dots (36)$$

$where$:
K_{DD}: The drawdown permeability (mD)
K_{BU}: The spherical build up permeability (mD)
q: The pretest chamber flow rate (cm/sec)
μ: The viscosity of the flowing fluid, usually it is mud filtrate (cp)
ΔP: The drawdown pressure (psi)
C_t: The total compressibility of formation fluid (psi^{-1})

P_e: The initial static formation pressure (psi)

P_s: The probe pressure where spherical build-up should occur (psi)

f_s: Time difference between the fluid flow between 2 different champers

In the absence of an intermediate viscosity value for the formation fluid, the equation delivers mobility for the reservoir. In logging programs that contain NMR and RFT tools, the NMR permeability index is calibrated to the calculated mobilities at each acquired depth. Despite these models could provide a permeability log through the interested zone, yet they lack accuracy and always require a reference to calibrate the results.

2.5. Facies Interpretation

The reservoir facies classification has been one of the major steps to unlock the reservoir complexity, calculate the existing potential, and explore the best areas to drill in any field. With the reservoir modelling advancements in the last two decades, the petrophysical interpretation and the reservoir parameters have played major roles in geological modelling. As it is impossible to core each and every well, logs were used to generate electrofacies through statistical calculations. Those logs have nothing to calibrate them to unless there are core measurements, and they cannot be widely distributed even within the same field as they usually lack consistency, particularly with the different logging tools in the same field. Most importantly, the facies classification should guide the permeability modeling in the reservoirs as permeability has proven itself independent of reservoir porosity. When facies logs are generated statistically, there is no valid permeability model that can be driven from such calculated facies.

Amaefule et al., (1993) developed a clustering technique, known widely as the Hydraulic Flow Units (HFU) to identify the different facies in a reservoir rock. The HFU concept is considered as a criterion of the reservoir units in which fluid flow properties are uniform due to the same pore throat properties (Kadkhodaie-Ilkhchi et al., 2013). The methodology employs both porosity and permeability to identify clusters that relate to each other and assign each a unique Flow Zone Indicator, known as FZI. The workflow utilises the routine core data measured in the lab, preferably under the reservoir conditions (McPhee et al., 2015), to develop an understanding of the pore geometry that exists in the different lithofacies (Amaefule et al., 1993). Independent of the porosity and permeability values from the core data, a clustered group indicates that the data points of this group share similar flow performance.

Further effectiveness of this technique is the possibility to extend the flow units classified from the cored sections to the uncored wells. Hence, the same facies definition developed from the cored intervals (Al-Ajmi et al., 2000).

A cumulative density plot can be established to define the thresholds of the different hydraulic flow units (Svirsky et al., 2004), with the base reference being a good reservoir geological description from cut cores or possibly a detailed description of the drill cuttings collected while drilling. **Figure 8** shows a typical example for the classification of the petrophysical facies with clear variations on the trends of the Log (FZI) values. Kadkhodaie-Ilkhchi et al., (2013) confirmed that the sedimentary rock types are identified based on the integration of the available core description and petrographic thin sections. This reflects the necessity to have the connection between the geological facies and the ones developed from the HFU technique. Accordingly, a disconnection between the identified groups and the geological facies would be a deficit that requires re-evaluation. Once a good facies model is in place, it can be used to assign reservoir parameters (e.g.: porosity, permeability, clay volume, saturation) in the 3D space, upon which hydrocarbons in place will be calculated.

Significant improvement in the lateral distribution for the petrophysical parameters in the rocks of little variation in the porosity, but large permeability variance, can be clearly witnessed through this approach. Once the facies are classified, each will have a different permeability model regardless of its porosity value. With high efficiency, the best approach to validate the results of the facies clustering is the core to modeled permeability correlation. **Figure 9** shows a porosity-permeability crossplot for the routine core measurements shown as different cluster trends from the poor (lowest permeability) to the best (highest permeability). In this example, the different curves depicted on this figure indicate the FZI average for each of the seven hydraulic units identified (Amaefule et al., 1993).
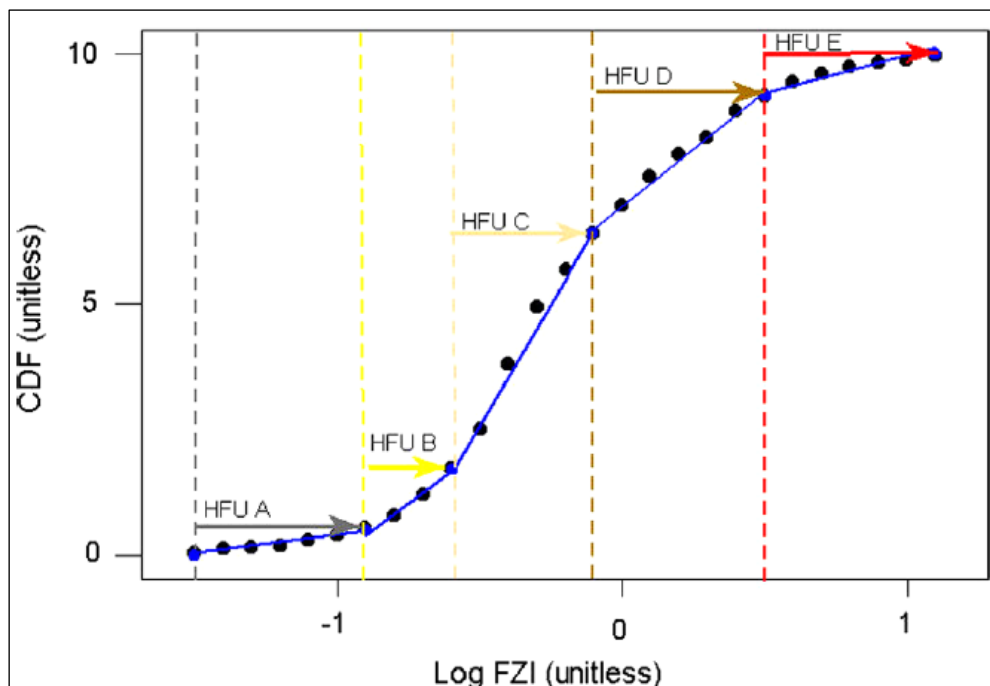
Figure 8: Cumulative frequency plot showing the classification of the petrophysical facies, (After Kadkhodaie-Ilkhchi, 2013)
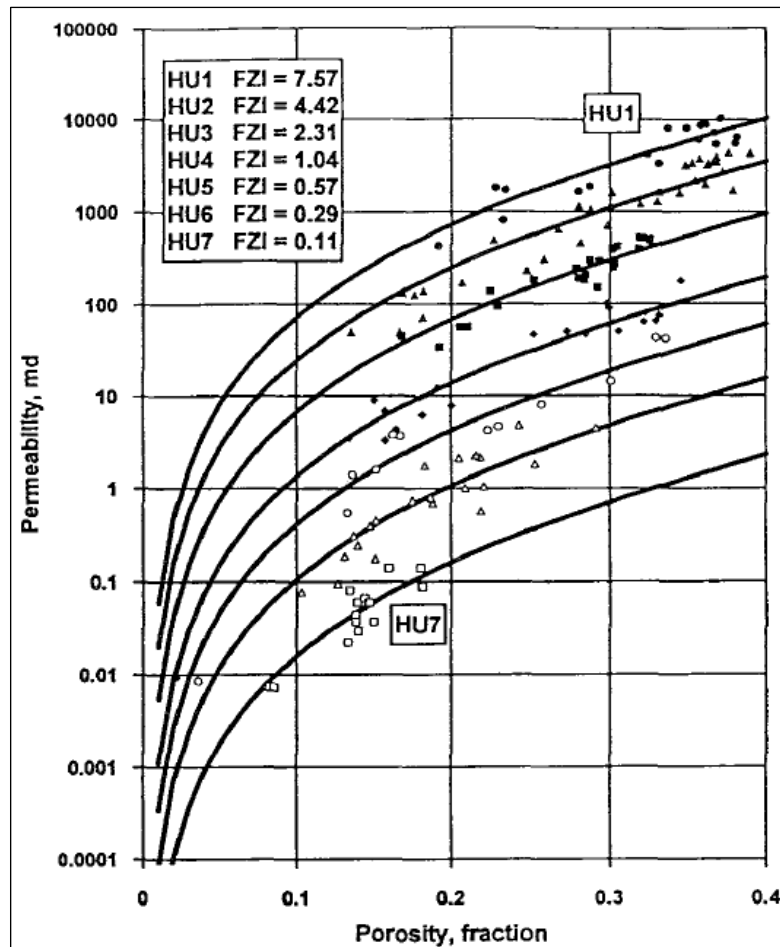
Figure 9: Plot between porosity and permeability showing classified hydraulic flow units (After Amaefule et al., 1993)

When a good facies model is generated, the water saturation in heterogeneous formations shows clear averaged trends through the interested zones that do not match the reservoir quality. Where the good quality rocks tend to show sharp transition zones and very low irreducible water saturations, they highly likely tend to show higher water saturations at large offsets from the free water levels, depending on the suppressed values of the used resistivity logs (McPhee et al., 2015). Therefore, advanced techniques that are dependent on core measurements have become mandatory to use if better saturations are to be calculated.

2.6. Saturation in Complicated Reservoirs

The petrophysical parameter that embraces a lot of ambiguity in the shaly sands is water saturation. Archie (1942) elaborated on "*the usefulness of electrical resistivity log in determining the reservoir saturation is governed by a) the accuracy with which the true formation resistivity can be determined; b) the scope of detailed data concerning the relation of the resistivity measurements to formation characteristics; c) the available information concerning the conductivity of connate waters; d) the extent of geologic knowledge regarding probable changes in facies within given horizons, both vertically and laterally*". Accordingly, the challenge remains unsolvable for the saturations that vary laterally in the case lateral facies variation, or vertically in the heterogeneous formations.

On the other hand, some reservoirs exhibit high hydrocarbons production with minimum water cut despite the logged resistivity generates high water saturation. Moreover, some of these reservoirs do not show any water production for several years despite the calculated water saturation is near 50 s.u. or even higher.

The shaly formations are known to have a common problem with conventional electrical logs due to their poor resolution. Harrison and Jing (2001) indicated that independent water saturation measurements from wells penetrating the transition zone, and covering a range of reservoir qualities, are recommended to constrain and calibrate the calculated water saturation. This can be carried out from the capillary-based saturation height functions. In these reservoirs, the irreducible water saturation is either higher than expectation, with which the water will not flow even at higher pressure drawdowns, or the calculated water saturation is not reflecting the reservoir production water cut, as the input logs are affected by the formation mineralogy or fast logging speed. In both cases, the irreducible water saturation is required as it could vary significantly from the estimated saturation based on the conventional resistivity-porosity technique. Obeida, (2005) stated that the calculation of the initial water saturation (Swi) is a critical step in any 3D reservoir modeling studies, where the saturation distribution will dictate the original oil in place (STOIP) estimation. Further, it will influence the subsequent dynamic modeling while running the history match and predictions. This reflects how the saturation distribution is not limited to the well evaluation itself, but to the further integration with the other disciplines of geology and engineering where petrophysics is translated statistically in the 3D spaces. This complexity has major room for improvement and puts the water saturation as an output of high uncertainty, next to the permeability.

As the Swi becomes a critical value to calculate, the fastest possible method to calculate it is from the NMR tools. Despite the tool does not provide a direct measurement for the irreducible saturation, it gives all the necessary inputs to calculate it, yet it will be dependent on the chosen cutoffs between the bound and the free fluids. If the reservoir rock is proven to be at its irreducible state, the total bulk volume of water will be considered all as bound water which will not flow upon the production of the reservoir. The Hydrocarbon Pore Volume in such case may be taken as NMR free fluid volume (Claverie et al., 2007):

$$HPV = \sum_{h1}^{h2} \varphi * S_{HC} = \sum_{h1}^{h2} \varphi * (1 - Swi) = \sum_{h1}^{h2} FFV \ldots \ldots \ldots (37)$$

The difference between the calculated Swi and the water saturation from Archie, or modified Archie equations that solve for the shaly formations, will reflect the amount of free water that exists in the reservoir rock. Having no variance between the two calculated logs indicates no free water in the formation. For a chosen T2 cutoff, the best calibration known to date is through measuring the relaxation time on saturated, and valid, reservoir samples in the core lab.

A second approach to measure the irreducible water saturation is through analysing the core capillarity on rock samples. Further, the capillary pressure profiles can be indirectly indicative to the reservoir rock quality, hence different facies. Thomas, (2018) indicated that the capillary pressure measurements can provide a major lead for facies classification. **Figure 10** presents different reservoir capillary pressure curves versus water saturation. The three capillary behaviours are clearly different from each other, where each has a different capillary entry pressure and different measured Swi. The best reservoir quality, Rock Type-1, has significantly lower capillary entry pressure relative to the poor facies (Rock Type-3), apart from the large variance in the irreducible water saturation. The permeability also decreases from rock type-1 to rock type-3, where much higher capillary pressure is required to apply the first hydrocarbons invasion in the smallest pore spaces. This criterion does not impact the permeability variations only, it could severely affect the estimated volume if not taken into consideration.

At a similar porosity range for all or the majority of the existing facies and low resistivity logs resolution, the water saturation will not show the saturation variations despite some of those porosities may have much better flow capabilities relative to the smaller pore throats, hence better hydrocarbons saturation. **Figure 11** presents a configuration over a case where there is a common free water level for different rock types. Well-1 had found oil in Rock Type-1, then encountered Rock Type-2 below its oil-water contact. The analysis would directly imply a contact much higher than the true case. Further, another well (Well-2) was drilled up-dip and penetrated Rock Type-4 below its contact, with the petrophysical logs once more confirming an existing higher contact, but for another facies. In such case, particularly in the absence of a valid pressure dataset, which is very common, a significantly underestimated oil in place volume will be calculated upon the wrong estimated contacts. In fact, this could still be the case even with the knowledge of a possible deeper free water level, as the logs become much more solid evidence, to which geoscientists would be inclined to when compared to few pressure measurements of less accuracy. This example shows the significance of understanding two major elements for any reservoir, the relation of the facies to their saturation profiles, and the capillary entry height of each of these facies in relation to the free water level.

In the saturation modeling workflow, it is crucial to consider that the capillary pressure and the measured saturation data were originally measured at surface ambient conditions at very low stresses relative to the reservoir conditions. McPhee et al. (2015) confirmed that there is a stress relief at atmospheric conditions results in an increase in both porosity and permeability of the samples. Therefore, correction must be applied to the core results before utilising the data in the modeling workflow (Juhasz et al. 1979).

The important application of the capillary pressure concept is how the reservoir fluids are in fact distributed across the thickness of the reservoir prior to its exploitation (Ahmed, 2001). This indeed solves the problem of the compromised water saturations calculated at reservoir depths with a considerable offset to the free water levels.
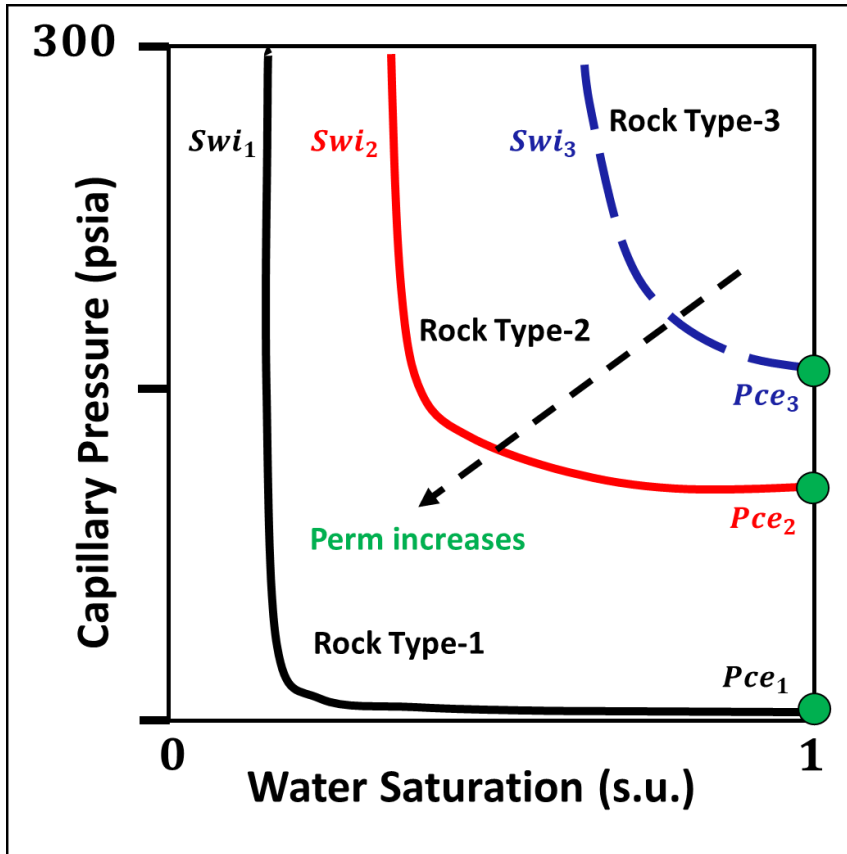
Figure 10: Capillary pressure profiles for three different reservoir facies (Modified after Thomas, 2018)
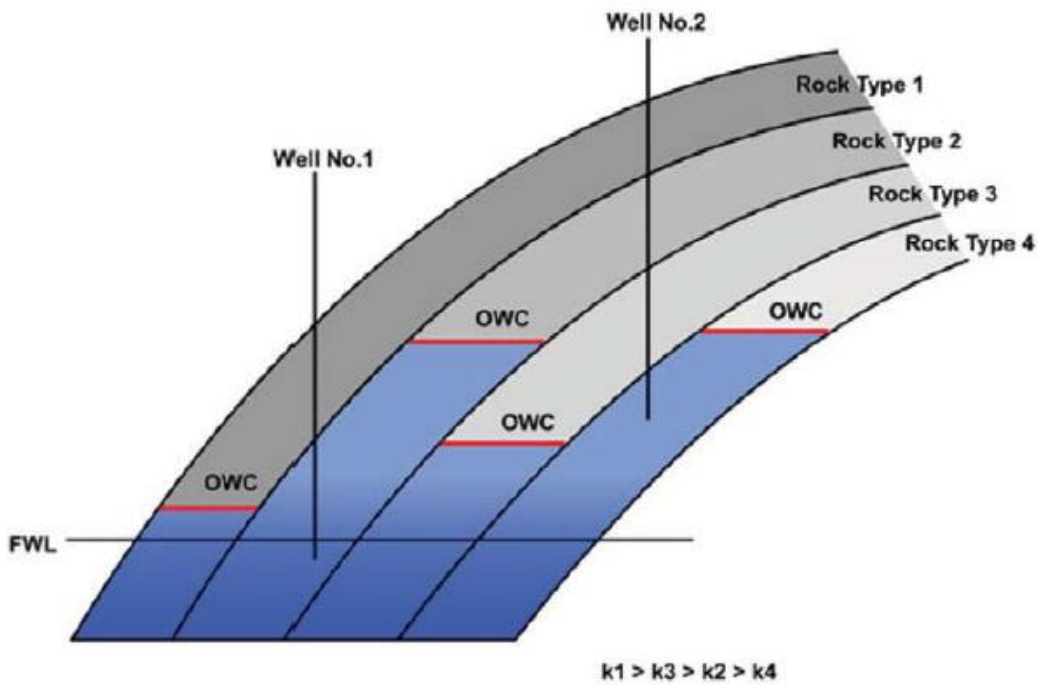
Figure 11: Structure showing different wells drilled and encountered misleading reservoir contacts (After Thomas, 2018)

The saturation height modeling will aim to run a resistivity independent quantitative saturation evaluation that can be compared with the resistivity-based and the NMR irreducible saturations. This provides three fully independent methods that provide the same output parameter. It is obvious the two logging-based methods will be limited to the acquired logs' vertical resolutions, and indirectly to the T2 cutoff used for the NMR saturation. In the saturation height modeling, despite the method are applicable to the cored and uncored wells, and in the presence of complicated facies regimes, the accuracy of those models remains a big challenge in the industry due to the limited core measurements, core applicability, and the accuracy of the measurements for the different wells.

In the following chapters, different integrations were carried out between cores and logs to solve for the three main uncertain outputs, facies, permeability and water saturation.

Chapter 3: The Equivalent Flow Zone Indicator

This chapter discusses a published peer-reviewed journal paper in *The Journal of Petroleum Science and Engineering.*

Elkhateeb A., Rezaee R., and Kadkhodaie A., 2019, Prediction of high-resolution reservoir facies and permeability, an integrated approach in the Irwin River Coal Measures Formation, Perth Basin, Western Australia, Journal of Petroleum Science and Engineering, **181** (2019) 1-12. https://doi.org/10.1016/j.petrol.2019.106226

3.1.Introduction

One of the very challenging petrophysical outputs is the reservoir facies and permeability which are considered major inputs in the reservoir static and dynamic modeling. Permeability is usually estimated through different methodologies. In general, three different approaches are used to derive permeability; the first is through Electric Logging (E-logs) tools, which give qualitative indirect permeability index estimation, such as nuclear magnetic resonance, repeat formation tester mobility measurements or empirical relationships between porosity and irreducible water saturation (Timur, 1968). Secondly, well testing, or drill stem tests, across a defined zone of interest after which the analysis of the well test results gives an estimation for the permeability over the tested interval. Thirdly, through core analysis that gives an absolute permeability value using single phase fluid (McPhee et al., 2015) either air, oil or brine. The first approach is considered the least effective and of the highest uncertainty amongst all. This is due to the lack of any calibration upon which the calculated permeability could be verified. The NMR permeability estimation is dependent on the Free Fluid Index (FFI) cutoff, which excludes any irreducible water in the formation. Yet, the permeability index from the NMR requires an independent calibration reference. The empirical equations are applicable to the intergranular pore system only, hence usually restricted to sandstone with reservoirs at irreducible saturation (Timur, 1968). Nonetheless, the log-based permeability is certainly still valuable information in the absence of any reference from the two other approaches, but it requires some caution while using as the only source for the reservoir permeability. The well testing is one of the best estimations for the permeability of a reservoir. However, it is reflecting the permeability of a complete zone of interest, which does not reflect each of the reservoir facies productivity to be used in reservoir modeling. The key for better reservoir characterization is very well based on the core samples upon which the log analysis outputs are calibrated, leading to less uncertainty. Therefore, the core results are always more valid reference and essential in complicated reservoirs, from which the facies can be identified, and the permeability can be assessed quantitatively. As shaly reservoirs are typically heterogeneous in nature, they require in-depth reservoir characterization. Accordingly, an accurate reservoir facies model would lead to better permeability calculation through the reservoir.

In complicated reservoirs, there may be high and low permeability intervals with equal porosity values (Amaefule, 1993). In such case, it is not recommended to generate a simple permeability model from the core data using simple linear relationships, which cover the full interested interval. The basis of this assumption is that porosity alone is not enough to explain the permeability variations, as the porosity is independent of the grain size distribution (Al-Ajmi et al., 2000). The Hydraulic Flow Units (HFU) concept developed a clustering technique to identify the different facies in a reservoir rock (Amaefule et al., 1993). The HFU concept is considered as a criterion of the reservoir units in which fluid flow properties are uniform due to the same pore throat properties (Kadkhodaie-Ilkhchi et al., 2013). The Flow Zone Indicator (FZI) is a popular rock typing technique based on the capillary tube model and hence the RQI parameter (Soleymanzadeh et al., 2018). Regardless of how complex the reservoir is, it has shown very good results, particularly in complicated reservoirs, either carbonates or clastics. Further effectiveness of this technique is the possibility to extend the generated flow units in the uncored wells and hence the same facies definition developed from the cored interval.

In this paper, a new technique with a complete workflow has been described that drives a continuous log equivalent to the flow zone indicator, named EFZI. This log allows a calculated flow zone indicator that can be used to reflect reservoir quality over any logged interval, from which facies can be derived and hence permeability for each detected facies. A complete workflow has been developed to perform the analysis and applied to the shaly sand of the Lower Permian Irwin River Coal Measures Formation in Cliff Head Field (Mory and Iasky, 1996; Mory and Haig, 2011). The routine core analysis has been studied to evaluate the core-dependent facies. Four facies have been classified through core analysis and used as a calibration reference for the EFZI log. The core thin sections were used to validate the EFZI facies. This allowed more coherency between the independent study inputs and reduced the uncertainty in the methodology to the minimum possible level.

The EFZI was calculated through the integration of the following datasets:

- The Nuclear Magnetic Resonance free fluid index calculated from the T2-Distribution log
- The density porosity from the high-resolution density log
- Core permeability and core porosity from at least one cored well
- Hydraulic flow units based on core measurements

3.2. Data and Methodology

Three wells will be used to test the new equivalent flow zone indicator technique, one of which has a conventional core through the interested shaly sand, with a complete set of conventional logs (e.g.: GR, density, neutron, resistivity). The second well was logged by a nuclear magnetic resonance tool that covers the full formation thickness in addition to the simple conventional logs. The third well contains only conventional logs. The three

wells encountered the reservoir section with 8.5-inch borehole. The borehole fluid was water-based mud of salinity value ranges between 25 to 30 g/l Chloride and mud weight of 9 to 9.6 pound/gallon. A complete petrophysical interpretation was carried out for the three wells, with the porosity from the core routine measurements used to calibrate the log-based porosity and the calculated permeability. The cored well has been used as the key calibration for the EFZI technique upon which the classified facies and the permeability models analysed were distributed to the other wells effectively.

3.2.1. Routine Core Data Analysis – Hydraulic Flow Units Classification

The porosity and permeability core data were available in Well-3. With an overburden stress of 1360 psi applied to the core samples, the helium was allowed to expand into the samples' pore spaces to determine the pore volume. The permeability to air is determined by applying air pressure on the plug samples creating air through the plugs, then the pressure is increased to the same confining stress and the Klinkenberg permeability is calculated, which is used in the study (McPhee et al., 2015). The porosity-permeability plot, from routine core measurements over the interested shaly sand interval, shows permeability variation of a different order of magnitudes for the plugs that show the same porosity (**Figure 12**). For instance, the plugs that have porosity range between 15-20 p.u. show a permeability range between 1 – 457 mD, with a coefficient of variance up to 0.73. This indicates very high reservoir heterogeneity and complex facies variation. Traditional approaches for the estimation of permeability are based on simple linear regressions (Abbaszadeh et al., 1996).
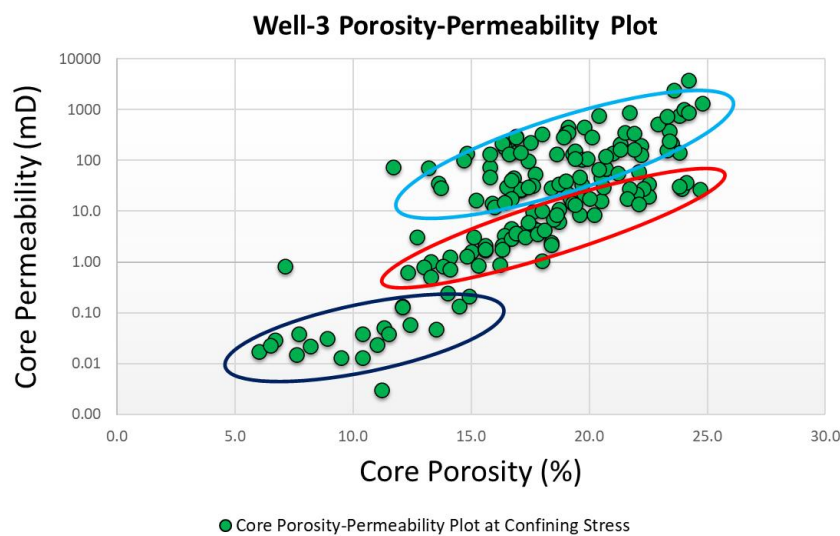
Figure 12: Core Porosity-Permeability plot. Visually, 3 separate trends can be roughly defined for this plot

Three different trends can be recognized instantly from the plot on a quick look basis; therefore, one simple permeability model that covers all facies will not cover the reservoir heterogeneity and will not result in comprehensive reservoir characterization. Guo et al., (2007) described the RQI/FZI as a more widely used

technique for facies evaluation in clastic reservoirs, through which the core samples of the same rock types will have similar FZI values. Add to this, the different theoretical and empirical correlations between porosity and permeability would require an independent source to calibrate the results, which were found to fail to return the proper permeabilities in complex rock textures (Ghadami et al., 2015).

Therefore, the data has been analysed using the Rock Quality Index or the Flow Zone Indicator approach. The reservoir facies are classified with the following equations:

$$RQI = 0.0314 * \sqrt{\left(\frac{K}{\varphi}\right)} \dots\dots\dots (38)$$

$$\varphi_z = \frac{\varphi}{1-\varphi} \dots\dots\dots (39)$$

FZI is defined as:

$$FZI = \frac{RQI}{\varphi_z} = \frac{0.0314 * \sqrt{k/\varphi}}{\frac{\varphi}{1-\varphi}} \dots\dots\dots (40)$$

where RQI is the Rock Quality Index; φ_z is the normalized porosity; FZI is the flow zone indicator; φ is the core porosity and k is core permeability. Four facies were identified for the shaly sand of the Irwin River Coal Measures Formation dependent on the flow zone indicator calculated from the core using equation 40. The facies shown in **Figure 13** are describing the reservoir complexity in Well-3, with each data aligned on the same trend reflecting one hydraulic flow unit (HFU-1 to HFU-4). On log-log plot of RQI versus φ_z, the samples with similar FZI value will lie on a straight line with a slope of 1, whereas the data of different FZI will lie on another parallel unit slope lines (Al-Ajmi et al., 2000), as per the following equation:

$$Log(RQI) = Log(\varphi_Z) + Log(FZI) \dots\dots\dots (41)$$

Accordingly, each of the samples that lie on the same line constitutes one hydraulic flow unit. The mean FZI is the intercept of the straight lines with $\varphi_z = 1$. **Table 2** shows the mean FZI value for each facies or hydraulic flow unit. The four hydraulic flow units are typically based on the variance of the frequency of the FZI calculated from the core data. The software used in the evaluation found four facies reflect the best classification for the number of rock types in this formation. In order to validate these results, the logarithmic value of the core flow zone indicator is shown in **Figure 14** on a cumulative frequency plot (Svirsky et al., 2004). Several distinct straight lines are formed on the plot, the number of the hydraulic flow unit in the reservoir is determined by the number of the straight lines on the cumulative frequency plot. At each intersection between two lines, a cutoff can be estimated between two different reservoir facies. The following cutoffs have been identified:

- Hydraulic Flow Unit-1, the poor rock type (HFU-1): Log (FZI) < (- 0.45)
- Hydraulic Flow Unit-2, (HFU-2): (- 0.45) < Log (FZI) < (0.13)

- Hydraulic Flow Unit-3, (HFU-3): (0.13) < Log (FZI) < (0.56)
- Hydraulic Flow Unit-4, the best rock type (HFU-4): Log (FZI) > (0.56)
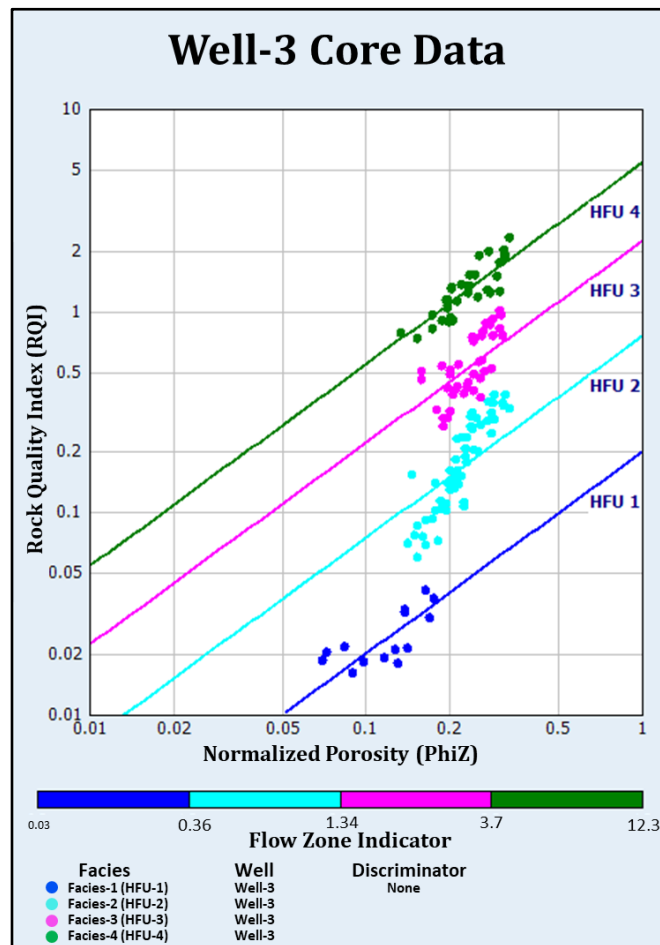
Figure 13: Log-Log plot for RQI versus Phiz
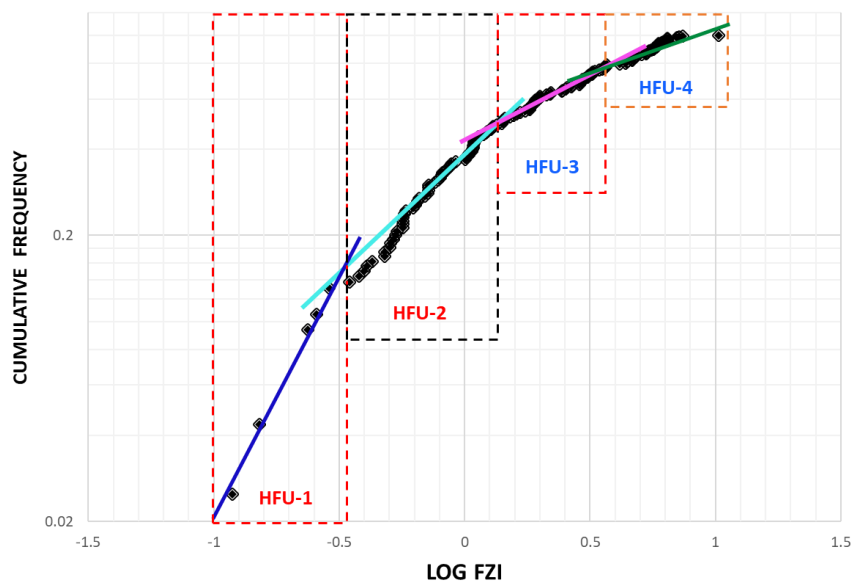
Figure 14: Cumulative frequency of the core flow zone indicator showing different hydraulic flow units; Distinct straight lines represent the number of the facies in the reservoir; Four facies have been determined (HFU-1 to HFU-4) in the Irwin River Coal Measures Formation from the core data

Table 2: *Mean Flow Zone Indicator for the Hydraulic Flow Units*

Hydraulic Flow Unit	Mean FZI
HFU-1	0.2
HFU-2	0.76
HFU-3	2.23
HFU-4	5.47

The flow zone indicator (FZI) is plotted on a histogram plot, **Figure 15**, to show which facies might be dominant compared to the others upon the above cutoff classification. The histogram indicates the number of the hydraulic flow units and the variance for the facies on the FZI distribution on semi-log scale. The red lines representing the boundaries between the facies (Hashim et al., 2017), each plotted using distinct colour matching the RQI-PhiZ plot.

From the histogram, HFU-2 and HFU-3 are showing similarity in the maximum points count while HFU-4 shows higher points count compared to the other two. However, the data density in the best facies (HFU-4) is less compared to the HFU-2 and 3, which indicates the reservoir has large variations in the rock quality, with a higher volume of low-quality sands. In the Irwin River Coal Measures Formation, those hydraulic flow units are reflecting different facies; Facies-1 is the lowest quality rock, mainly shale layers, Facies-2 represents the highly argillaceous sand to siltstone, Facies-3 represents the medium quality shaly sand and Facies-4 is the high-quality shaly sand with the best permeability.

Using the mean FZI values tabulated in Table-2, the following equation will yield a permeability log that describes each hydraulic unit quantitatively (Sokhal, 2016 and Mirzaei-Paiaman et al., 2018):

$$K = 1014 \, FZI^2 * \frac{\varphi_e^3}{(1 - \varphi_e)^2} \dots \dots \dots (42)$$

The porosity-permeability plot, **Figure 16**, shows the models created through the Flow Zone Indicator approach. It is clear that the porosity range of 15-23 p.u. dominates the dataset, with the permeability for the same porosity range varies several order of magnitudes. Applying one simple linear porosity-permeability model, in this case, will possibly underestimate the permeability for the good quality reservoir facies and will overestimate the same for other facies. In other words, the model ignores the scatter of the data around the fitted line and attributed any scatter to the measurement errors (Desouky, 2003).
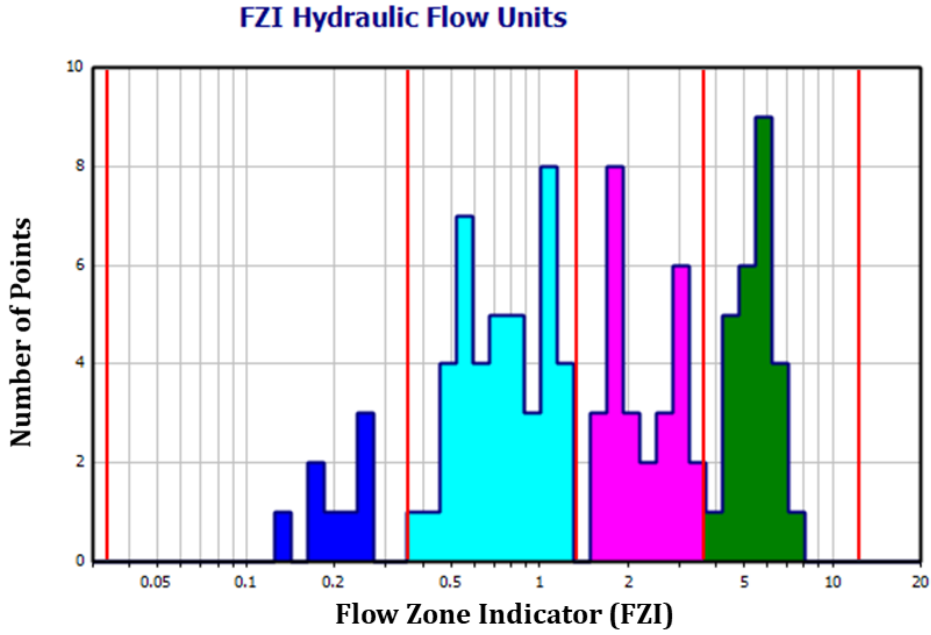
Figure 15: Facies classification based on the core Flow Zone Indicator histogram; The four classified facies from left to right are HFU-1 to HFU-4
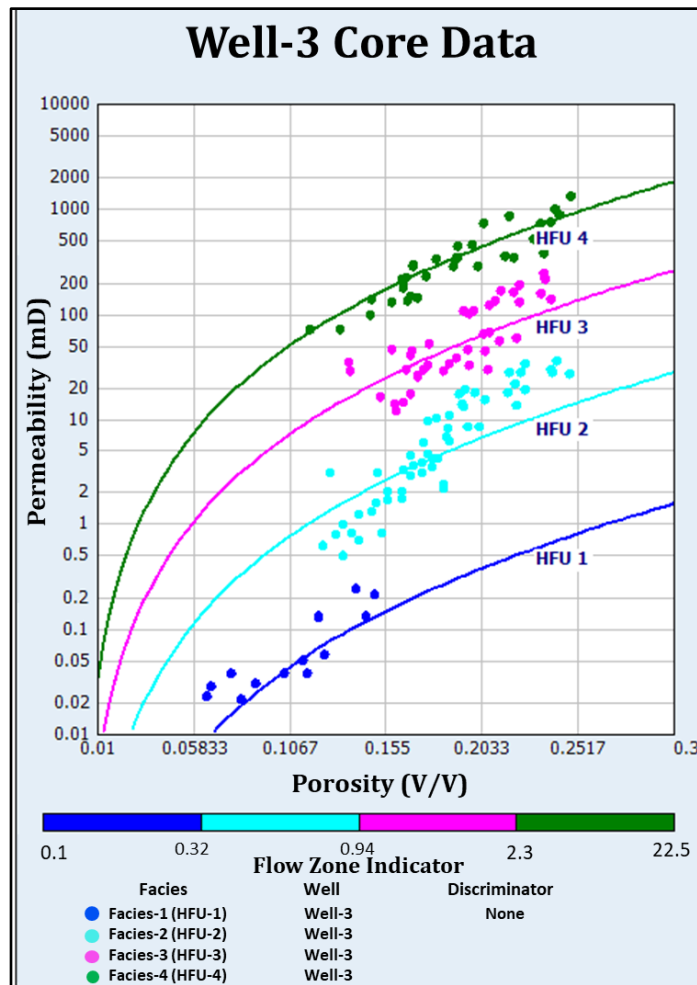
Figure 16: Core Porosity-Permeability plot showing the four HFUs classified from the core data

3.3. Workflow Used in the Analysis

The workflow used to derive the facies and reservoir permeability profile in the wells can be described in the steps shown in **Figure 17**, which will be explained in detail. Three main steps are shown; the core data analysis, the petrophysical analysis and the NMR interpretation, then finally the generation of the electrofacies using the EFZI technique followed by the permeability calculation. The EFZI log generated will reflect the reservoir quality in a very similar way to the FZI calculated from the routine core measurements. As the FZI technique is very effective in clastic reservoirs (Guo et al., 2007), the equivalent log will confidently reflect the lithological variations based on log data.
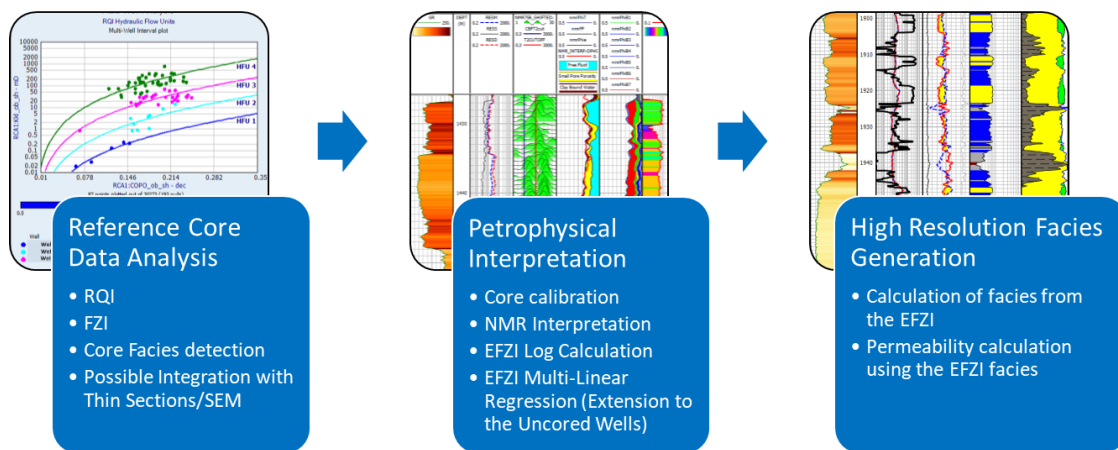
Figure 17: *Workflow of the EFZI technique for facies definition in complicated reservoirs*

3.3.1. NMR Integration – The Equivalent Flow Zone Indicator

The NMR data has been interpreted in Well-2, which covers the shaly sand interval. The T2-Distribution has been used in IP Software as a main input for the NMR interpretation. The T2-Distribution log has shown some variation across the sand units, with clear variance in the pore size distribution throughout the reservoir. **Figure 18** presents the NMR log in Well-2, with the triple combo logs and the petrophysical analysis. In track-6, the T2-Distrution log is presented in the usual waveform format, while in track-7 the same log is presented in image format. From the log in both NMR tracks, it is clear that the signature has changed with variance in the pore size where the signal shows the distinct bi-modal distribution between 1435 – 1444 mMD.

The NMR interpretation has been carried out as one main step in the workflow using the standard T2 cutoff values (3 ms for clay and 33 ms for free fluid cutoffs). The cutoffs were used for partitioning the total NMR porosity into clay bound water, capillary bound water and free fluid volumes. Through the NMR interpretation, the Bound Fluid (BF) and the Free Fluid (FF) are calculated from the following equations:

$$FF = Sum\ of\ all\ porosity\ bins\ above\ the\ T2\ Cutoff \dots\dots\dots(43)$$

$$BF = nmrPhi - Free\ Fluid \dots \dots \dots (44)$$

The NMR porosity bins were partitioned based on 10 partial porosities (1, 2, 4, 8, 16, 33, 100, 300, 1000, 3000 ms). The Timur Coates permeability equation is used to calculate the permeability index in mD (Coates et al., 1999) as per the following equation:

$$k = a * \left(\frac{FF}{BF}\right)^b * nmrPhi^c \dots \dots \dots (45)$$

where the FF is the free fluid index, the BF is the bound fluid volume, the nmrPhi is the total porosity from the NMR. The standard values for (a, b and C) parameters were used (10000, 2 and 4) respectively.
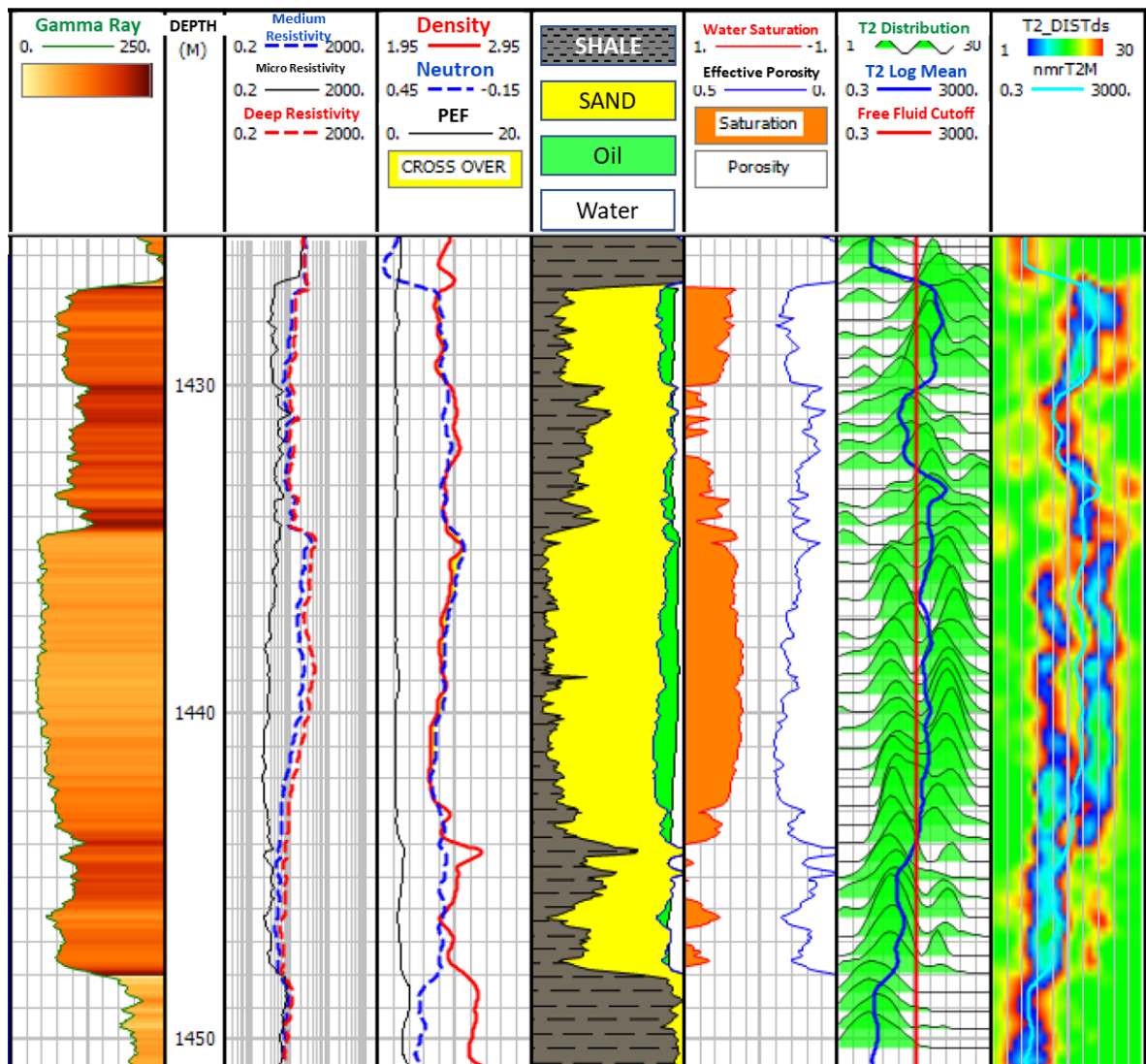
Figure 18: *The NMR log in with the petrophysical interpretation of Well-2; Track-1: GR log; Track-2: Resistivity; Track-3: Porosity logs; Track-4: Rock volume; Track-5: Porosity and water saturation logs; Track-6: NMR T2-Distribution; Track-7: T2-Distribution plotted in image format*

The free fluid index calculated has been used together with the density porosity to calculate a new facies-log. As the reservoir is shaly sand, the increase of the volume of the free fluids would directly indicate better flow with better rock quality, hence a

higher reservoir flow index over the thickness of the formation. The reservoir flow index calculated from the NMR and the density is named the "Equivalent Flow Zone Indicator" (EFZI). In order to calibrate the EFZI, the log will be compared to the FZI obtained from the core data in Well-3. The density porosity has been calculated as per the following equation:

$$DPHI = \frac{\rho_{ma} - \rho_b}{\rho_{ma} - \rho_{fl}} \dots \dots \dots (46)$$

The density porosity then was used as an input for the EFZI log calculated as follows:

$$EFZI = \frac{nmrFFI}{DPHI} \dots \dots \dots (47)$$

$where$:

$DPHI$: Density porosity

ρ_{ma}: Matrix density

ρ_b: Bulk density

ρ_{fl}: Fluid density

$nmrFFI$: NMR interpreted free fluid volume index

In the Irwin River Coal Measures Formation, the shale is proven to be dispersed in rock pore systems as will be discussed in the next section. Therefore, the EFZI log has been correlated directly to the core Flow Zone Indicator. Should the ratio between the free fluid to the total porosity increases, a larger pore space and better permeability would be expected, hence better reservoir facies.

The NMR interpretation is presented in tracks 4 to 7 in **Figure 19**. The permeability index from the NMR is plotted in track-4 and the fluid typing in track-5; (The free fluid index in blue, small pore porosity in yellow and the clay bound water in brown). The red curve is the density porosity where it shows a comparable porosity to the NMR total porosity. Track-6 shows the NMR porosity bins as per the time domains mentioned. Track-7 shows the Equivalent Flow Zone Indicator (EFZI) that is established over the entire shaly sand interval. In order to validate the EFZI trend, the log has been extended to Well-3 where there is full routine core analysis, where the flow zone indicator was calculated based on actual measurements.

The EFZI log calculated in Well-2 has been used as an input in the statistical Multi-Linear-Regression module in IP software. With the use of the normal conventional logs, the EFZI curve has been extended to the wells (3 & 4) that have no nuclear magnetic resonance data. Multiple logs were tested (e.g.: GR, sonic, density, resistivity), from

which the density, the neutron, the compressional slowness and the photoelectric factor have given the best results through the following equation:

$$EFZI = 10^{[a-(b*RHOB)-(c*NPHI)-(d*PEF)-(x*DTCO)]} \ldots \ldots \ldots (48)$$

where a = 6.44, b = 1.93, c = 4.03, d = 0.35 and x = 0.01
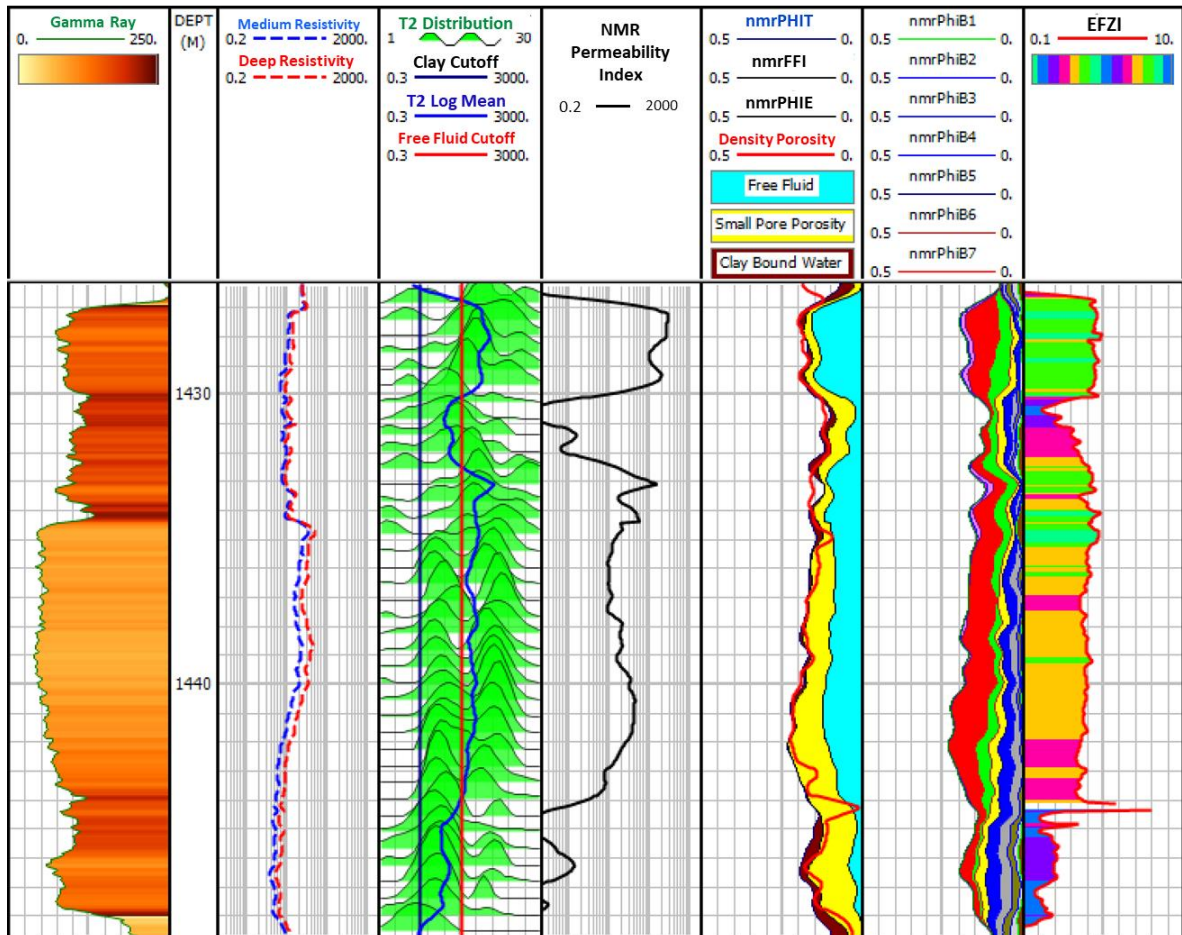
Figure 19: *The NMR interpretation for Well-2; Track-1: GR log; Track-2: Resistivity; Track-3: T2-Distribution with the clay and free fluid cutoffs; Track-4: NMR permeability index; Track-5: NMR porosity partitioned to fluid volumes, free fluid in blue, capillary bound water in yellow and clay bound water in brown; Trck-6: NMR bins porosity; Track-7: The equivalent Flow Zone Indicator (EFZI) from NMR and Density logs*

Figure 20 shows the petrophysical analysis for Well-3 in tracks 4 and 5, with the log porosity calibrated to the core porosity. The parameters used in analysing Well-3 were used for the other two wells as they are calibrated to the core measurements. The predicted EFZI log is presented in track-6 showing a very similar trend to the core-FZI. The EFZI log will be used as an independent indicator to predict high-resolution facies and permeability across the full Irwin River Coal Measures Formation. The core permeability data and the thin sections in this well will be used to calibrate and test the outputs.
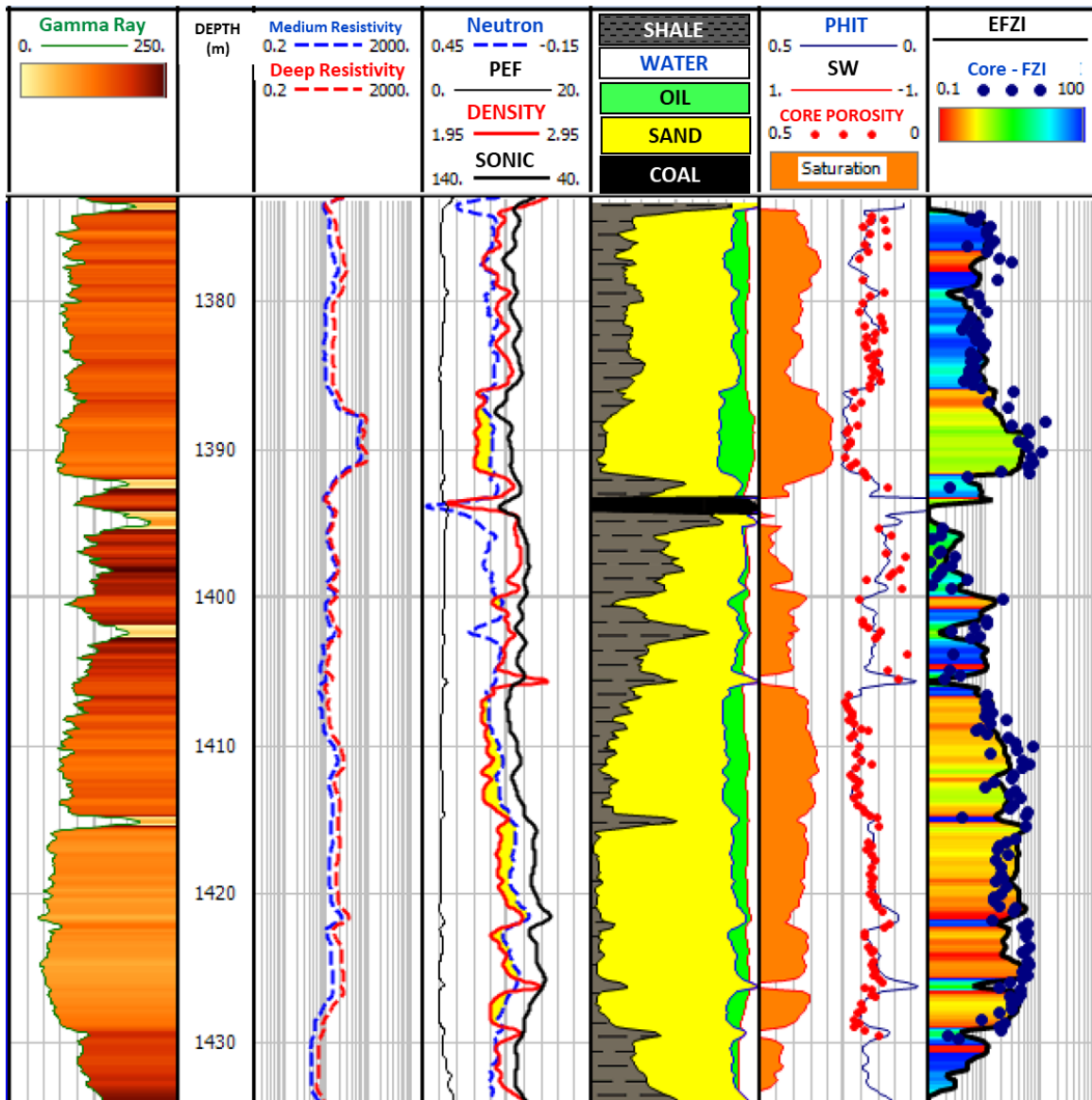
Figure 20: Well-3 log interpretation with the log porosity calibrated to core porosity; Track-1: GR log; Track-2: Resistivity; Track-3: Porosity logs; Track-4; Rock volume; Track-5: porosity and water saturation logs, the log porosity is matched to core porosity; Track-6: The Equivalent Flow Zone Indicator (EFZI) from NMR and Density logs matched to the FZI calculated from the routine core measurements

Well-4 has only the necessary dataset with no core and no advanced logs. The well was logged with conventional Logging While Drilling tools (e.g.: GR, Resistivity, Density and Neutron). The reservoir in this well consists of several sand layers of good hydrocarbon potential interbedded with highly argillaceous sand thin beds and lower quality shaly sand. The sand succession in this well is considered with high heterogeneity to test the validity of the predicted EFZI log. **Figure 21** shows the petrophysical analysis of Well-4 in tracks 4 and 5, and the predicted EFZI log in track 6. The results of the three wells are presented in the next section.
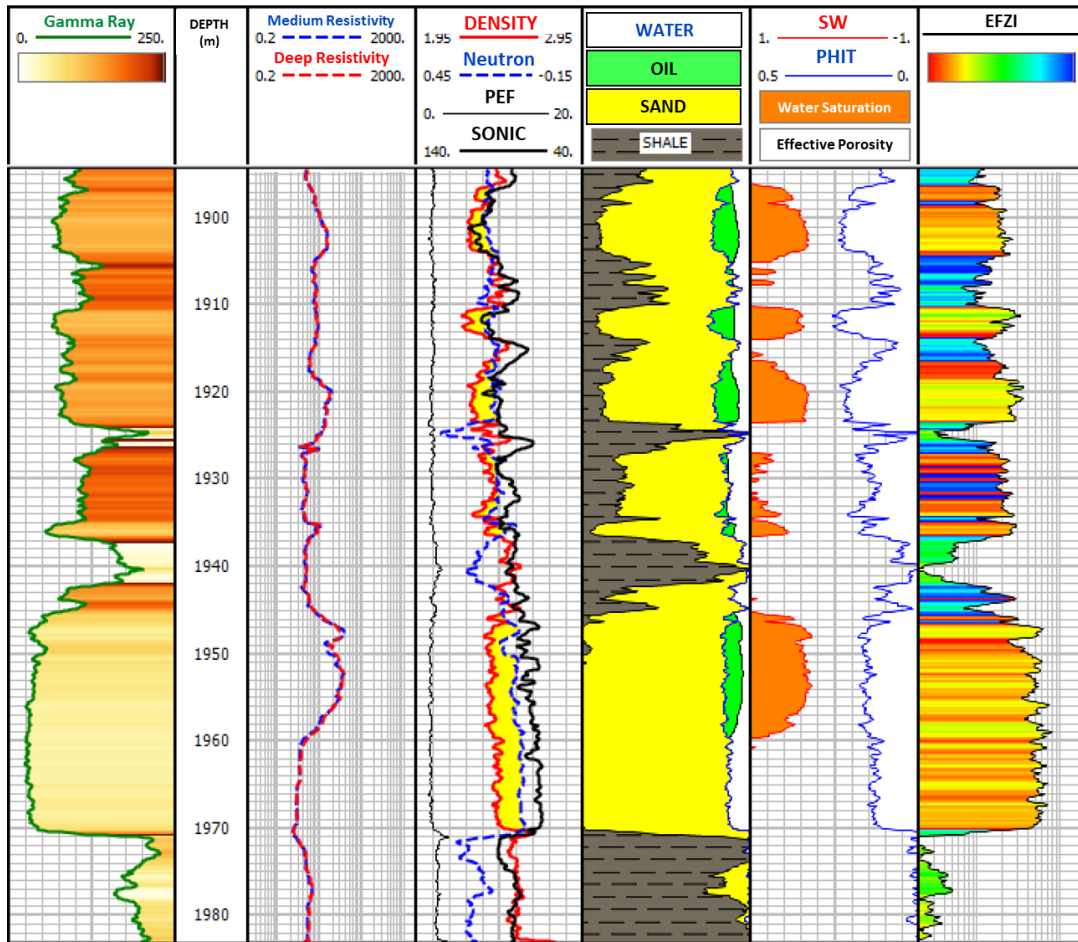
Figure 21: *Well-4 log interpretation; Track-1: GR log; Track-2: Resistivity; Track-3: Porosity logs; Track-4; Rock volume; Track-5: porosity and water saturation logs; Track-6: The Equivalent Flow Zone Indicator (EFZI) from NMR and Density logs*

3.4. Facies Analysis and Permeability Calculation Results

The core has given four different hydraulic flow units in the shaly sand of the Irwin River Coal Measures Formation. These four models were the base to test and predict the facies using the EFZI approach. Rearranging equation-42 to solve for the permeability of each facies yields the following power equation models based on the core data from Well-3:

$$HFU - 1: Perm = Phi^3 * \left(0.203/(0.0314 * (1 - Phi)\right)^2 \dots \dots \dots (49)$$

$$HFU - 2: Perm = Phi^3 * \left(0.761/(0.0314 * (1 - Phi)\right)^2 \dots \dots \dots (50)$$

$$HFU - 3: Perm = Phi^3 * \left(2.248/(0.0314 * (1 - Phi)\right)^2 \dots \dots \dots (51)$$

$$HFU - 4: Perm = Phi^3 * \left(5.5/(0.0314 * (1 - Phi)\right)^2 \dots \dots \dots (52)$$

The EFZI log has been used independently to predict facies across the interested shaly sand zone, and further extended in the lower clean zone in wells 2 and 4. The EFZI has been classified independently into four flow units as per **Figure 22**. Four distinct straight lines reflect the number of the hydraulic flow units on the cumulative frequency plot, from which four groups are distinguished, representing four different facies. The intersections between the lines represent the cutoffs to be used for the facies classification. The identified values are as follows:

HFU-1: Log (EFZI) < (- 0.8)

HFU-2: (- 0.8) < Log (EFZI) < (- 0.34)

HFU-3: (-0.34) < Log (EFZI) < (- 0.18)

HFU-4: Log (EFZI) > (- 0.18)
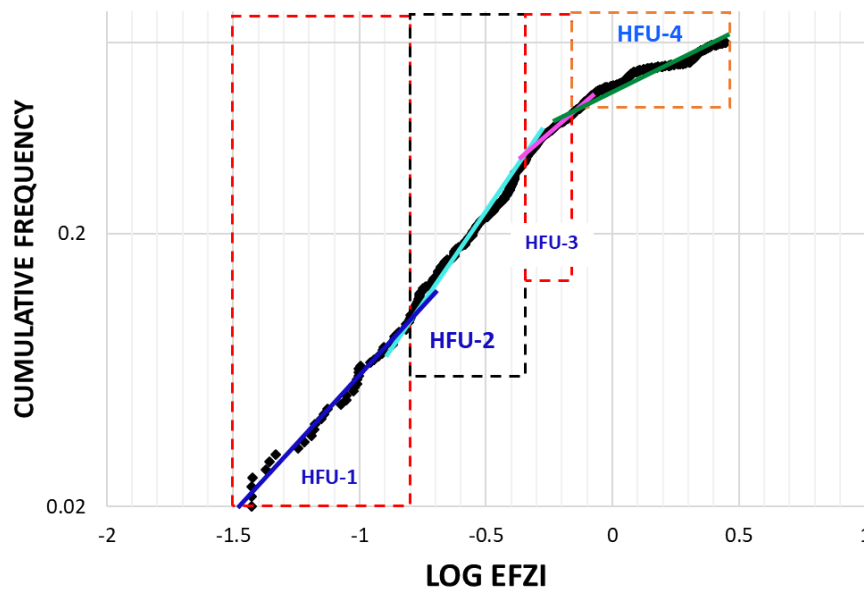
Figure 22: *Cumulative density plot for the EFZI log to obtain the optimum number of flow units; Four facies represented by distinct straight lines in the Irwin River Coal Measures Formation (HFU-1 to HFU-4)*

The EFZI logs in each well have been used to distribute the facies as per **Figure 23**. Four typical types of facies were established in the other two wells. The facies then has been turned into the high-resolution facies log dependent the EFZI. The facies logs are plotted on the correlation panel in track-5 in all the wells.

The top part of Figure 23 shows the EFZI histogram for the three wells, with facies classified into four flow units. The first facies is mainly shale, the second facies is the fine grained highly argillaceous sands to siltstone with a large amount of clay volume, which directly affected the reservoir quality and heavily reduced the permeability. The third facies represents the medium quality facies of fine to medium grain shaly sand, while the fourth is the best shaly sand that consists mainly of coarse grain size. The lower part of Figure 23 shows a correlation panel for the three wells with the GR log presented in the first track, track-2 shows the EFZI-based permeability in black. The red dots in Well-3 represent the core permeability to which the models were calibrated. The core

measurements are in good match with the modeled permeability. The porosity logs in track-3, the new EFZI facies in track-4 and the EFZI log in track-5. The EFZI dependent facies classification was extended to thick intervals of less shale content within the same reservoir in wells 2 and 4. In this case, Irwin River Coal Measures Formation has a deeper clean sand member for which the facies was estimated based on the EFZI technique. In case the NMR log has covered formations of very different characteristics, the same technique can be applied with different multi-linear regression correlations for each reservoir separately.
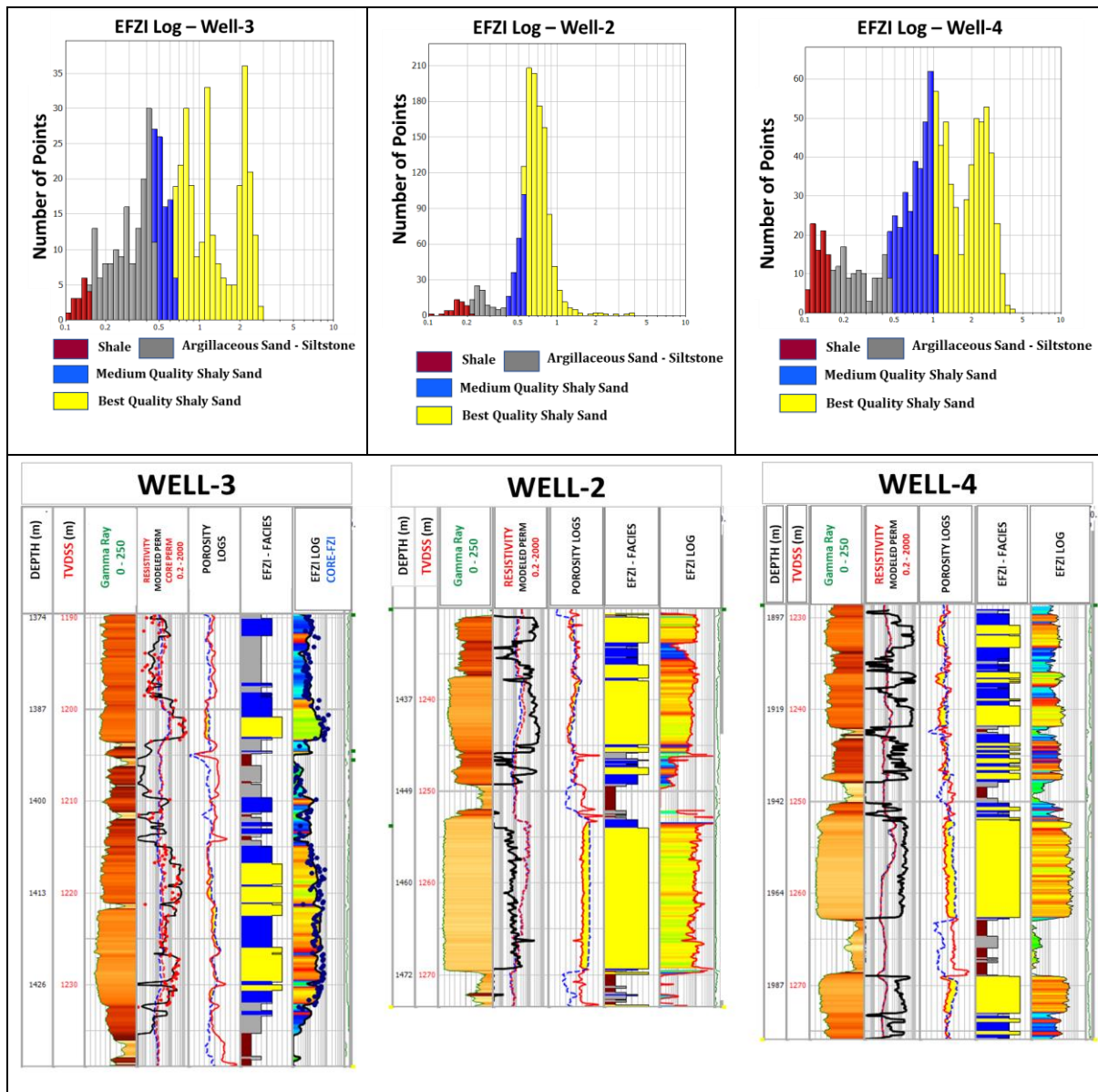
Figure 23: *The final results of the EFZI high-resolution facies and EFZI-permeability prediction; The top part showing the histograms for the EFZI facies classification; The lower section shows well stratigraphic correlation for the three studied wells; Track-1: GR log; Track-2: Resistivity and permeability in bold black, Well-3 shows EFZI-based permeability log matched to core permeability in red dots; Track-3: Porosity logs; Track-4; EFZI high-resolution facies; Track-5: The Equivalent Flow Zone Indicator (EFZI) from NMR and Density logs, In well-3 the EFZI log is plotted with the core calculated FZI*

3.5. Thin Section and Integration for Rock Types Calibration

The cored interval covered the complete sand package in Well-3. Some thin sections were analysed to quantitatively assess the generated HFUs from the EFZI analysis. In this section, we describe the thin section for the above created facies and how each flow unit is uniquely correlated to a unique rock type.

Facies-1, HFU-1, is the shaly part of the Irwin River Coal Measures Formation. The permeability for this facies has a maximum of 0.2 mD and has not been covered by any thin sections. This is reflected by the brown facies on the correlation panel.

Facies-2, HFU-2, is the fine grained argillaceous sand to siltstone that has the intergranular pore spaces filled up to 70-80% with authigenic clays, particularly Kaolinite. **Figure 24** shows the depths 1381.84 m and 1391.86 m, with porosity values of 13.3 and 18.4 porosity units respectively, where the kaolinite (K) filled almost all the pore system (dispersed clay) leaving very little interconnected porosity. The core permeability for the first sample is 1.07 mD at ambient conditions and 0.5 mD at the reservoir confining stress, while the second sample permeability is 4.5 mD and 2.5 mD for the ambient and effective stress respectively. This has indicated how tight this shaly sand is due to the clays that fill in the effective pore system, classified as dispersed shale. This facies is presented in dark grey in the correlation panel. Some other minerals exist in the samples including Potassium Feldspars (KF), Garnet (Ga), metamorphic rock fragments (MRF) and some Illite (I). Primary and secondary porosities were also identified in the thin sections, (PP and SP respectively).

Facies-3, HFU-3, is a moderate-quality sand compared to HFU-2, with more porosity introduced to the system. The rock consists of fine grained sandstone with the pore system greatly reduced by the quartz overgrowth (QO) cementation and authigenic dispersed kaolin (K). **Figure 25** shows two thin sections; The sample at 1418.17 m (porosity: 17.1 porosity units) has core permeability at ambient conditions of 36.4 mD and at an overburden of 26.8 mD. For the sample at 1420.77 m (porosity: 15.2 porosity units), the permeability is 25.9 and 16.3 mD for the ambient conditions and effective stress respectively. Some secondary porosity (SP) exists with illitic clays (I), micaceous rock fragments (MRF) and garnet (Ga) as an accessory mineral. This facies is presented in blue colour on the correlation panel.

Facies-4, HFU-4, is presented in yellow colour on the correlation panel, represents the best quality shaly sand in the Irwin River Coal Measures Formation. This rock type consists of coarse grained subarkose sandstone with modest primary intergranular porosity. The porosity reduction is due to the dispersed authigenic kaolin (K) and quartz overgrowth (QO) cementation. The permeability of the samples shown in **Figure 26** is 1005 mD for the sample at 1390.84 m and 174 mD for the sample at 1415.46 m at ambient conditions. At overburden, the values are 864 mD and 140 mD for the same. The porosity for the two samples are 21.7 and 14.8 porosity units respectively.
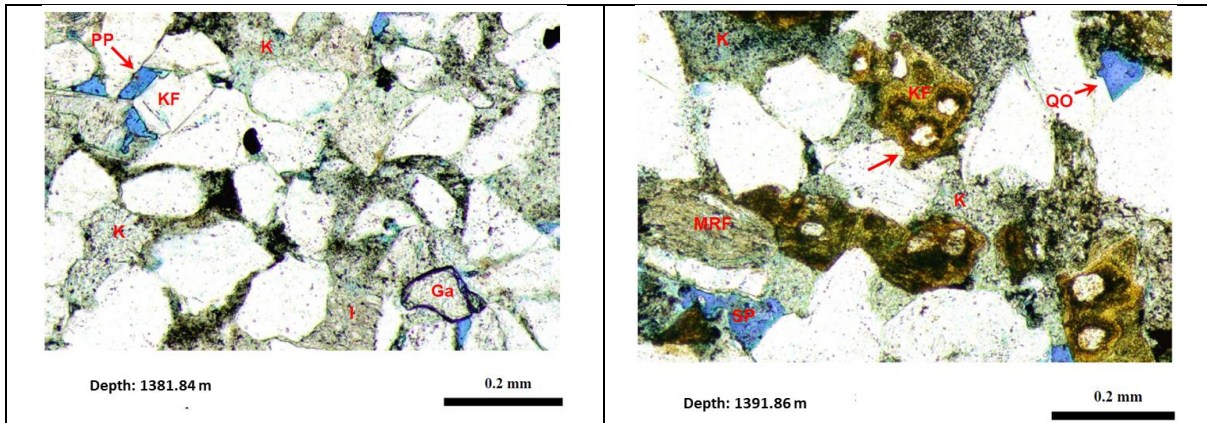
Figure 24: Facies-2, HFU-2, Primary macropores (PP) and little secondary porosity (SP) are poorly interconnected with the authigenic kaoline (K) filling most of the pores, other micaceous rock fragments (MRF) are present in addition to garnet (Ga), illite (I), potassium feldspars (KF) and minor quartz overgrowth (QO), (After Roc Oil, 2005)
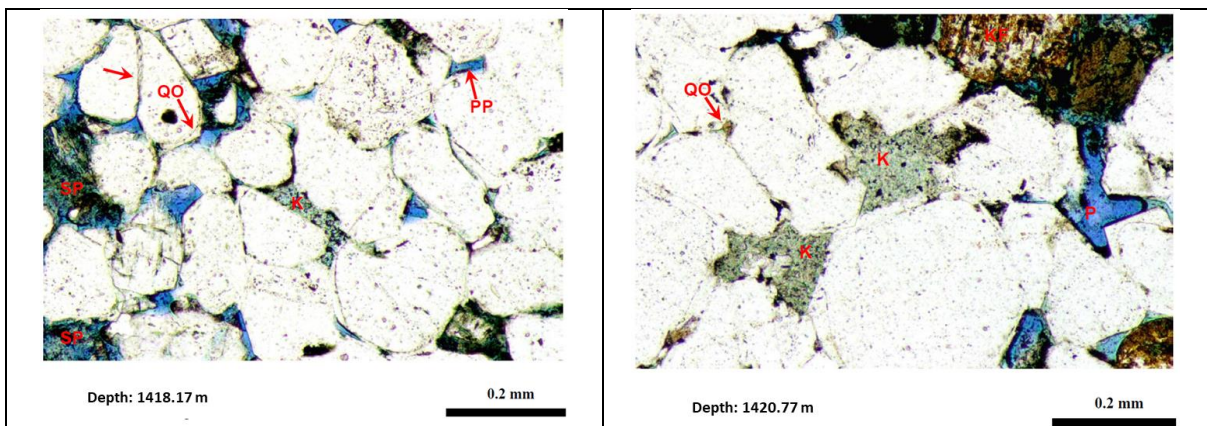
Figure 25: Facies-3, HFU-3, the porosity is greatly reduced by quartz overgrowth (QO) and authigenic kaoline (K). Primary porosity (PP) and macropores (P) can be identified with some secondary porosity (SP), (After Roc Oil, 2005)
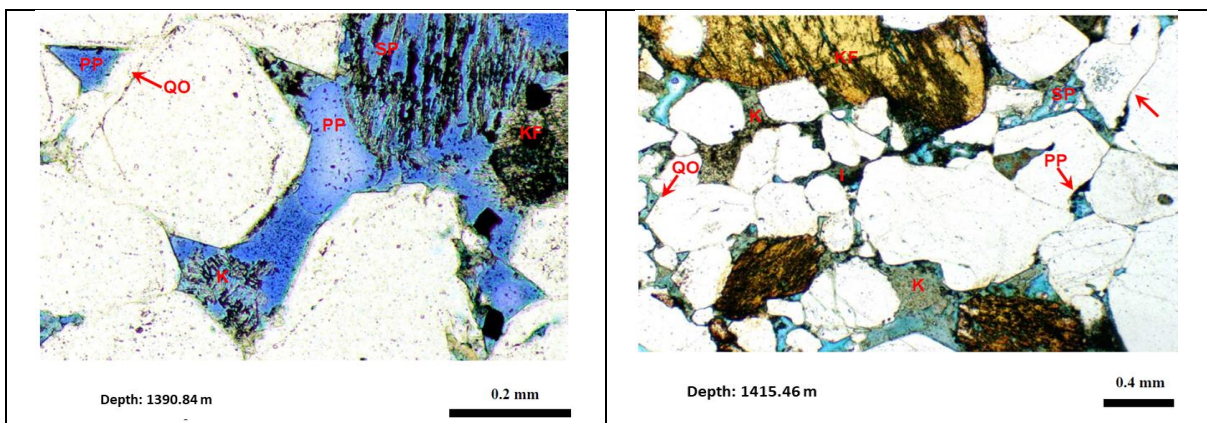
Figure 26: Facies-4, HFU-4, The best facies with the best reservoir quality with some local kaoline (K); Primary porosity (PP); secondary porosity (SP); Quartz overgrowth (QO), potassium feldspars (KF), (After Roc Oil, 2005)

It is clear how the permeability changes between the three facies, (HFU-2 to HFU-4), with the main factor being the amount of Kaolin in the pore spaces. The quartz overgrowth is considered another major factor as well, yet it is largely affecting the lower clean sand section of the Irwin River Coal Measures Formation due to the excessive decrease in porosity (<7 p.u.) in Well-2. The petrophysical parameters from the integrated interpretation are tabulated in **Table 3**, from which the variance between the rock types

is clear for the permeability. Facies-2 shows a range between 1.4 to 3.7 mD, facies-3 ranges from 16 to 62 mD., while facies-4 ranges from 206 to 519 mD. This matches the range for the thin section plugs very well.

Table 3: Petrophysical parameters table for the studied wells

Wells	Total Thickness TVD Meters	Net Pay Meters	Net Sand Meters	Average Porosity V/V			Average Oil Saturation V/V			Average Permeability mD		
				HFU-2	HFU-3	HFU-4	HFU-2	HFU-3	HFU-4	HFU-2	HFU-3	HFU-4
Well-2	22.00	11.00	13.60	0.12	0.12	0.16	0.05	0.50	0.62	1.4	16	206
Well-3	49.50	32.50	38.50	0.16	0.18	0.19	0.51	0.57	0.66	3.7	53	392
Well-4	22.00	8.00	15.00	0.16	0.20	0.22	0	0.47	0.61	3.5	62	519

The facies results from the EFZI are plotted on the density-neutron crossplot for the three wells in **Figure 27**. The shaly sand trend is very clear from the dataset starting with the best rock type points lie on the sandstone line in yellow, moving to the more shaly sands in blue, highly argillaceous sand in green and shale in brown colour.

With these results, it is believed the EFZI could be used in heterogenous sandstone reservoirs of complicated facies. The NMR free fluid index can be used to predict a flow zone indicator log with a direct approach. The resulted EFZI log is a high-resolution facies indicator in the absence of the core data. This workflow represents a new independent technique that can be utilized as a comprehensive answer for predicting very challenging parameters with or without the core availability, yet would be a very useful approach in legacy data, analogues and offset wells.
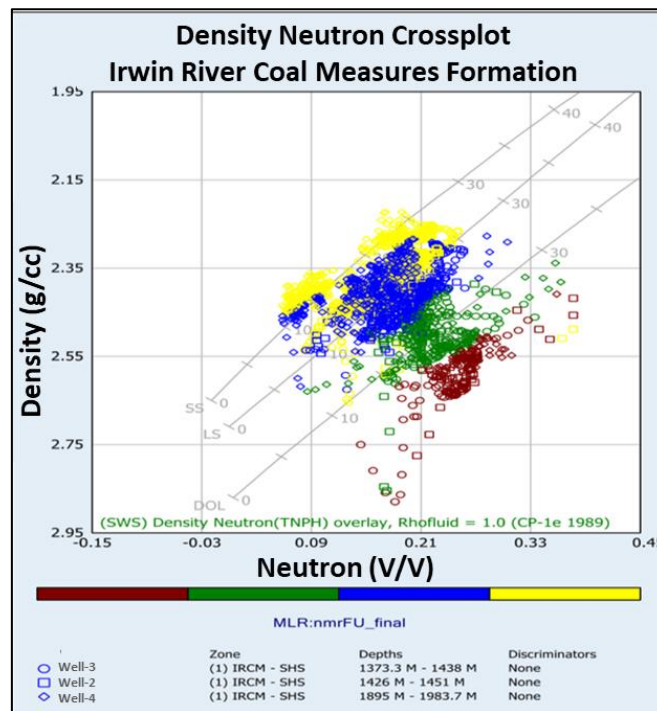
Figure 27: Density-Neutron crossplot showing the EFZI facies

3.6. Conclusion

Three wells have been used to study and test a new technique for facies prediction in the sands of the Irwin River Coal Measures Formation of the Lower Permian age in Perth Basin. The nuclear magnetic resonance log has been integrated with the density porosity to predict a direct flow zone indicator log that covers the full zone of interest. The Equivalent Flow Zone Indicator (EFZI) was created and extended to two other wells in this study using Multi-Linear Regression statistical technique. The EFZI log created showed very effective prediction for high resolution facies and permeability logs, which were calibrated to the available core measurements and rock thin sections. The predicted high-resolution facies through the EFZI were used to calculate the reservoir permeability using the four models estimated from the core porosity-permeability plot. A quantitative assessment for the classified facies dependent on the EFZI was carried out using core thin sections with four unique rock types identified, which matched the EFZI results. The modeled permeability results have shown a very good match with the core permeability. The EFZI technique can help to calculate very valuable challenging reservoir parameters in existing offset wells or analogues and can be used on legacy data.

Chapter-4: Log-Dependent Modeling

This chapter discusses a published conference paper in The Australasian Exploration Geoscience Conference held in Perth, 2019.

Elkhateeb A., Rezaee R., and Kadkhodaie A., 2019, Log Dependent Approach to Predict Reservoir Facies and Permeability in a Complicated Shaly Sand Reservoir, Presented in the Australasian Exploration Geoscience Conference, 2019:1, 1-5, https://doi.org/10.1080/22020586.2019.12072924

4.1. Introduction

In complicated reservoirs, there may be high and low permeability intervals with equal porosity values (Amaefule et al., 1993). In such a case, it is not recommended to establish a simple permeability model from the core data using a simple linear relationship. The basis of this assumption is that porosity alone is not enough to explain the permeability variations, as the porosity is independent of the grain size distribution (Al-Ajmi et al., 2000). Hydraulic Flow Units (HFU) concept developed a clustering technique to identify the different facies in a reservoir rock (Amaefule et al., 1993). The Hydraulic Flow Units are considered as a criterion of the various reservoir units in which fluid flow properties is uniform due to the same pore throat properties (Kadkhodaie-Ilkhchi et al., 2013). Further effectiveness of this technique is the possibility to extend the generated flow units to the uncored wells, as well as the same facies definition developed from the cored intervals. The flow zone indicator (FZI), driven from the rock quality index (RQI), is used to describe the facies of the reservoir in detail. Regardless of how complex the reservoir is, the FZI technique has shown very good results, particularly in complicated formations, either carbonates or clastics.

In this paper, a new technique is described that drives a continuous log equivalent to the flow zone indicator estimated from the core measurements. This log allows a continuous FZI log that can be used to derive facies over any logged interval, and hence permeability for each detected facies. The methodology is applied to the shaly sand of the Lower Permian Irwin River Coal Measures Formation (Mory and Haig, 2011) in the Perth Basin. Two wells with a comprehensive suite of conventional and advanced logs were used in this evaluation, one of which contains full routine core analysis. The application of this technique, including the validation of the results, was done through the integration of the following datasets:

- The Nuclear Magnetic Resonance free fluid index calculated from the T2-Distribution log
- The density porosity from the high-resolution density log
- The repeat formation tester mobility
- Core permeability and core porosity from the cored well

Four electrofacies models have been classified within the interested shaly sand interval. In addition to a detailed facies modeling obtained through the analysis, the permeability

has been quantitatively calculated and calibrated to the mobility from the repeat formation tester tool. To test the validity of the defined facies, the core thin sections have been used to ensure the electrofacies match the lithofacies. Both facies and permeability logs show very good resolution honouring the core data. Hence, this method represents a log dependent approach for reservoir characterisation.

4.2. Methodology

Two wells are used in this evaluation, Well-2 includes a conventional set of logs (e.g.; GR, resistivity, density, neutron, sonic) and NMR log, while Well-3 was cored through the reservoir section and logged with conventional tools only. The workflow starts with the NMR interpretation using the T2-Distribution log. With a typical T2-Cutoff values for clastic reservoirs, the pore volume was partitioned into clay bound water, capillary bound water and free fluid volumes. Ten porosity bins were computed from the 30 vector element T2-Distribution. As part of the workflow, a simple calculation for the total porosity using the density log is done through the following equation:

$$DPHI = \frac{\rho_{ma} - \rho_b}{\rho_{ma} - \rho_{fl}} \dots \dots \dots (53)$$

where DPHI: Density porosity; ρ_{ma}: Matrix density; ρ_b: Bulk density; and ρ_{fl}: Fluid density.

Figure 28 shows the NMR interpretation in Well-2. Track-1 presents the GR log; Track-2 shows the resistivity from which the hydrocarbon volume will be calculated. The T2-Distribution is presented in track-3; The porosity is partitioned into clay bound water, capillary bound water, free water and hydrocarbon volumes in track-4, with the density porosity matches the total NMR porosity; Track-5 shows the bin porosities. There is no free water indication from the NMR interpretation, accordingly, all the possible water in the rock is at irreducible state.

The density porosity and the NMR free fluid, including free water and hydrocarbon, are used to generate a reservoir index, equal to EFZI (Elkhateeb et al., 2019) presented in Chapter-3, as per the following equation:

$$R_{Index} = EFZI = \frac{nmrFFI}{DPHI} \dots \dots \dots (54)$$

Where R_{Index} is the reservoir index; $nmrFFI$ is the free fluid volume; and the $DPHI$ is the density porosity. Should the ratio of the free fluid index to the total porosity increase, a larger pore size, hence better permeability and reservoir facies, is expected. Nevertheless, caution needs to be taken in case this is applied to a gas reservoir, as the free fluid or NMR porosity will be suppressed with the gas low hydrogen index.
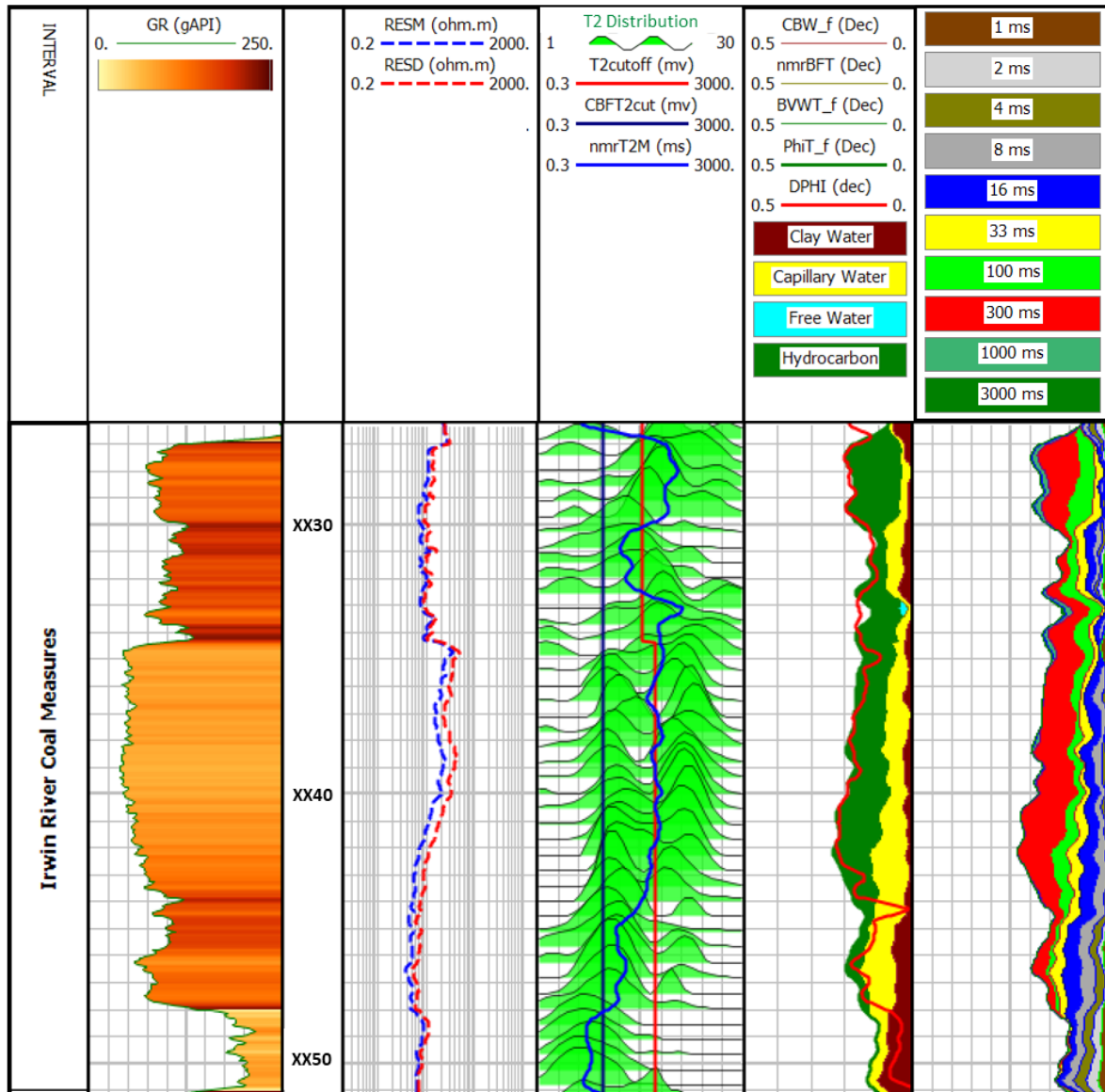
Figure 28: NMR interpretation for Well-2 in the Irwin River Coal Measures Formation

Figure 29 shows the porosity logs in track-3; fluid volumes from the NMR in tarck-4; Reservoir Index in track-5; the porosity and water saturation from the petrophysical interpretation in track-6 and the rock volume in track-7.

Well-3 was cored across the Irwin River Coal Measures Formation for which the core porosity and permeability results are available. Within the shaly sand, the porosity in the good quality reservoir ranges between 15 to 20 p.u. However, the permeability range is between 1 mD to 1 Darcy indicating high reservoir heterogeneity for the same porosity range. Therefore, an advanced statistical approach is necessary to distinguish between the different facies in the porous sand. The Rock Quality Index (RQI), or the Flow Zone Indicator (FZI), is a very effective approach to analyse the electrofacies, which is applied to Well-3 core data. Following equations 38 to 40, the RQI is calculated to generate the FZI for each of the plug samples.
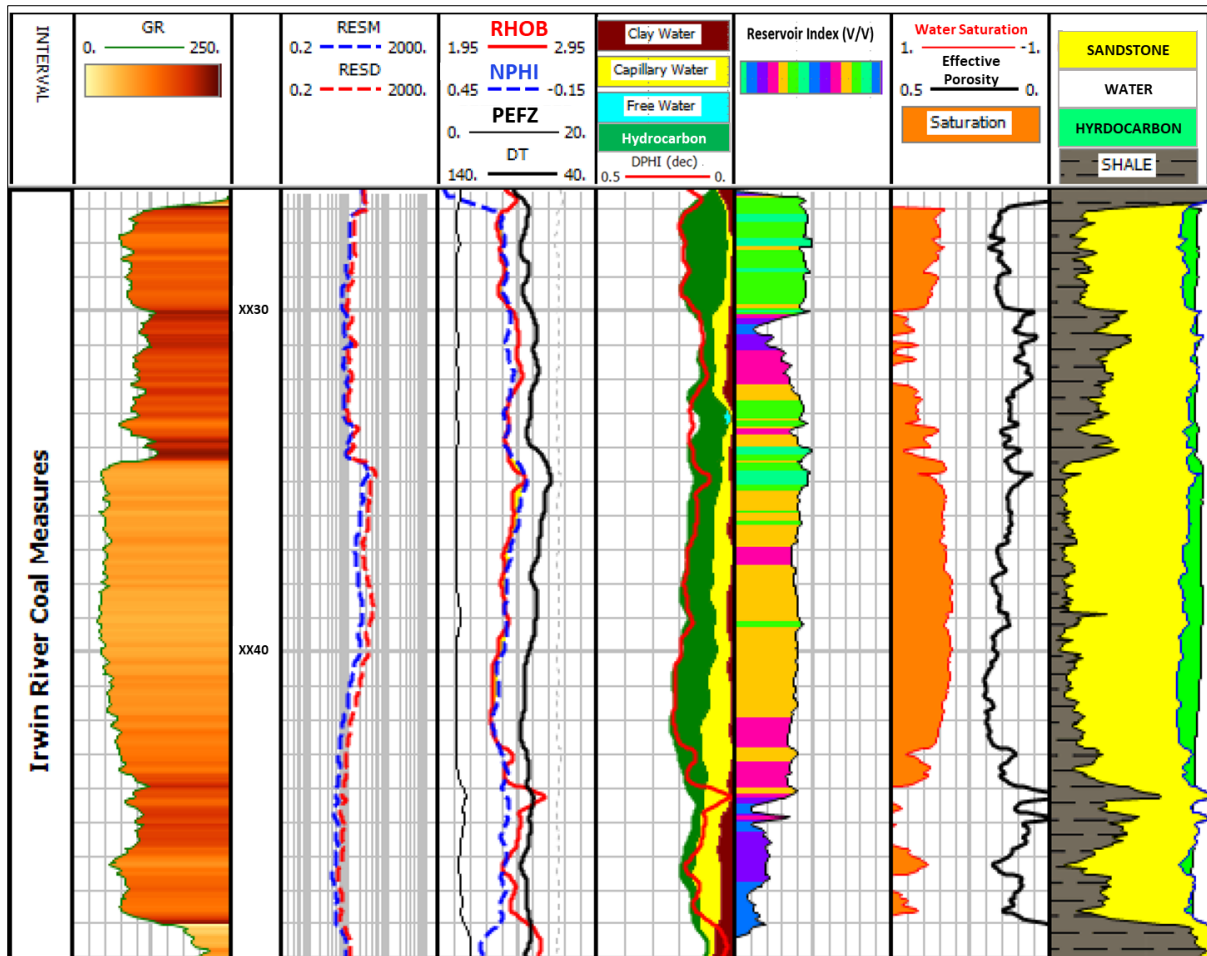
Figure 29: The reservoir index calculated from the NMR and density logs presented in track-5 and log analysis in tracks 6 and 7

Well-3 log interpretation is done as part of the workflow to ensure the log porosity matches the core porosity and to calculate the saturation profile in the reservoir. Figure 30 presents the log interpretation in tracks 4 and 5. To test the reservoir index method, the reservoir index log is extended to Well-3 through Multi-Linear-Regression (MLR) using the available conventional logs. As both the FZI calculated from the core measurements and the Reservoir Index are reflecting rock properties, they have been correlated to each other on log scale and showed a very good match as shown in track-6.
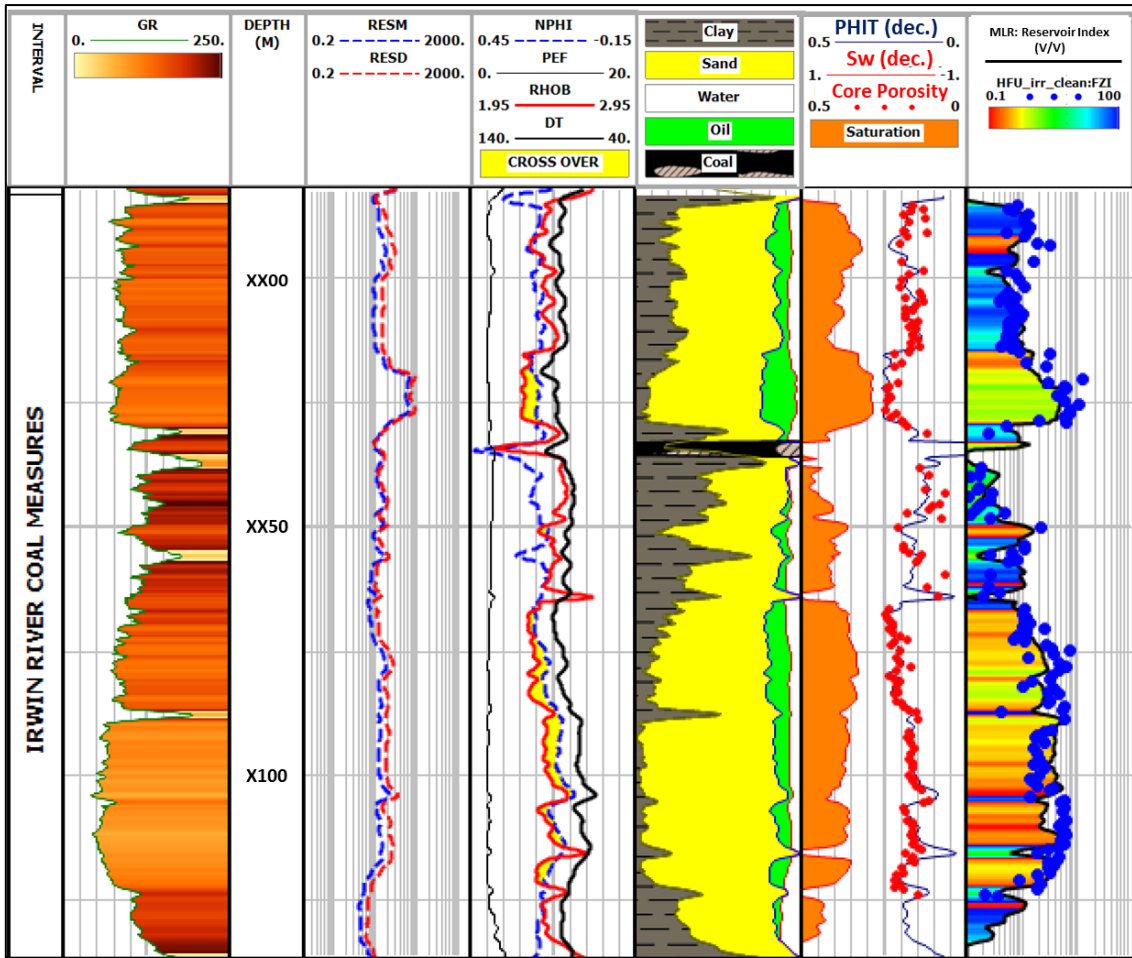
Figure 30: Well-3 log interpretation; Track-5 shows the log porosity matched to core porosity; Track-6 presents the Reservoir Index match with the core-based FZI

4.3. Reservoir Electrofacies

The Reservoir Index has been used as an independent tool to characterize the Irwin River Coal Measures formation. Four hydraulic flow units were classified across the complete reservoir section. **Figure 31** shows the logarithmic value of the Reservoir Index on a cumulative frequency plot (Svirsky et al., 2004). Four different trends are recognised each representing one facies. The following cutoffs established from the plot are as follows:

HFU-1: Log $(R_{Index}) < (- 0.8)$

HFU-2: $(- 0.8) <$ Log $(R_{Index}) < (- 0.34)$

HFU-3: $(-0.34) <$ Log $(R_{Index}) < (- 0.18)$

HFU-4: Log $(R_{Index}) > (- 0.18)$

Upon these cutoffs, the facies can be established through the logs using a reverse calculated Reservoir Quality Index:

$$RQI_{Log} = R_{Index} * \varphi_Z \dots \dots (55)$$
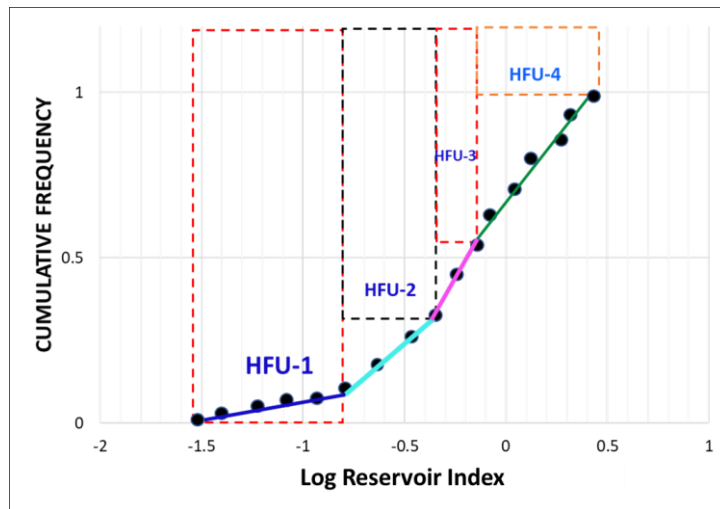
Figure 31: *Reservoir Index showing the hydraulic flow units*

Where the normalised porosity φ_Z is the normalised log porosity and the reservoir index is calculated based on equation 54. The RQI versus the normalised porosity is plotted on log-log plot in **Figure 32**. On the plot generated for Well-3, the rock type with similar FZI value will lie on a straight line with a slope of 1, whereas the data of different FZI will lie on another parallel unit slope lines (Al-Ajmi et al., 2000).
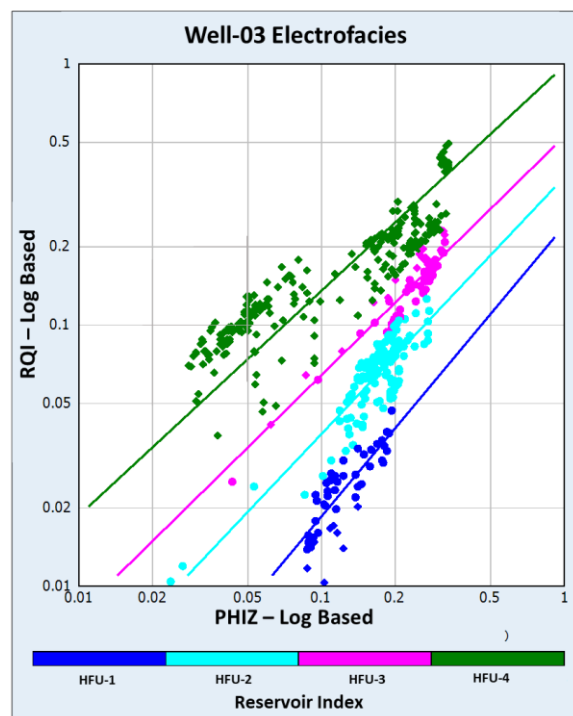
Figure 32: *RQI versus PHIZ based on logs for Well-3*

The classified electrofacies, or the hydraulic flow units, have been categorised into four different rock types, with the first (HFU-1) represents mainly the shale layers, HFU-2 represents the very fine grained to siltstone rock, HFU-3 represents the medium quality shaly sand and HFU-4 is the best quality shaly sand.

The following equation yields a permeability log that describes each hydraulic unit quantitatively (Sokhal et al., 2016):

$$K = 1014 \, FZI^2 * \frac{\varphi_e^3}{(1 - \varphi_e)^2} \dots \dots (56)$$

Based on the log-log plot of RQI versus the normalised porosity, each of the facies has a unique FZI value at the intercept of the straight lines with $\varphi_z = 1$. The values generated for the facies are used to calculate permeability dependent on logs. **Figure 33** shows the classified electrofacies log in track-3 and the permeability calculated using equation 56 in track-4. However, this permeability requires a calibration reference to validate the output. The repeat formation tester mobility, shown in blue points in track-4, is a very useful reference to validate the permeability from the Reservoir Index technique. From the comparison, the calculated log achieves a very good match to the formation tester mobilities. Add to this, the permeability index describes the layering variation with high resolution. Where the mobility showed large variation from XX50 m downwards, the permeability log has seen these changes through the change of the electrofacies log and achieved a very good match.

Further calibration with core measurements is needed to test the validity of this method. The next section describes the facies from the thin section and the statistical analysis for the routine core data.
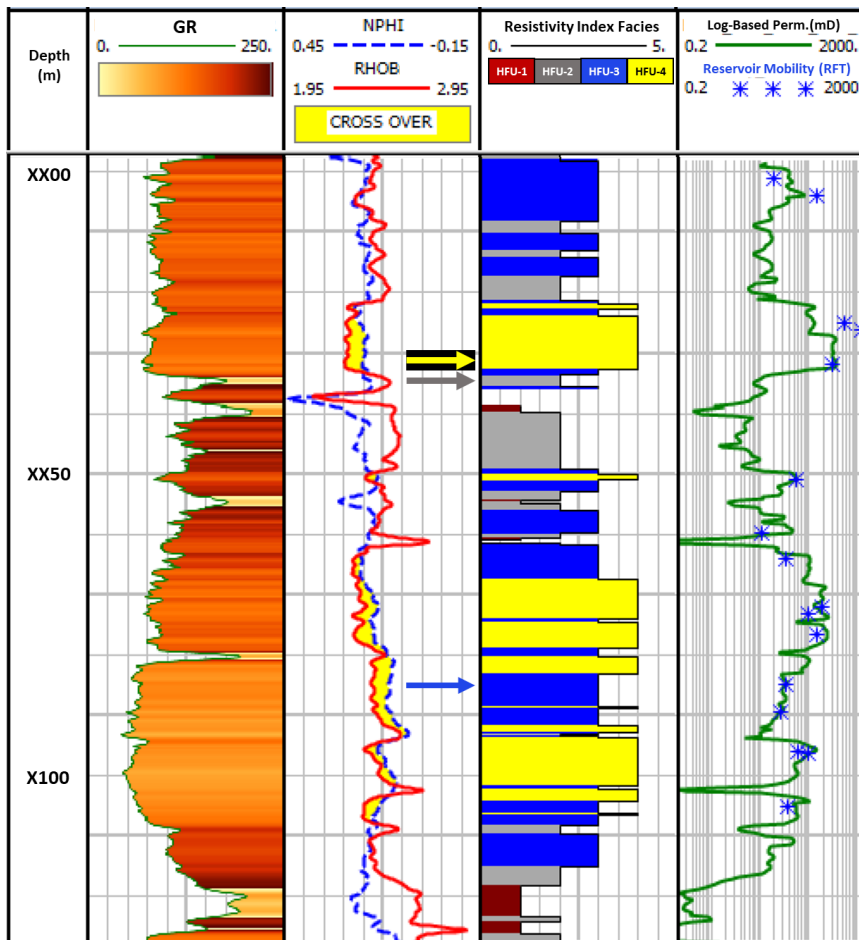
Figure 33: *Well-3 with track-3 showing the facies log; Track-4 shows the permeability index calibrated to the repeat formation tester mobilities*

4.4. Core Integration and Results Calibration

The core thin sections, selected at the depths shown with arrows that have the same colours on the above log plot, have been used to ensure the electrofacies cutoffs are set correctly. The first facies (Brown on the above log plot) is representing mainly the shale layers. HFU-2 (Grey) is the fine-grained argillaceous sand to siltstone. The pore spaces for this facies are filled up to 70 - 80% with Kaolinitic authigenic clay. **Figure 34** shows a thin section representing this facies, for which the core permeability is 2.5 mD. The Kaolinite fills almost all the pore volume leaving very little free pore space.

HFU-3 (Blue) is representing the moderate quality shaly sands in which more porosity is introduced to the rock system. The rock consists of medium-grained sandstone of higher permeability compared to facies-2. Two factors have a direct effect on the reservoir quality, the dispersed Kaoline and the quartz overgrowth. **Figure 35** shows a thin section for this facies, which has a permeability value of 27 mD.

HFU-4 (Yellow) is the best quality reservoir facies that contains the highest permeability. The rock consists of coarse-grained sandstone affected by moderate to severe quartz overgrowth and less authigenic kaolinite. **Figure 36** indicates much better permeability compared to the lower quality facies. In this sample, the permeability is 864 mD.

The electrofacies have been extended through the reservoir interval in the two wells based on the cutoffs presented. In order to test the permeability index relative to routine core analysis, the core data was plotted on the same Log-Log plot for RQI versus normalised core porosity. A core dependent permeability is calculated using the high-resolution facies log created from the Reservoir Index. The unique FZI values for the four electrofacies are 0.21, 0.8, 2.2 and 5.5 for HFU-1, HFU-2, HFU-3 and HFU-4 respectively as shown in **Figure 37**.

The results of the facies and permeability logs are presented in **Figure 38**. The 4 classified electrofacies are presented in a continuous high-resolution log. Track-1 in both wells shows the GR log, Track-2 shows the permeability log calculated based on equation 56 and the unique FZI values from Figure 37. Track-3 presents the porosity logs while Track-4 shows the electrofacies log based on the Reservoir Index approach. Well-3 has more complicated lithology and a thicker reservoir section. However, an excellent match to core permeability has been achieved through the log dependent electrofacies models.
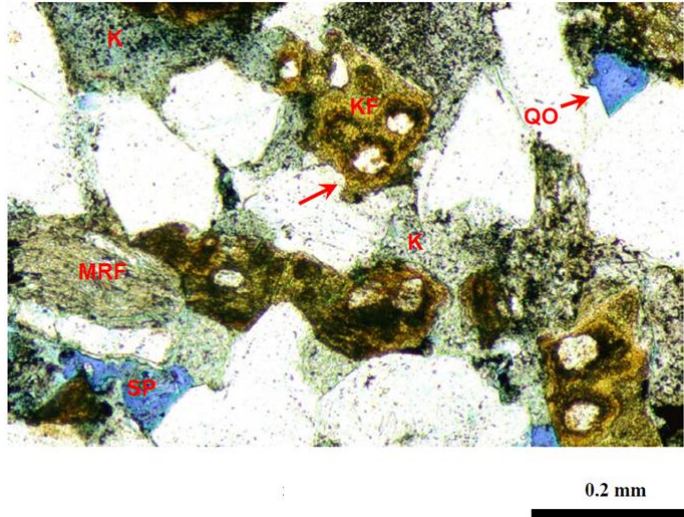
Figure 34: HFU-2 with Kaolinite filling the pore spaces, (After Roc Oil, 2005)
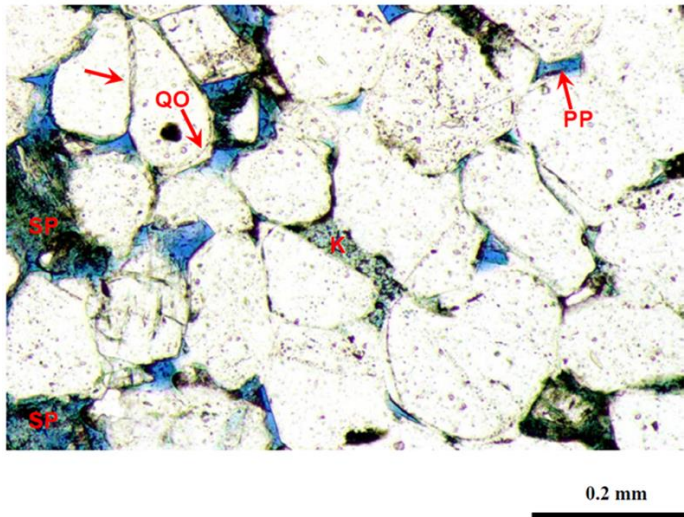
Figure 35: HFU-3 core facies showing quartz overgrowth and kaolin filling the pore spaces, (After Roc Oil, 2005)
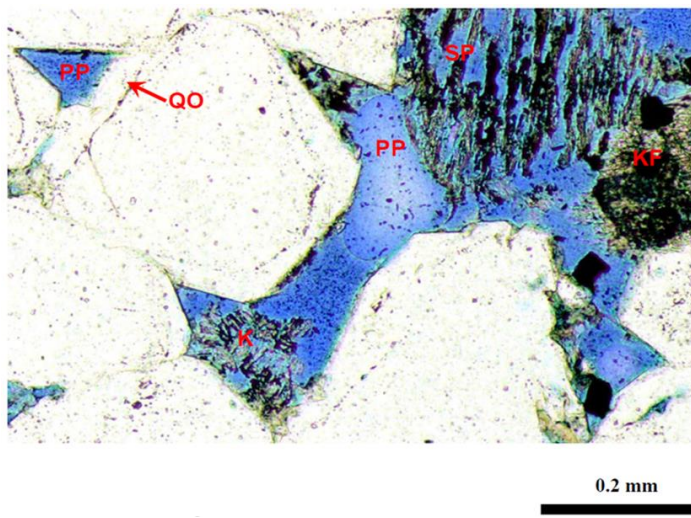
Figure 36: HFU-4 consists of coarse-grained sandstone of high quartz overgrowth and less kaolinite, (After Roc Oil, 2005)
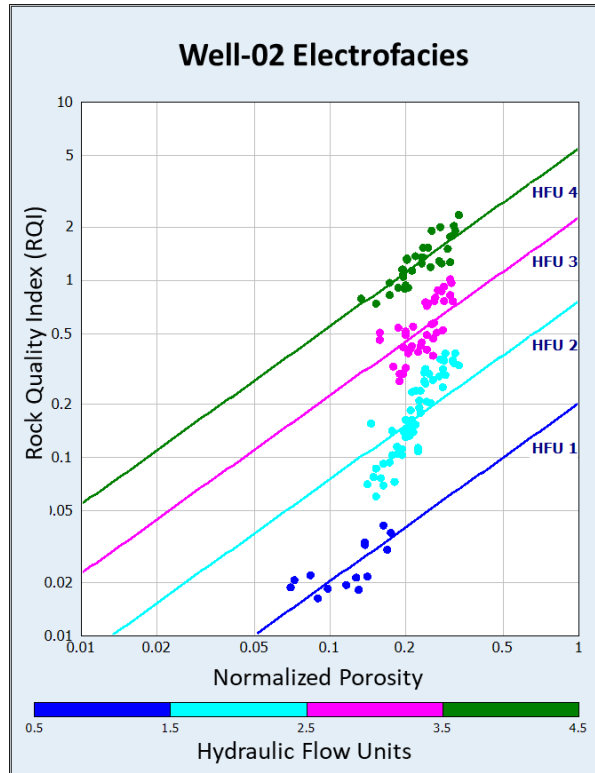
Figure 37: RQI versus normalised core porosity
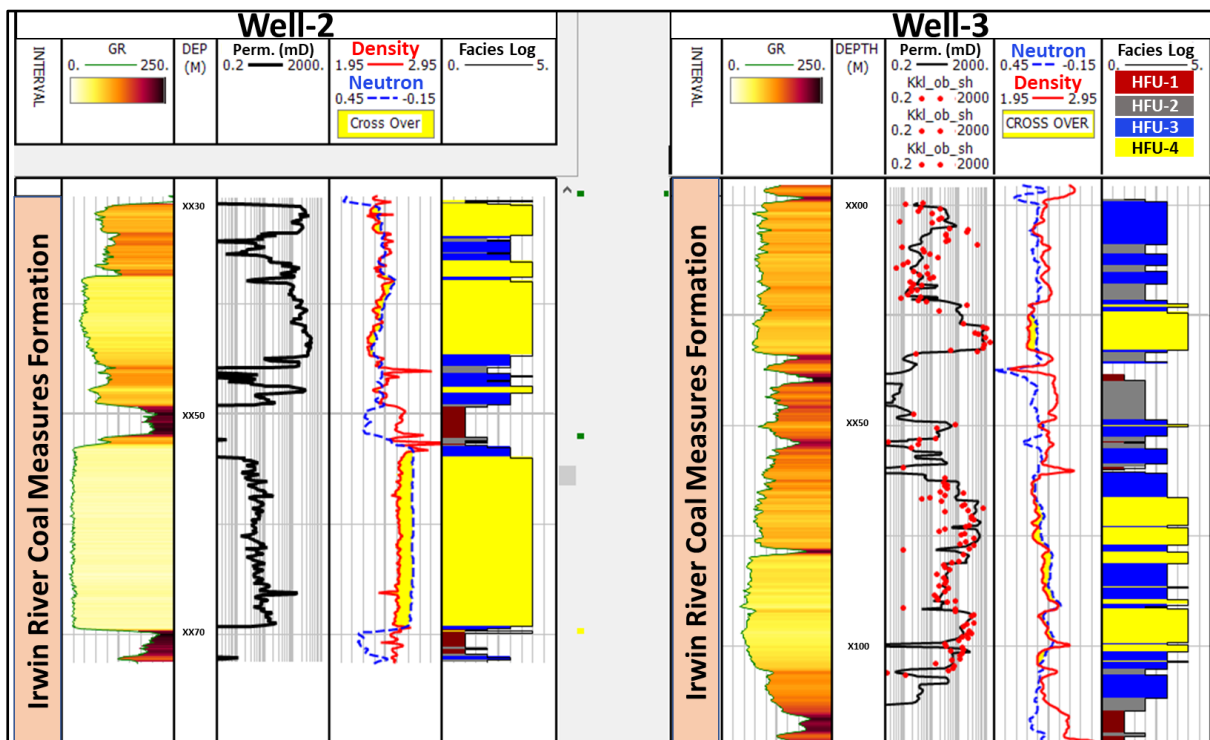
Figure 38: Well-2 and Well-3 electrofacies log; The permeability in Well-02 matches the core permeability

4.5. Conclusions

An integration has been carried out between NMR and the density to predict a direct flow zone indicator log that covers the full zone of interest. The created log can be used as a reservoir index to generate a continuous high-resolution facies in heterogenous reservoirs; in addition to a permeability index that can be matched to mobility from the repeat formation tester tools. Two wells were used to test this technique in the shaly sand of the Irwin River Coal Measures Formation, one of which contains full routine core measurements. The reservoir modelled permeability through the log dependent electrofacies showed very encouraging results with the routine core measurements. The described workflow will help in the establishment of comprehensive facies model in the absence of any core data. Nevertheless, this technique needs calibration in gas reservoir cases due to the gas effect on the NMR porosity. Add to this, the log dependent permeability will require calibration using either core measurements or calculated formation mobility. The reservoir index method is considerably simple technique for very valuable and challenging outputs, which can be used in wells with conventional logs only.

Chapter-5: High Resolution Saturation Modeling

This chapter discusses a published peer-reviewed journal paper in *The Journal of Petroleum.*

Elkhateeb A., Rezaee R., and Kadkhodaie A., 2021, A New Integrated Approach to Resolve the Saturation Profile Using High-Resolution Facies in Heterogeneous Reservoirs, *Journal of Petroleum*, 2021, pp. 1-12.

5.1. Introduction

The formation evaluation of complex reservoirs includes several challenges, one of which is the compromised reservoir properties that are dependent on averaged well-logs in shaly sand formations. Accordingly, core analyses played a major role in calibrating the actual rock properties and well logs. Contrary to simple reservoirs, a simple porosity to permeability relationship is no longer valid, so as any criteria of log analysis that is dependent on a supposed simple relation between the rock quality and the reservoir flow. In many reservoir cases, the calculated saturation profile may not represent the hydrocarbon flow proven either by production history, or at least the well testing. In fact, some advanced logs such as the Nuclear Magnetic Resonance (NMR) may provide valuable information, but considerably different from the actual formation nature, unless they are calibrated to core measurements. In this paper, a comprehensive study in Cliff Head Field is presented through the heterogeneous Early Permian clastic succession in Cliff Head area. The reservoir sections include the High Cliff Sandstone Formation, defined as interbedded sandstone, conglomerate and siltstone and underlying the Irwin River Coal Measures, Clarke et al. (1951). The formation was deposited in shallow marine to shoreface environments, with the fauna indicating an Artinskian age, (Archbold, 1957). The overlying Irwin River Coal Measures Formation, introduced by Clarke et al. (1951), consists of rapidly alternating siltstone and fine to medium grained sandstone, with carbonaceous shale and lenticular coal beds, (McWhae et al., 1958 and Mory et al., 2005). The environment of deposition for the Irwin River Coal Measures represents various delta plains, (Segroves, 1971), deposited in the Artinskian age of the Early Permian, (McWhae et al. 1958). Further, Mory et al. (1996) confirmed the Irwin River Coal Measures as fluvial-deltaic deposits. The top reservoir sand encountered in the Cliff Head area is the Dongara Sandstone of the Kungurian age, (Segroves, 1971 and Kemp et al. 1977). Mory et al. (1996) indicated the age of the Dongara Sandstone as late Early Permian to early Late Permian and described the formation as clean to bioturbated silty sandstone underlying the Kockatea Shale, and equivalent to Beekeeper and Wagina Formations towards the North of the basin. The formation is deposited in a shallow marine environment, (Rasmussen, 1986), restricted to the Northern part of the Perth basin, (Mory et al. 2005). The stratigraphic column of the Northern Perth Basin presenting the units in the Cliff Head Field was shown earlier in **Figure 2**, (Geoscience Australia, 2020).

The Irwin River Coal Measures Formation is divided into two very different units, one shaly sand that is the main reservoir in the field, and an underlying tight clean sand. To resolve the saturation profile as one of the most vulnerable rock properties to uncertainty, a new workflow has been applied to 4 wells of variable degree of complexity. The capillary pressure measurements acquired during the Special Core Analyses are utilized to reflect the actual irreducible saturation profile and to calculate the original saturation in thinly bedded zones, McPhee et al. (2015). Moreover, the measurements clearly identify the difference between the different rock types. The shaly sand succession has shown compromised logs resulted in high water saturation at elevated heights in the reservoir. One major challenge in the shaly sands is having productive layers identified as non-reservoir due to the lower facies quality, Bhatti et al., (2020), Rezaee et al., (2006) and Al Hinai et al., (2013) highlighted the relationship between the pore throat size and the permeability in complex rock systems, which reflects a possible high heterogeneity that cannot be resolved through the formation porosity. With the complexity found in the shaly sand rocks, capillary pressure data has been used to resolve the water saturation profile more accurately. As the reservoir saturation in the log interpretation is dependent on the formation porosity estimated from the conventional logs, an accurate calculation for the reservoir saturation is yet to be challenging through the saturation height modeling workflow. Hence, an independent factor is required to characterize the fluid saturation quantitatively in such complicated reservoir systems.

A new advanced workflow that separates the distribution of the water saturation across the height above the FWL from the formation porosity is presented in this study using 4 wells from Cliff Head Field. The wells have shown an interesting heterogeneity through the clastics succession where the porosity ranges between 15 and 25%, while the permeability varies significantly for the same range from tens of millidarcies to nearly 1 Darcy. The EFZI advanced high-resolution electrofacies classification technique is utilized to characterize the electrofacies and the formation permeability, which is verified by core measurements (Elkhateeb et al., 2019). Despite the water saturation was obtained through the resistivity logs, yet the hydrocarbon saturation remains with high uncertainty due to the several factors involved such as the compromised logs affected by formation shaliness and the reservoir Archie parameters. A more solid evidence of the present uncertainty is that the saturation results through the normal workflow was not reflecting the excellent reservoir production from well testing. To resolve the accuracy of the formation saturation profile, an advanced saturation height modeling workflow is generated that is EFZI-dependent. The resulted saturation represented the formation saturation at an irreducible state proven by NMR logs, with the advantage of its applicability in the cored and the uncored wells. The full workflow is described in detail in the following sections.

5.2. Data and Methodology

Four wells were used to test the new saturation height modeling dependent on the Equivalent Flow Zone Indicator technique. To build the facies model, routine core measurements through the interested clastics succession were used with a complete set

of conventional logs (e.g.: GR, density, neutron, resistivity) in Wells 1 and 3. The NMR is available in Well-1 and 2, with which the water saturation could be calculated independent of resistivity at the irreducible water saturation state. Further, 7 capillary pressure measurements between the two wells are available. A complete advanced petrophysical interpretation was carried out for the four wells, with the log porosity and permeability calibrated to the core routine measurements where applicable. The extended facies in the uncored wells were used to distribute the saturation profile through advanced saturation height modeling. **Figure 39** shows the full workflow adopted in this study for advanced saturation height function modeling.
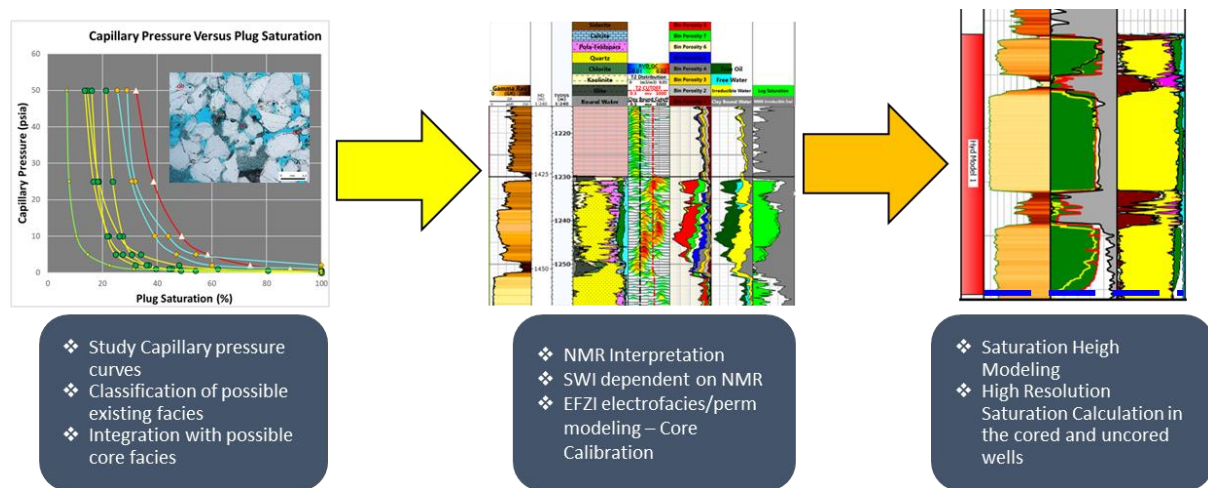
Figure 39: *Workflow used to characterize the reservoir and calculate high resolution rock properties*

5.2.1.   Capillary Pressure Data Analysis

The rock capillarity has proven an extraordinary input to the reservoir characterization and saturation evaluation. Two of the three wells in this study were logged by the NMR Tool that covered several zones of interest of considerable reservoir quality differences. Two out of three wells have capillary pressure data, which covered all the target reservoirs. The core porosity and permeability of the studied samples are very variable due to reservoir heterogeneity (**Table 4**). As can be seen in the Table, there is no good correlation between porosity and permeability due to the reservoir heterogeneity, where the highest porosities show lower permeability relative to the lower porosities.

Table 4: *Samples porosity and permeability values*

Sample	Core Porosity (%)	Core Permeability (mD)
S-16	17.4	633
S-35	8.8	230
S-13	19.7	34
S-15	18.5	16.7

S-42	14.8	87.9
S-37	16.5	445
S-6	22.1	298
S-44	18.1	825

Figure 40 shows the capillary pressure measurements done by the centrifuge method for 7 samples classified based on the average permeability values for the plugs, which matches the irreducible water saturation values. The capillary pressure and the measured saturation data were originally measured at lab conditions at very low stresses relative to the reservoir conditions. McPhee et al., (2015) confirmed that there is a stress relief at atmospheric conditions results in an increase in both porosity and permeability of the samples. The application of the Juhasz method yields effective results for stress correction as per the following equations, (Juhasz et al., 1979).
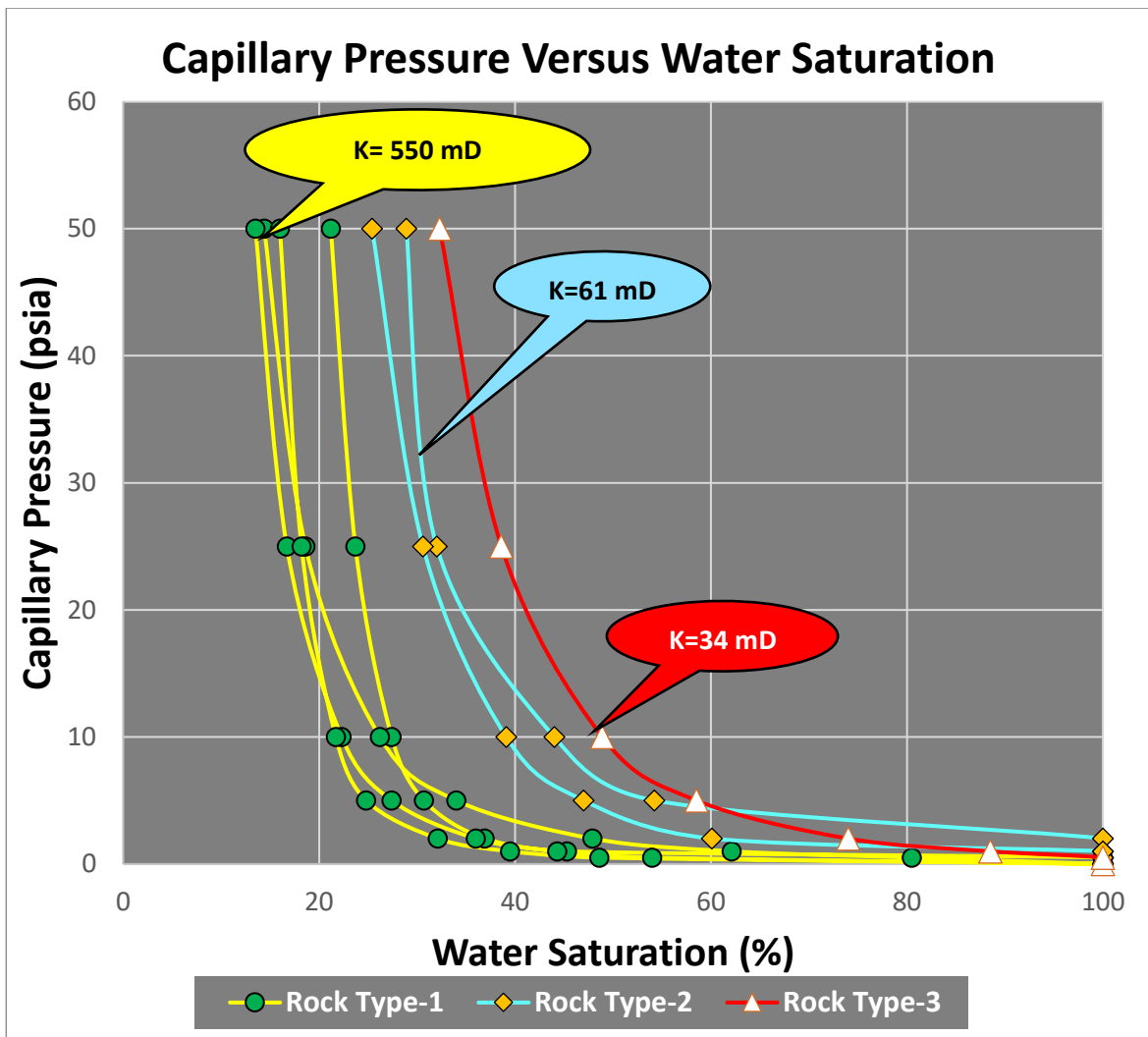
Figure 40: Capillary pressure data in Cliff Head Field

$$Pc^* = Pc_{lab} \left[\frac{\emptyset_{res}}{\emptyset_{lab}}\right]^{0.5} \dots\dots\dots (57)$$

$$Sw_{nw}^* = S_{nw_{lab}} \left[\frac{\emptyset_{res}}{\emptyset_{lab}} \right] \dots \dots \dots (58)$$

where Pc^* and Sw_{nw}^* are the stress corrected capillary pressure and plug saturation, Pc_{lab} and $S_{nw_{lab}}$ are the same at ambient conditions. The $\emptyset_{lab}$ is the total porosity as measured in the laboratory under the ambient conditions and $\emptyset_{res}$ is the stress corrected porosity. The data requires another correction for reservoir fluids conditions taking into consideration the contact angle and the Interfacial Tension, (Purcell, 1949). The conversion is done through the following equation:

$$Pc_{res} = Pc_{lab} * \left[\frac{(\sigma Cos\theta)_{res}}{(\sigma Cos\theta)_{lab}} \right] \dots \dots \dots (59)$$

Where the Pc_{res} is the corrected capillary pressure to the reservoir conditions (psia), the θ is the contact angle and the (σ) is the rock interfacial tension (IFT). McPhee et al., (2015) have listed the values for the contact angle and the Interfacial Tension in an oil-water system. The contact angle for such a system at lab conditions is 0° and the IFT is 72 dynes/cm, while at the reservoir conditions the values are 30° and 30 dynes/cm for the contact angle and IFT respectively. The important application of the capillary pressure concept is how the reservoir fluids are in fact distributed across the thickness of the reservoir prior to its exploitation (Ahmed, 2001). Final conversion to reservoir height is required to represent the saturation profile at any certain depth above the reservoir free water level.

$$HAFWL = 144 * \frac{Pc_{res}}{(\rho_{water} - \rho_{oil})} \dots \dots \dots (60)$$

Where HAFWL is the Height Above the Free Water Level (ft.), ρ_{water} and ρ_{oil} are the densities for the water and oil respectively (lb/ft3). The saturation height modeling will aim to run a resistivity independent quantitative saturation evaluation and compare it with resistivity-based and the NMR irreducible saturations. Figure 41 shows the capillary pressure dataset corrected to the reservoir conditions. The left y-axis presents the capillary pressure, while the right side for the same shows the height above the free water level in meters, the x-axis presents the saturation corrected to reservoir conditions.

5.2.2.   The Core Thin Sections – An Integration with the Rock Capillarity

The target zones in the Irwin River Coal Measures Formation have been covered by core thin sections that allowed further understanding of the reservoir nature. By studying the various thin sections, 4 distinct lithofacies are identified reflecting 4 different rock types, 3 of which are covered by capillary pressure measurements. Figure 42 shows the first reservoir distinct facies of the poorest quality rock identified in Well-

3 at depth 1391.85 mMD. The rock consists of medium-grained arkose, moderately sorted with potassium feldspars (KF) that is partially replaced by some pyrite locally and abundant authigenic kaolinite (K.). The permeability of this rock is 4.4 mD, despite that the measured core porosity is 19%. The Kaolinite, identified as dispersed clay (Elkhateeb et al., 2019), is clearly filling the pores in the reservoir, which has significantly affected the permeability of this rock type (Rock Type-3). The irreducible water saturation of this facies is 32%.
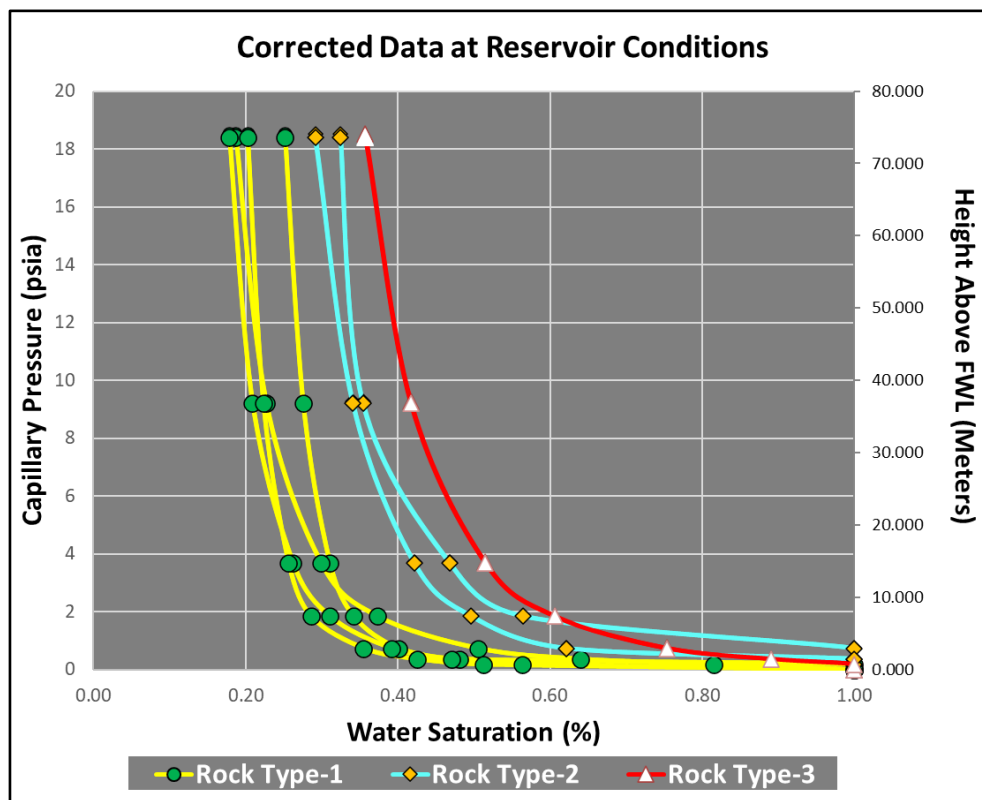
Figure 41: *The corrected capillary pressure measurements to the reservoir conditions*
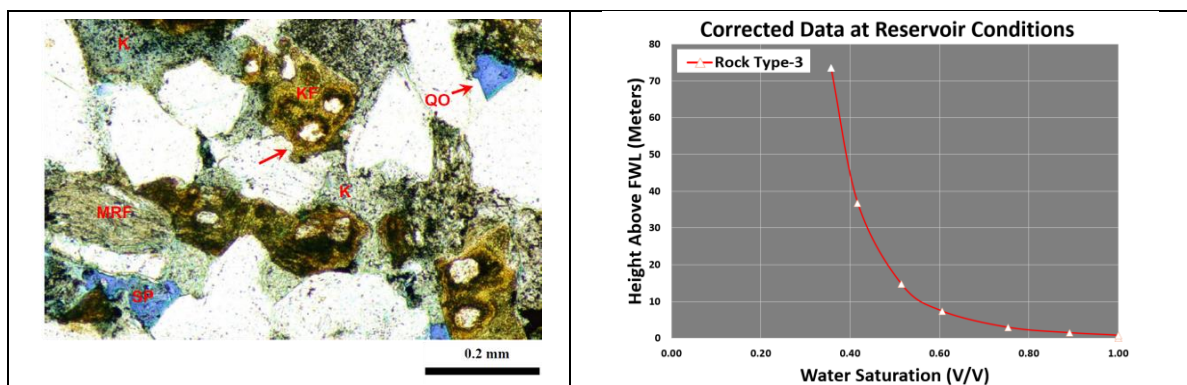
Figure 42: *A core thin section matching the poor quality rock type identified from the capillary pressure curves where the authigenic Kaolinite (K) filling the pore spaces, a clear Quartz overgrowth (QO) and potassium feldspars (KF) occupied by few pyrite fragments are common in the rock sample, (After Roc Oil, 2005)*

Rock Type-2 is moderately microporous, medium-grained arkose with abundant authigenic kaolinite that fills the pore spaces. Detrital Clays (Dclay) are present in this rock type. A clear element that affected the rock formation pore volume is the quartz overgrowth (QO). **Figure 43** shows a thin section for Rock Type-2 from Well-2 at depth 1447 mMD. The porosity and permeability of this sample are 16% and 20.7 mD respectively. In this rock type, the permeability is higher despite the low porosity when compared with RRT-3. The SWir, based on the PC curve, for this Rock type is 27.2%.
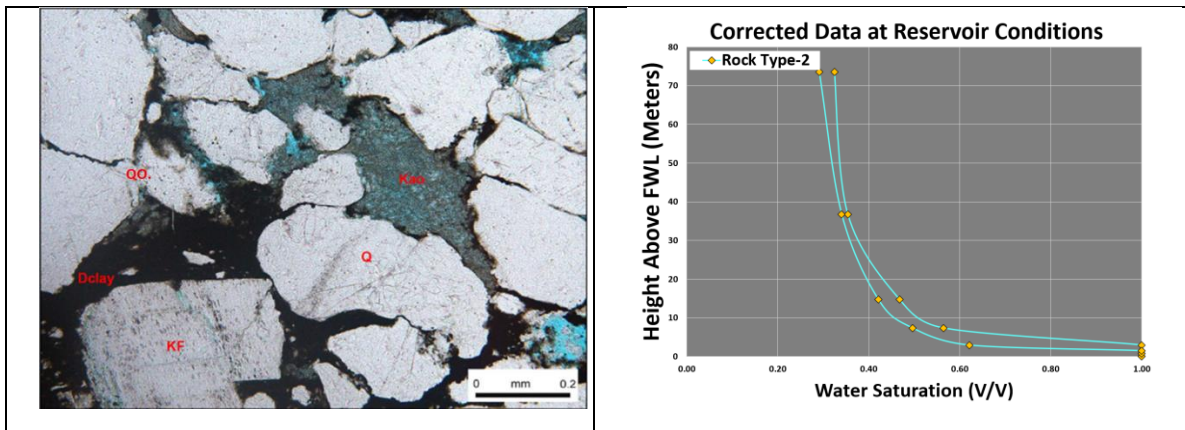
Figure 43: Thin section for Reservoir Rock Type-2 in which the Kaolinite (Kao.) occupies the pore spaces with some Detrital Clays (Dclay). The Quartz overgrowth (QO) is common cementation with the presence of potassium feldspars (KF), (After Roc Oil, 2004)

The best quality lithofacies in the shaly sand is represented by Reservoir Rock Type-1 in the Irwin River Coal Measures Formation. In this rock type, the pores still have some authigenic kaolin occupies the pores and a clear identified quartz overgrowth (QO), but with much better permeability. **Figure 44** shows a thin section that represents this facies with 22% porosity and average permeability value of 550 mD. The irreducible water saturation of this facies is clearly much lower relative to the other two discussed facies with an average value of 16%.
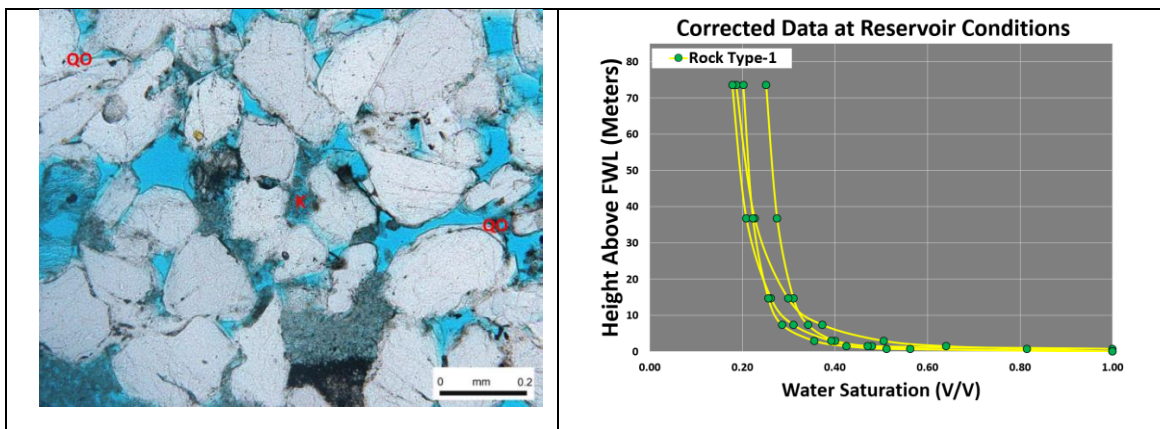
Figure 44: Thin section showing Reservoir Rock Type-1 reflecting much higher permeability and common intergranular pores relative to other facies. The Kaolin (K) still occupies the pore spaces with Quartz overgrowth (QO) cementation, (After Roc Oil, 2004)

The last identified Reservoir Rock Type (RRT-4) is the low porosity, or the tight, clean sand of the Irwin River Coal Measures Formation (**Figure 45**). The recorded reservoir properties of this sample are 8.8 porosity units and the permeability is 300 mD, but no valid capillary pressure measurements were recorded for this facies. The Clays in this rock are negligible with a clear predominant quartz overgrowth (QO) acting as a cementing agent.
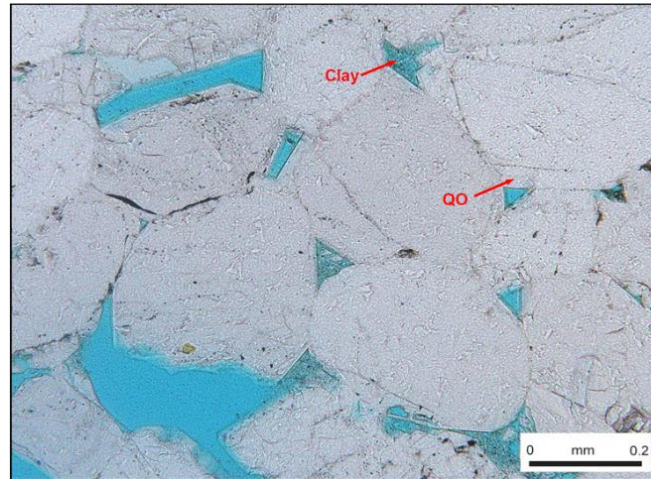
Figure 45: The Clean Sand facies presenting Reservoir Rock Type-4 in the Irwin River Coal Measures Formation. The rock is with intergranular pores that are well interconnected with minor clay content and clear Quartz overgrowth (QO) acting as cementing material, (After Roc Oil, 2004)

5.2.3. Identification of Reservoir Archie parameters

The cored wells have tested the values of the Formation Resistivity Factor and the Resistivity Index-Saturation to estimate the Cementation Factor (m) and Saturation Exponent (n) in the different formations. **Table 5** summarizes the estimated Archie parameters for each cored formation (Roc Oil, 2004).

Table 5: Identified Archie parameters in Cliff Head Field for all reservoir rocks

Formation / Unit	Cementation Factor (m)	Saturation Exponent (n)
Dongara Sandstone	1.98	2.71
Irwin River Coal Measures – Shaly Sand	1.94	2.754
Irwin River Coal Measures – Clean Sand	1.91	2.47

5.2.4. Nuclear Magnetic Resonance

The NMR has been proven a very effective tool that provides a formation porosity independent of reservoir lithology (Coates et al., 1999). A great outcome from the NMR interpretation is the irreducible water saturation (Swi_{NMR}) that can be calculated using the Free Fluid Index (FFI) and the NMR porosity ($TCMR$). The following equation was used to calculate the irreducible water saturation:

$$Swi_{NMR} = 1 - \left(\frac{FFI}{TCMR}\right) \dots \dots \dots (61)$$

There are no available core magnetic resonance measurements to identify the precise T2 cutoff. Nevertheless, very solid information about the reservoir productivity had been collected in Well-1 through an extended well test during which the shaly and the clean sands in Well-1 were allowed to flow through 27 meters thickness for a continuous 8 days. The reservoir flowed at a rate of 3,000 barrels of oil per day with negligible to no water cut (Roc Oil, 2003). This will indirectly support a Nuclear Magnetic Resonance interpretation that shows negligible to no free formation water dependent on a selected T2-Cutoff value. The final well test results are listed in **Table 6**.

Table 6: Test Results in Well-1 (After Roc Oil, 2003)

Parameters	Well Test Results
Tested Thickness	27 Meters
Productivity Index	3.00 stb/psi
Permeability-Thickness (K-h)	62,500 mD.ft
Pressure Depletion	Not indicated
Initial reservoir pressure	1840 psia
Reservoir Temperature	75° C @ 1225 mSS
Water Cut	Negligible to none
Oil Gravity	31° to 33° API
Viscosity	5.5 to 6.25 centipoise
GOR	32 to 38 SCF/BBL
Wax	20% with pour point of 33° C
Asphaltene	<1%

The NMR interpretation has been carried out in wells 1 and 2 to calculate the irreducible saturation and to start the log evaluation for the electrofacies using the Equivalent Flow Zone Indicator (EFZI) method. Several samples from the T2 Distribution log has been selected to validate the cutoff, each selected to represent a certain rock type from the best quality to the poor quality. The data has been plotted on a semi-log plot versus the T2 relaxation time (**Figure 46** and **Figure 47**). It is found that all the classified rock types share one valley that separates the small pores with bound fluid from the large pores with free fluids, despite the variance in the logs signature. A clear variation between the rock types are obvious with a clear variation in the cutoff value, where the shaly sand appears to have a faster cutoff value relative to the clean sands. The shaly sand is found to be producing a free fluid volume of net oil at a value of 70 milliseconds, while the clean sands were found to produce the same at a 100 millisecond T2 cutoff value. Comparing the different rock types classified has revealed also that the volume of the free fluids in the good quality rock (RRT-1) is nearly double the bulk irreducible volume for poor quality rock (RRT-3). Furthermore, upon the application of such variable Free Fluid Cutoff, the NMR interpretation has shown oil-free water matching

the well test results. The resulted saturation will represent purely the irreducible water saturation in the reservoir through a resistivity-independent method that has not been affected by any type of mineralogy or formation tightness. The saturation from the NMR interpretation has been compared directly to the resistivity based water saturation calculated using the Simandoux shaly sand saturation model, (Simandoux, 1963), which is referred to as the best known of the shaly sand saturation solutions (Cannon, 2016).

$$\frac{1}{R_T} = \frac{\emptyset^m * Sw^n}{a * R_W} + \frac{V_{clay} * Sw}{R_{clay}} \dots \dots \dots (62)$$
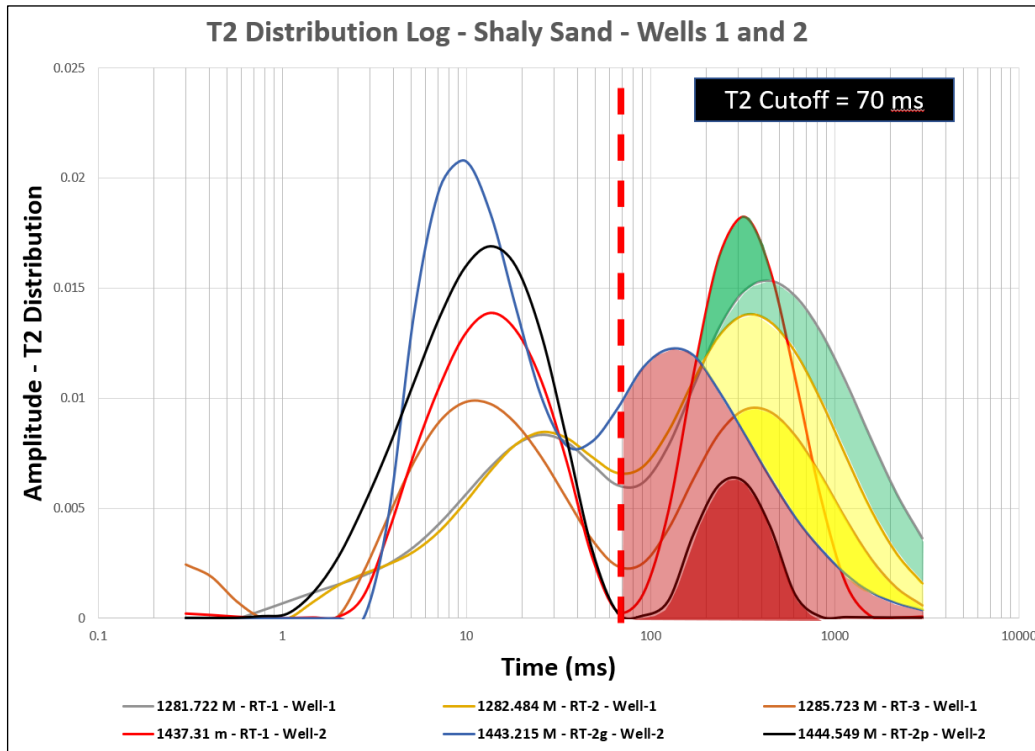
Figure 46: T2 Distribution log plotted versus relaxation time showing the shared cutoff value for all the shaly sand rock types
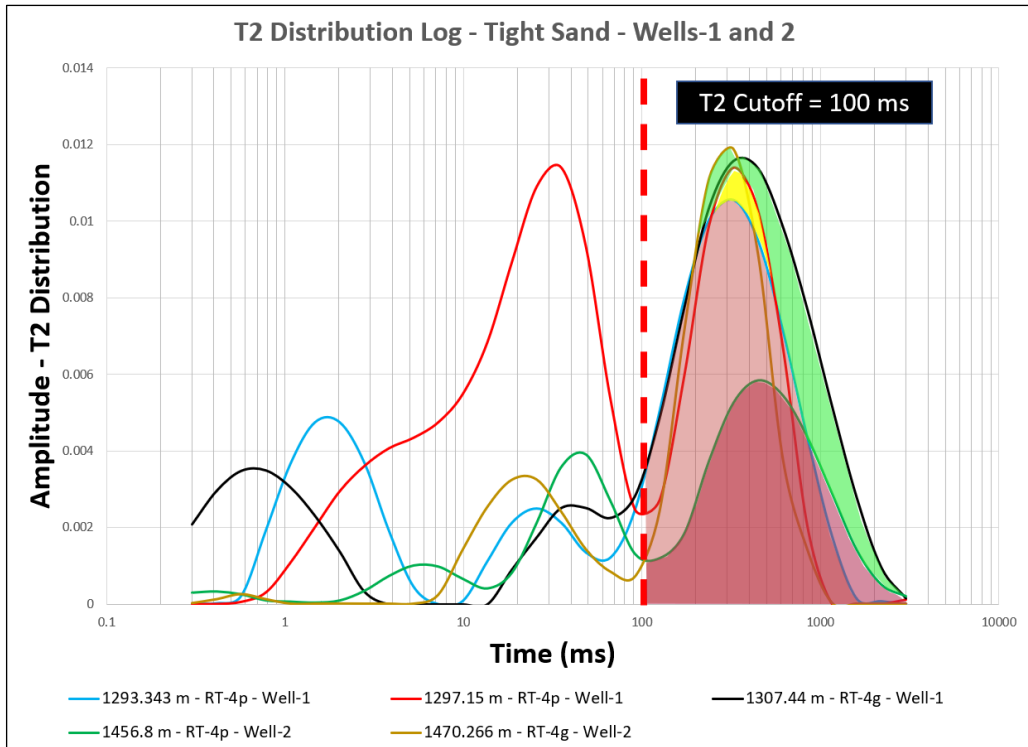
Figure 47: *T2 Distribution log plotted versus relaxation time showing the shared cutoff value for all the clean tight sand rock type in the Irwin River Coal Measures Formation*

With the availability of complete fluid characterization from the NMR interpretation, the reservoir facies characterization using the Equivalent Flow Zone Indicator technique will be carried out using equation 47 (Elkhateeb et al., 2019). The methodology allows a high-resolution facies log and permeability characterized in heterogeneous reservoirs.

The classification of the clastics succession in the Cliff Head Field wells started by initializing the EFZI plot on a cumulative frequency chart for all interested zones (Figure 48). In this plot, several distinct straight lines are formed with each representing a certain Hydraulic Flow Unit (Svirsky et al., 2004). A total of 9 distinct reservoir electrofacies were classified for three formations; 3 for The Dongara Shaly Sands, 4 for The Shaly section of the Irwin River Coal Measures and 2 for the underlying tight sands.
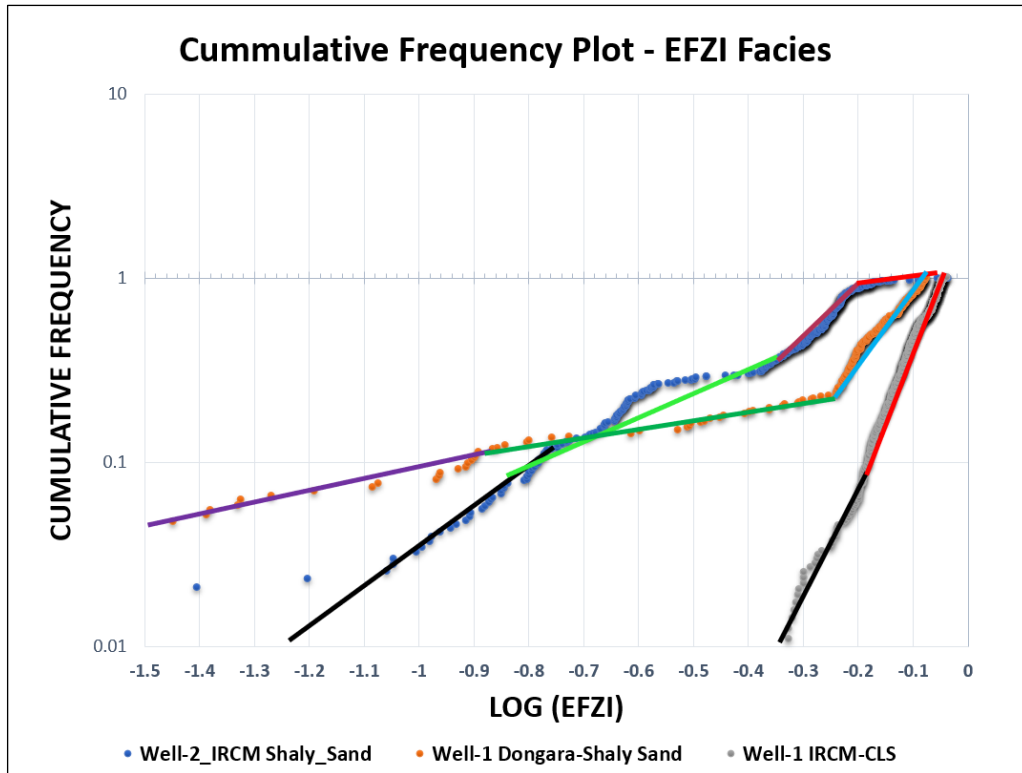
Figure 48: Cumulative frequency chart for the available facies in the Cliff Head Field Clastics succession

Table 7 lists the thresholds of the classification for the 9 identified electrofacies and their relation to the identified Reservoir Rock Types (RRT).

Table 7: The identified Rock Types and the electrofacies classification using the Equivalent Flow Zone Indicator technique

Formation	Reservoir Rock Type (RRT)	Hydraulic Flow Unit (HFU)	Cumulative Frequency Threshold Log (EFZ)
Dongara Sandstone	RRT-3	HFU-1	<-0.87
	RRT-2	HFU-2	>-0.87 , >-0.24
	RRT-1	HFU-3	>-0.24
Irwin River Coal Measures – Shaly Sand and High Cliff Sandstone	RRT-3	HFU-4	<-0.8
		HFU-5	>-0.8 , < -0.34
	RRT-2	HFU-6	> -0.34, <-0.18
	RRT-1	HFU-7	>-0.18
Irwin River Coal Measures – Clean Sand	RRT-4	HFU-8	<-0.17
		HFU-9	>-0.17

The best application of these identified facies to test them is to run an EFZI-dependent permeability modeling and match the core measurements available in Wells 1 and 3. The Hydraulic Flow Units concept has developed a clustering technique to classify the facies for a reservoir rock (Amaefule et al., 1993). Furthermore, Soleymanzadeh et al.

(2018) indicated that the Flow Zone Indicator approach is a popular rock type technique that is based on a capillary tube model and hence Rock Quality Index Parameter (RQI). Accordingly, in complicated reservoir rocks, a single linear relationship between porosity and permeability cannot describe the rock heterogeneity. Rather the capillarity is reflecting groups of rock types that are connected to a unique permeability model. In general, the different theoretical and empirical correlations between porosity and permeability would require an independent source to calibrate the results, with which simple factors were found to fail to return the proper permeabilities in complex rock textures (Ghadami et al., 2015). The FZI is considered an independent factor that showed consistency in the nature of the various rock types (Elkhateeb et al., 2019 and Garrouch et al., 2018). To calculate the Flow Zone Indicator, equations 38 to 40 were applied to complete the facies analysis workflow as explained earlier in Chapter-3.

5.2.5.   The High-Resolution Saturation Height Modeling

The saturation height modeling has been carried out to characterize the saturation in the clastics succession in Cliff Head Field. In order to set up the variation between the previously defined rock typing models, an integration between the classified EFZI facies and the capillary pressure saturation height has been done to model an effective high-resolution saturation profile. Using the Leverett-J Function modeling for each rock type, a saturation height function has been defined to fit each of the classified rock types independently as per the following models. **Figure 49** shows the J-Function versus water saturation for each rock type.
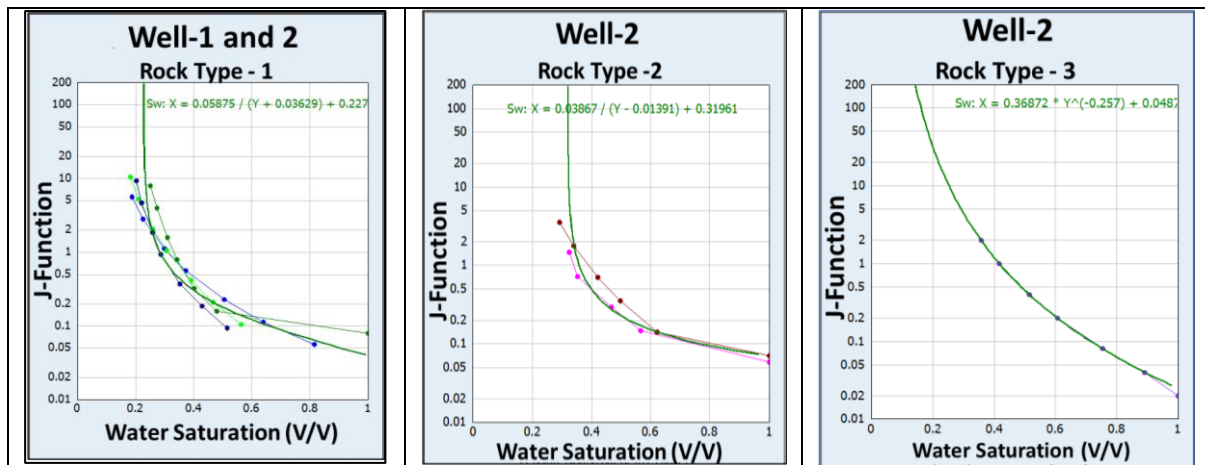
Figure 49: *Leverett-J plotted against the water saturation for the capillary pressure corrected curves*

$$Swi_{RRT-1,4} = 0.05875/(J + 0.03629) + 0.22766 \dots\dots\dots (63)$$

$$Swi_{RRT-2} = 0.03867/(J - 0.01391) + 0.31961 \dots\dots\dots (64)$$

$$Swi_{RRT-3} = 0.36872 * J^{-0.257} + 0.0487 \dots\dots\dots (65)$$

where (J) is the Leverett-J Function, (Ahmed, 2001), calculated as per the following equation:

$$J = 0.21645 * \left(\frac{Pc}{\sigma Cos\theta}\right) * \sqrt{\frac{K}{\emptyset}} \dots \dots \dots (66)$$

where Pc is the capillary pressure, K is the EFZI-dependent formation permeability and $\emptyset$ is the calculated formation porosity. The saturation height modeling has been carried out using the rock typing classified for the clastics succession, further extended to the uncored horizontal well, which had a considerable offset to the free water level, through a long high heterogenous drilled section.

The saturation height modeling will act as a third independent water saturation computation across the target zones for all rock types. In such a complicated reservoir, it is very hard to allocate the correct saturation-height model to a certain rock type where the porosity is not a discriminating factor. Yet, the permeability solely cannot act as a final defining factor since there could be two facies of high and low permeabilities that are showing the same porosity. To assign the correct saturation model to a certain rock type, at a specific reservoir height, the EFZI facies and the permeability were integrated in the saturation height modeling workflow based on the following equation:

$$Swi = f(K_i, EFZI_i) \dots \dots \dots (67)$$

In Cliff Head Field, the resulted saturation profile will represent the reservoir at its irreducible state due to the oil-free water produced in the well testing. Furthermore, the modeling can be used on a real time basis, with the lack of resistivity logs, where the water saturation can be calculated while drilling through the characterized facies log using equations 63 to 65.

5.3. Modeling Results

This integrated formation evaluation has allowed the development of a new workflow to characterize two formation properties quantitatively, permeability, and water saturation. Moreover, a generation of the irreducible water saturation as a continuous log with the possibility to extend the results to any uncored well. Further an independent calibration for the T2 Cutoff value for the magnetic resonance log interpretation.

5.3.1.   Petrophysical Evaluation and NMR Interpretation Results

The petrophysical interpretation has been carried out, applying the SCAL determined Archie parameters, using the mineralogical inversion analysis. The clays used in the evaluation are the kaolinite and illite as the main clays in the zones of interest proven by the core examination. Wells 1 and 2 NMR logs were interpreted to provide an

independent source for the saturation calculation, which will be compared relative to the calculated saturation based on resistivity and porosity logs. **Figure 50** shows a correlation between wells 1 and 2. Track-1 shows the Gamma-ray log; Track-2 shows the mineralogical petrophysical interpretation for both wells integrated with the analysed fluid characterization from the NMR interpretation; Track-3 shows the T2 Distribution log with the variable T2 Cutoffs; Track-4 presents the porosity bins partitioned to 10 partial porosities (1, 2, 4, 8, 16, 33, 100, 300, 1000 and 3000 ms). Clearly, there is a difference in the pore structure where the bin porosity 9 constitutes the majority of the pores in Dongara Shaly sands relative to bin porosity 8 in the Irwin River Coal Measures Shaly Sand, which indicates a smaller pore size for the latest proven by the core thin sections. Track-5 presents the NMR interpretation utilizing the variable T2 Cutoffs where the grey is the Clay Bound Water, the yellow is the small pore bound water porosity, the free fluids are partitioned into two volumes; Free water in blue and the free hydrocarbons in dark green. Track-6 presents the calculated irreducible water saturation from the NMR interpretation shaded in grey, while the resistivity log-based Simandoux water saturation is shaded in green.
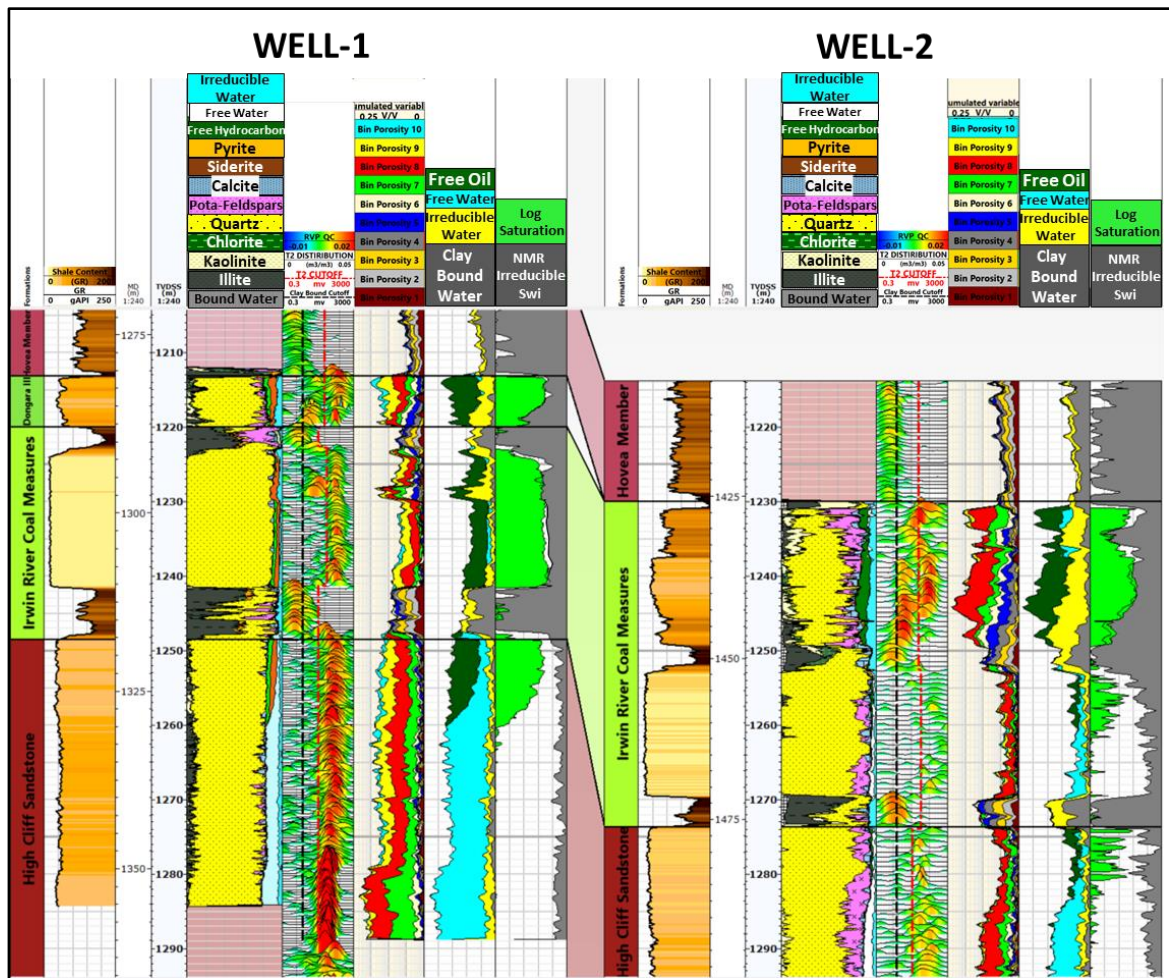
Figure 50: *Petrophysical analysis and NMR interpretation integration in Wells 1 and 2. Track-1: GR log, scaled from 0 to 250 GAPI, with shading indicating the formation shaliness; Track-2: The mineralogical petrophysical modeling, scaled from 0 to 1, showing the shale comprises of three clay types, kaolinite, Illite and chlorite; Track-3: The NMR T2-Distribution array with two cutoffs, the clay bound water (black) and the variable T2*

There is a very good match between the two saturations in the shaly sand intervals (Dongara and Irwin River Coal Measures) despite the very different sources of the calculated saturations. There is a clear variance between the two logs in Well-1 in the High Cliff Sandstone Formation, and in the tight Sand in Well-2, above the contact at 1261 mSS. One would interpret this as a transition zone in which it is possible to have an increased free water volume next to the reservoir hydrocarbon fluids. However, the facies in the High Cliff Sandstone Formation is represented by the best quality rock type, with which it is expected to have a thinner transition zone. The saturation height modeling will confirm the actual saturation in this zone.

5.3.2. Permeability Calculation

The permeability has been calculated utilizing the core-based classified electrofacies equations through the porosity-permeability plot in Well-1 and Well-3. The two wells are for different formations of different reservoir characteristics, therefore they have been separated into two different plots, one for the Dongara Sandstone and the Irwin River Coal Measures clean sands in Well-1, and the second for Shaly sands of the Irwin River Coal Measures in Well-3 as shown in **Figure 51** and **Figure 52** respectively.

Nine permeability models have been used to run the permeability calculations for all the facies, all in the form of power equations. For the Dongara Sandstone and the tight Clean Sands, the equations are:

$$K_{HFU1} = \emptyset^3 * \left(3.305/(0.0314 * (1 - Phi))\right)^2 \dots \dots \dots (68)$$

$$K_{HFU2} = \emptyset^3 * \left(6.03/(0.0314 * (1 - Phi))\right)^2 \dots \dots \dots (69)$$

$$K_{HFU3} = \emptyset^3 * \left(10.376/(0.0314 * (1 - Phi))\right)^2 \dots \dots \dots (70)$$

$$K_{HFU8} = \emptyset^3 * \left(13.796/(0.0314 * (1 - Phi))\right)^2 \dots \dots \dots (71)$$

$$K_{HFU9} = \emptyset^3 * \left(16.933/(0.0314 * (1 - Phi))\right)^2 \dots \dots \dots (72)$$

For the Shaly Sands of the Irwin River Coal Measures, equations 49 to 52 have been utilized following the studied facies in Chapter-3 for the Hydraulic Flow Units 4 to 7 (Elkhateeb et al., 2019):

From the cross plots, it is clear the significant variance between the rock types, particularly in the shaly sands. There is an overlap for the reservoir porosity with

variance in the permeability of several order of magnitudes. **Figure 53** presents the results of the high-resolution EFZI facies and the permeability logs.
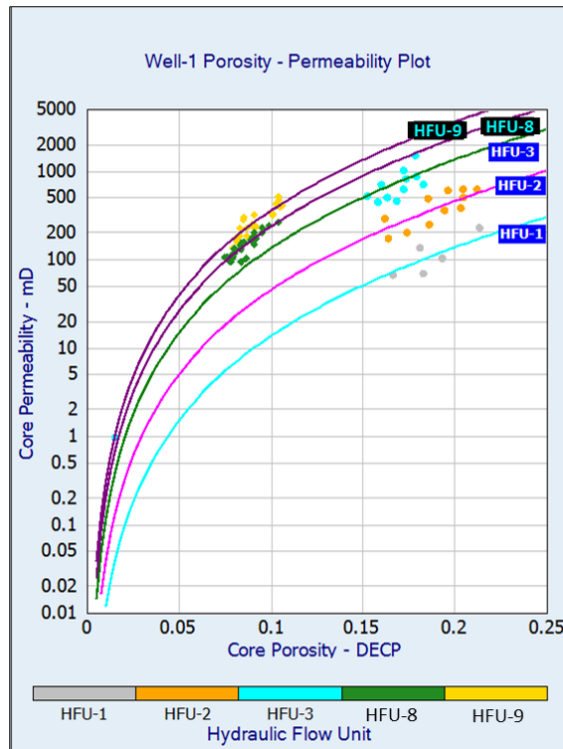
Figure 51: *Porosity vs. Permeability plot showing the HFUs classification in the Dongara and the Clean sands of the Irwin River Coal Measures Formation*
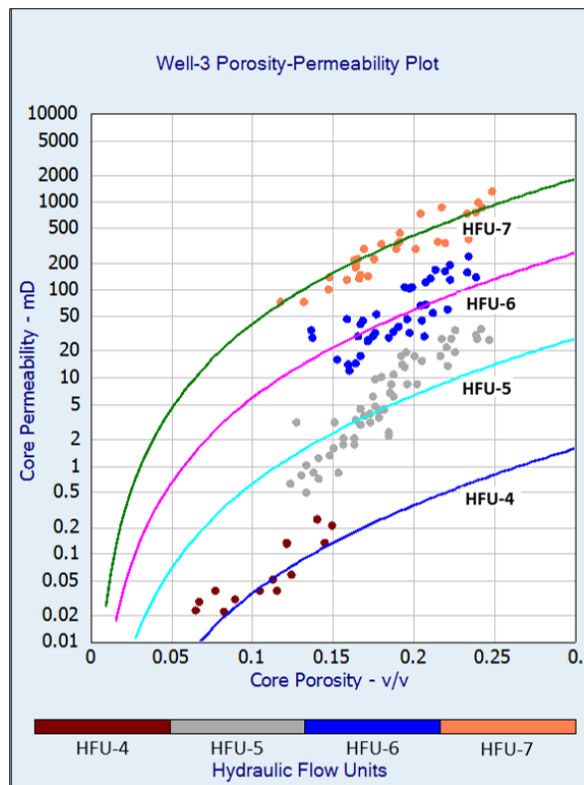
Figure 52: *Porosity vs. Permeability plot showing the HFUs classification in the Shaly sands of the Irwin River Coal Measures Formation*

The wells are showing the Gamma-ray log in Track-1; Track-2 shows the porosity logs, density in red and neutron in blue; Track-3 shows the core porosity in Wells 1 and 3 matching very well the log calculated porosity in Black; Track-4 shows the EFZI facies; Track-5 presents the EFZI high resolution permeability log matching the core permeability in wells 1 and 3. From the results, the porosity in the shaly sands in Wells-2 and 3 seem to be consistent in the range, however, the permeability varies, so as the facies identified, significantly between the sand layers. This is where the capillarity effect reflects the interaction between the rock and fluids, controlled by pore geometry in such a case (Harrison and Jing, 2001).
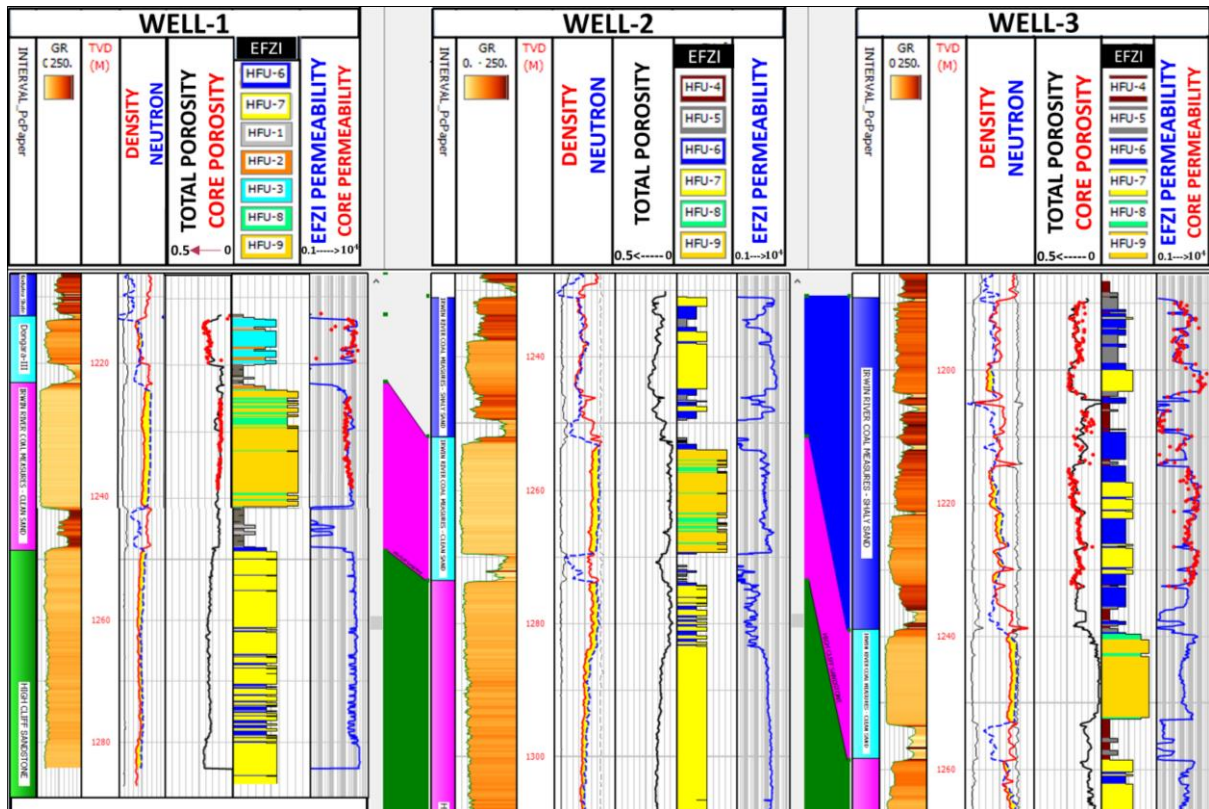
Figure 53: The EFZI classified facies and the calculated permeability showing very good match to the core permeability. Track-1: The GR log, scaled from 0 to 250 GAPI, with the shading indicating shaliness of the formation; Track-2: The density (red) scaled from (1.95 – 2.95 g/cc) and the neutron (blue) scaled from (0.45 – (-0.15)) according to the limestone scale; Track-3: The calculated total porosity (black) and where applicable, in wells 1 and 3, the core plug porosity (red dots) plotted showing very good match to log porosity; Track-4: The classified equivalent flow zone indicator facies (EFZI); Track-5: The EFZI permeability (blue) showing a good match with the core permeability (red) in wells 1 and 3, both scaled between 0.1 - 10,000 mD

5.3.3. Saturation Height Modeling

The saturation height modeling is considered another independent evaluation for the saturation profile from a completely independent source. In Cliff Head Field, the water saturation profile is representing the irreducible water saturation for all the reservoir intervals proven by well testing. Studying the capillarity behaviour of the various rock types revealed a connection to the permeability of the rock rather than the porosity. The EFZI methodology results have provided a quantitative facies heterogeneity model, with

which the calculated permeability has shown a great match with the core permeability. In the saturation height modeling process, two independent factors have been integrated to calculate a high-resolution water saturation profile above the free water level, which are the EFZI classified facies and the high-resolution permeability. The capillary pressure curves at reservoir conditions have been converted to the height above the free water level using equation 60. Following the conversion, the application of equations 63 to 66 yields an independent saturation profile in both cored and uncored wells.

Several combined thresholds between the permeability and the EFZI facies have been utilized to distribute the reservoir fluids into the rock at the different heights above the reservoir contact. The following equations represent the base upon which the models are selected using the lithofacies.

$$Swi_{RRT-1,4} = f(K(> 150 \leq 1000\ mD), HFU - 3\&7, 8\&9) \dots\dots\dots (73)$$

$$Swi_{RRT-2} = f(K(> 20 \leq 150\ mD), HFU - 2\&6) \dots\dots\dots (74)$$

$$Swi_{RRT-3} = f(K \leq 20\ mD, HFU - 1, 4\&5) \dots\dots\dots (75)$$

Figure 54 presents the results of the high-resolution saturation height modeling in the first 3 wells. The reservoir extends up to 71 meters true vertical thickness above the free water level in Well-3, which will help to test the integration methodology on a long vertical thickness for the reservoir section. Track-1 shows the Gamma-ray log; Track-2 shows the different water saturation logs calculated using 3 different methods, the yellow is the resistivity based SW, the red is the saturation height modeling SW dependent on the EFZI facies, and the black is the SWI from NMR interpretation.

The results have shown very interesting coherency where the log-based water saturation (Yellow) has matched the NMR irreducible saturation (Black) and the saturation height modeling (Red) in Well-1. This indicates valid Archie parameters and proves the validity of the variable NMR T2 Cutoff applied in the interpretation, calibrated to measured Archie parameters from the SCAL measurements. The saturation heigh model has shown extraordinary results upon a calibrated core facies and calibrated permeability log. In the Cliff Head Sandstone section above the FWL in Wells 1 and 2, the new saturation height model results showed the true saturation for such facies with thin transition zone matching the best quality rock type, which was not accurately addressed in the resistivity based saturation. The shaded red zones next to the depth track are representing the height above the free water level (1261 mSS) where Well-3 has encountered the thickest hydrocarbon thickness among the three wells. In Wells 2 and 3, the results have shown some variance relative to the log-based Simandoux saturation due to the that the resistivity is suppressed by the formation shaliness, which resulted in averaging the resistivity value for the sands and shales. On

the other hand, the Lower section in Well-3 below 1240 mSS in the clean tight reservoir of the Irwin River Coal Measures Formation shows the log-based SW lower than the modeled saturation. This is due to the formation tightness that affected the resistivity log values. Accordingly, the application of this workflow allows the calculation of the water saturation in the absence of any resistivity log in the borehole.
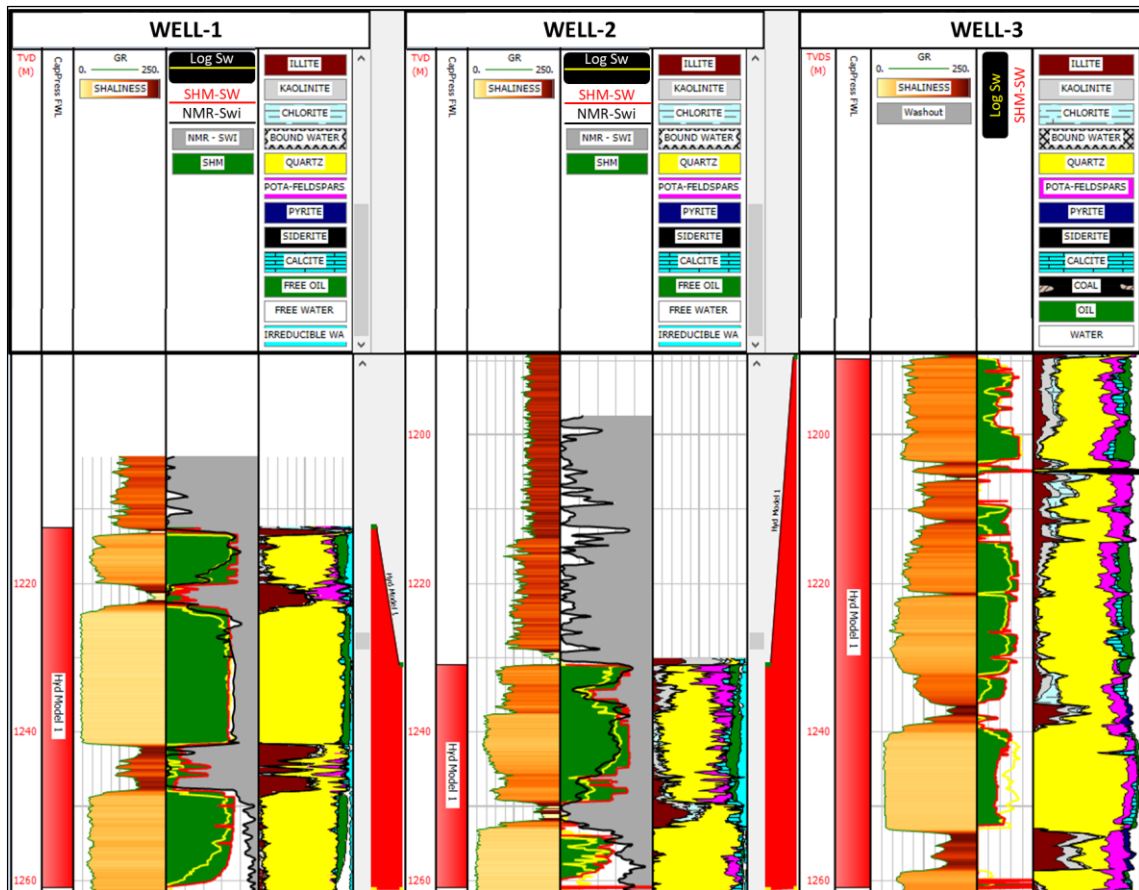
Figure 54: Saturation Height Modeling results based on the EFZI facies modeling. Track-1: The GR log scaled from 0 to 250 GAPI; Track-2: The calculated water saturation from the different applications, scaled from (1 – 0), first the resistivity based model (yellow), second the irreducible water saturation from NMR (black) and the saturation height modeling (red); Track-3: The mineralogical petrophysical modeling scaled from 0 to 1

The modeling workflow has been extended further and tested on the fourth well that was drilled horizontally through the shaly sand of the Irwin River Coal Measures Formation (**Figure 55**). The long section was drilled with an offset of 45 meters above the FWL, at the highest point of the trajectory, and encountered a complex facies variation along the lateral section. The reservoir shows high heterogeneity with high shale content and intercalation between shales and sands, which resistivity response will not account for. The modeled saturation profile has shown a much higher resolution saturation profile that is originally based on the core data and extended to the subject well.

It is believed that the methodology can be used as a high-resolution real time workflow to provide three petrophysical parameters of high challenge, the facies, the permeability, and the saturation profile all on high resolution mode.
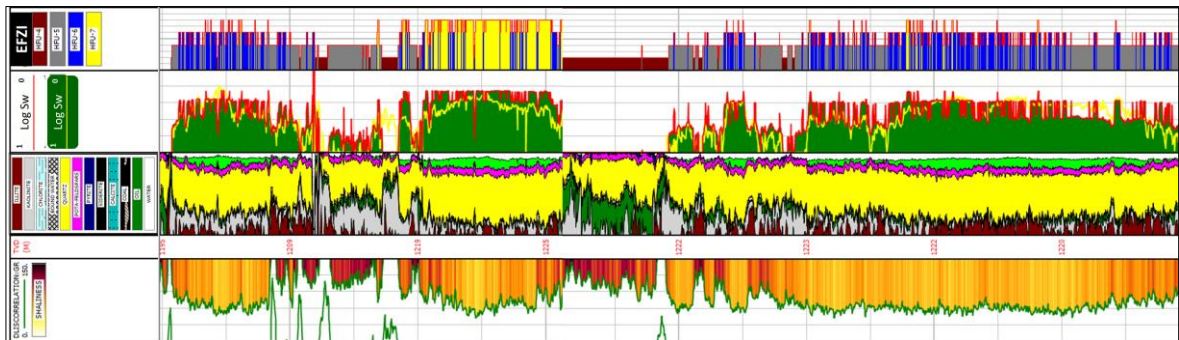
Figure 55: *Well-4 testing the EFZI-Based saturation height modeling through long horizontal well with high degree of facies variation. Track-1: The GR log scaled between 0 and 150 GAPI with shading indicating shaliness of the formation; Track-2: The mineralogical petrophysical modeling; Track-3: The calculated water saturation from the different applications scaled from $(1-0)$, the resistivity based model (yellow) and the saturation height modeling (red); Track-4: The EFZI classified facies*

5.4. Conclusions

An integrated workflow has been carried out to validate and reduce the uncertainty in the water saturation through the high heterogeneous formations. Four wells have been used to test the workflow that were drilled through the Early Permian clastics succession in the Perth Basin. The core capillary pressure data was found to describe 4 different reservoir lithofacies supported by core thin sections in 3 different formations. In the light of the identified lithofacies, the EFZI methodology was utilized to classify nine electrofacies across all the interested reservoir sands upon which the permeability log has been calculated. A very good match to the core permeability has been achieved. The water saturation involved a challenge to be accurately estimated for each reservoir facies due to the high irreducible saturation found in the shaly sands. Therefore, three methods were used to calculate the saturation profile; A resistivity-based water saturation, the NMR irreducible water saturation utilizing variable T2 cutoffs and an EFZI dependent saturation height modeling. The results were found to be very encouraging supported by an extended Drill Stem Test during which negligible to oil-free water was produced for a long period of time. The integrated workflow was tested in Four wells of different degrees of complexity, which showed very consistent results. The EFZI dependent saturation height modeling is proven very effective tool to estimate the water saturation in high heterogeneous rocks, which can be extended to any uncored wells. The workflow can be used as a real time estimation for the permeability and saturation profiles in deviated and horizontal wells in the absence of formation resistivity log.

Chapter-6: Discussion and Conclusion

6.1. Research Outcome

This chapter aims to discuss the results of the previous publications and summarise the research project. The research aimed to design a better approach to integrate the petrophysical inputs in modernised workflows; further, to perform the best possible interpretation to the data to generate the least uncertain outputs. It is found that simple workflows can perform relatively wells in simple reservoirs, when it comes to heterogeneity, formation saturation and permeability are very hard to calculate with reasonable accuracy. Therefore, techniques in the research aimed to generate workflows that allow those two parameters to be linked to the reservoir lithofacies, in the best modelled facies scheme possible.

The mineralogical interpretation, known as inversion modeling, is found to be the best approach in case core measurements are available, either routine or special core analysis, in addition to the geological description, studied core thin sections, or advanced suite of logging tools. The best output would be indeed possible in knowing how to employ each dataset effectively in the interpretation. A contradiction between the formation evaluation and either geology or engineering indicates a deficit that requires assessment, whether at an early stage or later stage of the analysis.

To perform the best evaluation for complex reservoirs, the lack of core measurements is used to obstruct the generation of valid outputs. The research has confirmed the possibility to characterise the complex reservoirs with the least uncertainty upon depending on valid reservoir facies description, which can be related to logs. The integration between a robust formation density logged on high resolution mode, and the free fluid volume measured from NMR generates a continuous log that holds information about reservoir electrofacies. Studying the geological description, which is available from different sources such as cuttings, or core thin sections done on cuttings or core, can connect the electrofacies to the lithofacies. Accordingly, a high resolution facies log can be calculated in any number of wells provided they encountered the same formation. A very detailed permeability modeling can be done through this methodology with high accuracy. In the availability of rock capillary measurements for different rock types, the water saturation can be calculated using saturation height modeling dependent on the generated facies. Where a well test data is available, solid information becomes in hand that allows calibration for the results, and powerful guidance towards the reservoir's irreducible water saturation.

6.1.1. Petrophysical Analysis Overview

The petrophysical analysis for the studied reservoir was performed using the inversion mineralogical modeling with the integrated facies and core analyses, but both

the permeability and water saturation were calculated using different methods. **Table 8** presents the final petrophysical parameters from all the used methods. The net calculation results have confirmed the accuracy from the presented analysis in the last chapters and indicated where the differences existed. Firstly, the net pay calculation was done using the NMR porosity and Swi in one model, and the inversion analysis in another. Both calculations show very similar net pay except where a contact was encountered in Well-2 clean sand interval. However, when it comes to the reason to perform the petrophysical analysis, and how this affects the bigger goal of prospect evaluation and volumes for a reservoir rock, the net pay does not dictate any areas away from the borehole locations, while the parameters themselves, porosity, clay volume, saturation and permeability, translate the fluid volume and its flow path in the 3D area. The difference in formation porosity is very little between the NMR and the inversion analysis, which did not exceed 1.6% in Well-1 Dongara Sandstone. This confirms consistency between the porosity measured by NMR and the calculated porosity.

On the other hand, the water saturation results are interesting as it reflects what was discussed in Chapter-5 for wells 1 and 2 where the log-based saturation matched the NMR irreducible saturation in the shaly sand. The maximum difference observed is 2.6% only in Well-2, which indicates correct parameterisation in the interpretation. In Well-2 in the clean sand, the NMR saturation becomes much lower than the log-based saturation due to the encountered contacts in such zone, with which effectively the NMR is providing a different parameter (Swi) than the inversion analysis (Resistivity Log-Based Sw). The saturation height model showed average saturation ranges between 5 to 12 units less amongst all the wells in the shaly sands. The saturation height model by its nature represents the true saturation that is dependent on the matched facies at a certain reservoir height, irrespective of resistivity, depending on true core capillary pressure measurements. When the resistivity log was not affected much by the existing clays in the reservoir (e.g.: the clean sands of the Irwin River Coal Measures in all wells), the difference diminishes to 1% as seen in wells 1, 3 and 4.

The permeability by far is of the largest uncertain parameter of all. A clear large difference between the NMR permeability index and the EFZI model can be observed in wells 1 and 2. Despite this confirms that any permeability resulted from the NMR log is only indicative and can be far from being accurate, it does reflect the importance of characterising complex reservoirs before issuing permeability figures depending on any wireline or LWD log. As discussed in Chapter-3, the one possible figure that may reflect the reservoir permeability is the one driven from the well test analysis in the value of (Permeability*Thinkness) in mD.ft., otherwise core is the best option to reflect permeability value for each depth. From the listed parameters, the core average permeabilities shown in the last column for wells 1 and 3 are closely matching the EFZI permeability model. The EFZI model can be dependent on logs only as indicated in Chapter-4. However, without the existence of at least one NMR log in the studied area, such a methodology cannot be carried out.

One of the best outcomes from the EFZI method is the possibility to calculate the final parameters for each facies separately. This provides an immediate view of the distinct differences between the classified facies groups. **Table 9** presents the petrophysical parameters for the Dongara Sandstone and the Irwin River Coal Measures Formation through the clean and the shaly sands.

The calculated formation porosity shows a 1 to 2% difference between the wells in the shaly sands. Yet the permeability exhibits very large variations of several orders of magnitude. Dongara Sandstone shows 2% porosity variation between RRT-1 and RRT-2, with an average porosity of 16% indicating moderate formation porosity. The permeability in the formation shows a significant reduction from 741 to 187 mD for the two rock types respectively. In the shaly sands of the Irwin River Coal Measures Formation, RRT-1 and RRT-2 still have a porosity difference of a maximum 2%, whereas the permeability difference has reached up to 800% between the two rock types. RRT-1 average porosities still show high values relative to the good rock types and could be very similar (e.g.: Well-5 porosity is 17%), but the permeability exhibits few millidarcies reflecting much tighter rock. Nevertheless, the flow is still possible from this poor rock type should hydrocarbons are proven with good offset above the free water level.

Further, the water saturation for each rock type can be identified separately to reflect the existing potential for each. A clear difference in the values exists between the rock types where the best quality rock holds the highest hydrocarbon saturation. Some of the wells have very good potential in poorer rock types (e.g. Well-4 shaly sands) where the water saturation is between 48 to 50% for all the facies. This can significantly help in production planning in such complex reservoirs, and help to identify the best zones to advance to production stages relative to others.

With such parameterisation method, an immediate view over the expected reservoir flow would be available, which supports both geoscience and engineering disciplines to quickly detecting any possible water source and mitigate the reservoir existing risks. Hence, supporting reservoir best performance.

Table 8: Petrophysical Parameters in the Dongara Sandstone and the Irwin River Coal Measures

Well	Zone Name	Analysis	Gross	Net Pay	N/G	Av. Phi	Av. Sw	Av. Vcl	Av. Perm	Core Perm
			(M.)	(M.)	(v/v)	(v/v)	(v/v)	(v/v)	(mD)	(mD)
Well-1	Dongara Sandstone	SHM	10				0.26			
		Inversion		5.83	0.59	0.164	0.376	0.1	505.356	410
		nmrSwi		5.8	0.584	0.148	0.36		22.454	
	IRCM - Clean Sand	SHM	25				0.339			
		Inversion		17.38	0.689	0.093	0.328	0.001	285.262	205
		nmrSwi		16.84	0.667	0.086	0.31		6.236	
Well-2	IRCM – Shaly Sand	SHM	21				0.32			
		Inversion		11.99	0.574	0.18	0.441	0.102	227.564	
		nmrSwi		12.17	0.583	0.167	0.415		13.534	
	IRCM – Clean Sand	SHM	22				0.47			
		Inversion		0.92	0.043	0.06	0.539	0.043	61.858	
		nmrSwi		8.37	0.388	0.058	0.267	Contact	0.424	
Well-3	IRCM – Shaly Sand	SHM	50				0.38			
		Inversion		23.9	0.481	0.186	0.43	0.112	212.437	165
	IRCM – Clean Sand	SHM	19				0.465			
		Inversion		1.83	0.094	0.069	0.45	0.001	65.305	
Well-4	IRCM – Shaly Sand	SHM	29				0.384			
		Inversion		5.96	0.207	0.203	0.491	0.091	357.594	
	IRCM – Clean Sand	SHM	18				0.466			
		Inversion		4.67	0.253	0.128	0.476	0.034	795.121	
Well-5	IRCM – Shaly Sand	SHM	54				0.372			
		Inversion		26.5	0.487	0.171	0.432	0.208	74.173	

Table 9: Petrophysical Parameters classified by facies in the Dongara Sandstone and the Irwin River Coal Measures

Well	Reservoir	Total Thickness	Net Pay	Net Sand	Average Porosity (V/V)			Average Water Saturation (V/V)			Average Clay Volume (V/V)			Average Permeability (mD)		
		TVD (M.)	(M.)	(M.)	RRT-1	RRT-2	RRT-3	RRT-1	RRT-2	RRT-3	RRT-1	RRT-2	RRT-3	RRT-1	RRT-2	RRT-3
Well-1	Dongara Sandstone	9.95	5.83	6.65	0.17	0.15	0.18	0.37	0.42	0.37	0.08	0.18	0.11	740.6	186.9	93.35
	IRCM - Clean Sand	25.25	17.38	20.20	0.09	0.09	0.08	0.33	0.77	0.86	<0.01	0.14	0.25	285.3	34.16	6.46
Well-2	IRCM - Shaly Sand	20.89	11.99	18.42	0.18	0.17	0.11	0.42	0.52	0.73	0.10	0.11	0.26	287.4	38.04	1.09
	IRCM - Clean Sand	21.56	0.92	11.57	0.06	0.05	0.09	0.54	0.91	0.94	0.05	0.08	0.21	60.80	1.14	0.43
Well-3	IRCM - Shaly Sand	49.73	23.9	44.54	0.20	0.18	0.16	0.38	0.48	0.52	0.09	0.13	0.20	401.2	50.03	3.45
	IRCM - Clean Sand	19.42	1.83	5.60	0.04	0.10	0.10	0.40	0.83	0.98	<0.01	0.05	0.26	21.24	6.07	0.36
Well-4	IRCM - Shaly Sand	28.73	5.96	23.95	0.21	0.20	0.15	0.49	0.50	0.48	0.08	0.14	0.09	435.9	66.69	1.17
	IRCM - Clean Sand	18.47	4.67	12.93	0.13	0.10	0.10	0.48	0.97	1.00	0.03	0.20	0.22	795.1	5.89	0.47
Well-5	IRCM - Shaly Sand	54.36	26.50	43.14	0.18	0.17	0.17	0.42	0.42	0.46	0.14	0.21	0.27	313	43.30	3.67

For a further presentation of the reservoir's important parameters, histograms have been used to interpret the results of the permeability and water saturation. "*Histograms are a useful tool for illustrating variation in a log reading and properties that are derived from it. Even if they are not used to pick parameters, histograms are used to show how properties are distributed*" (Kennedy, 2015). Currently, each software platform includes a module that allows users to plot histograms due to its effectiveness in understanding the results of the analysis. **Figure 56** presents the permeability results in all the wells for the EFZI permeability (blue) and the NMR permeability index (yellow) where the NMR tool was logged in the interested section. From all the graphs, the EFZI permeability has described the low and the high permeable zones much better compared to the NMR permeability index. In fact, the NMR permeability seems to follow a limitation of around 100 mD, driven by the calculated Free fluid from NMR interpretation relative to the bound fluid volume. In the wells 3 to 5 where no NMR logs were available, The EFZI permeability has described a very wide range of values dependent on the core integration and the EFZI classified facies. In the horizontal well (Well-5), high permeability range prevails the histogram as the majority of the section was targeting obviously the best sand units possible. Nevertheless, when the quality of the sands degraded, the EFZI model was able to identify the difference very well.

Similarly, the water saturation from the models applied have been compared to each other on histograms as per **Figure 57**. Wells 1 and 2 have been integrated with one plot to show the variation between the modelled saturations. A clear coherency was observed between all models, with obvious concentrated lower saturation values for the saturation height modeling reflecting the good facies encountered in Well-1 Dongara Sands and the clean sands of the Irwin River Coal Measures.

Well-3 shows a good match between the saturation height model and the mineralogical analysis, which confirms the little variance from Table-8. The saturation height in wells 4 and 5 shows lower values, with coherence towards the high water saturation generally. This indicates the resolution of the saturation height has seen the better layered facies in the reservoir and assigned the correct water saturation value at the different heights above the free water level. Further, this matches the higher permeability values that prevailed in Well-5 due to the horizontalization in the best sand layers.
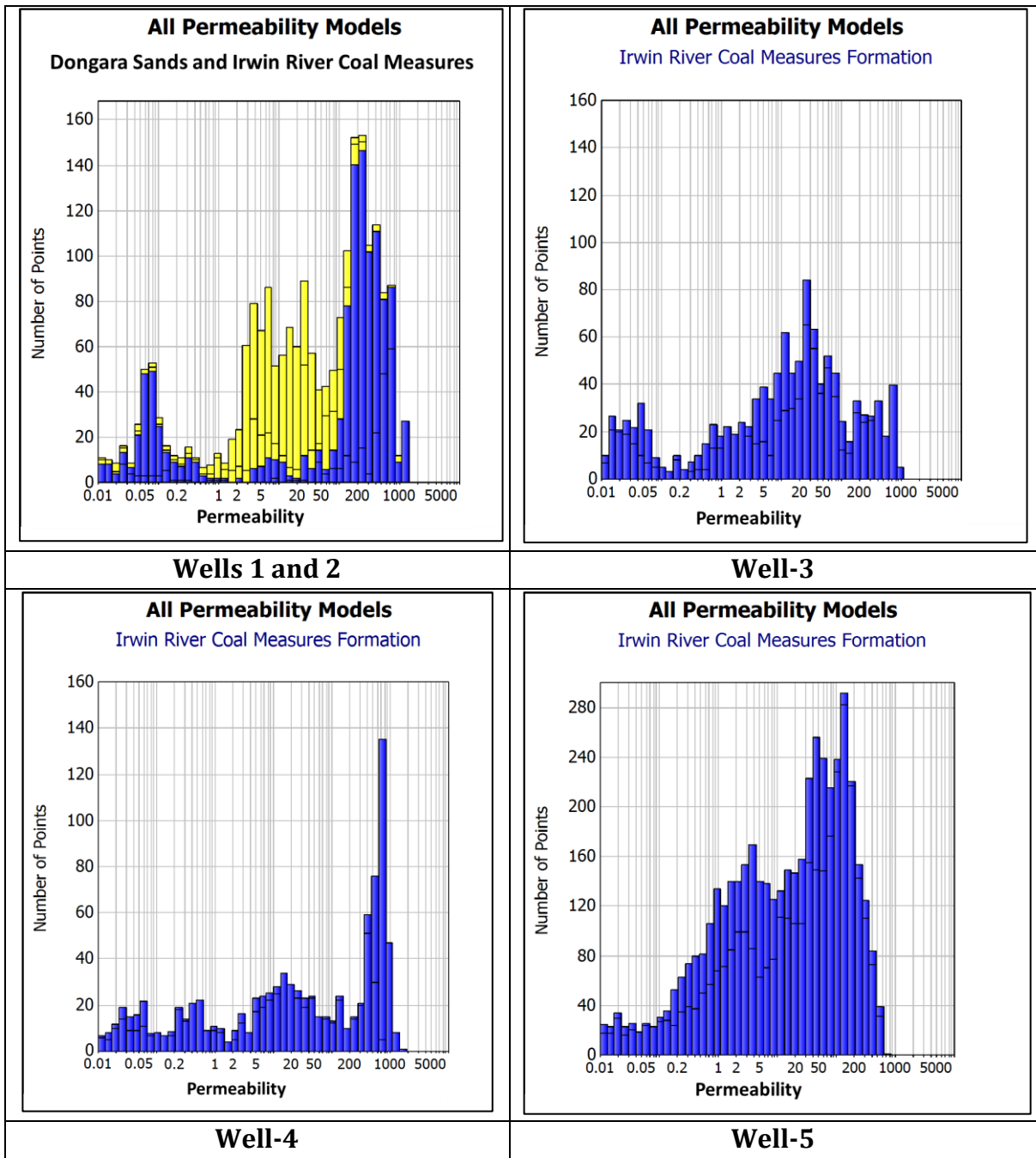
Figure 56: The permeability results (Wells 1 to 5) for two models, the EFZI permeability (blue) and the NMR permeability index (yellow)

| Wells 1 and 2 | Well-3 |
| Well-4 | Well-5 |
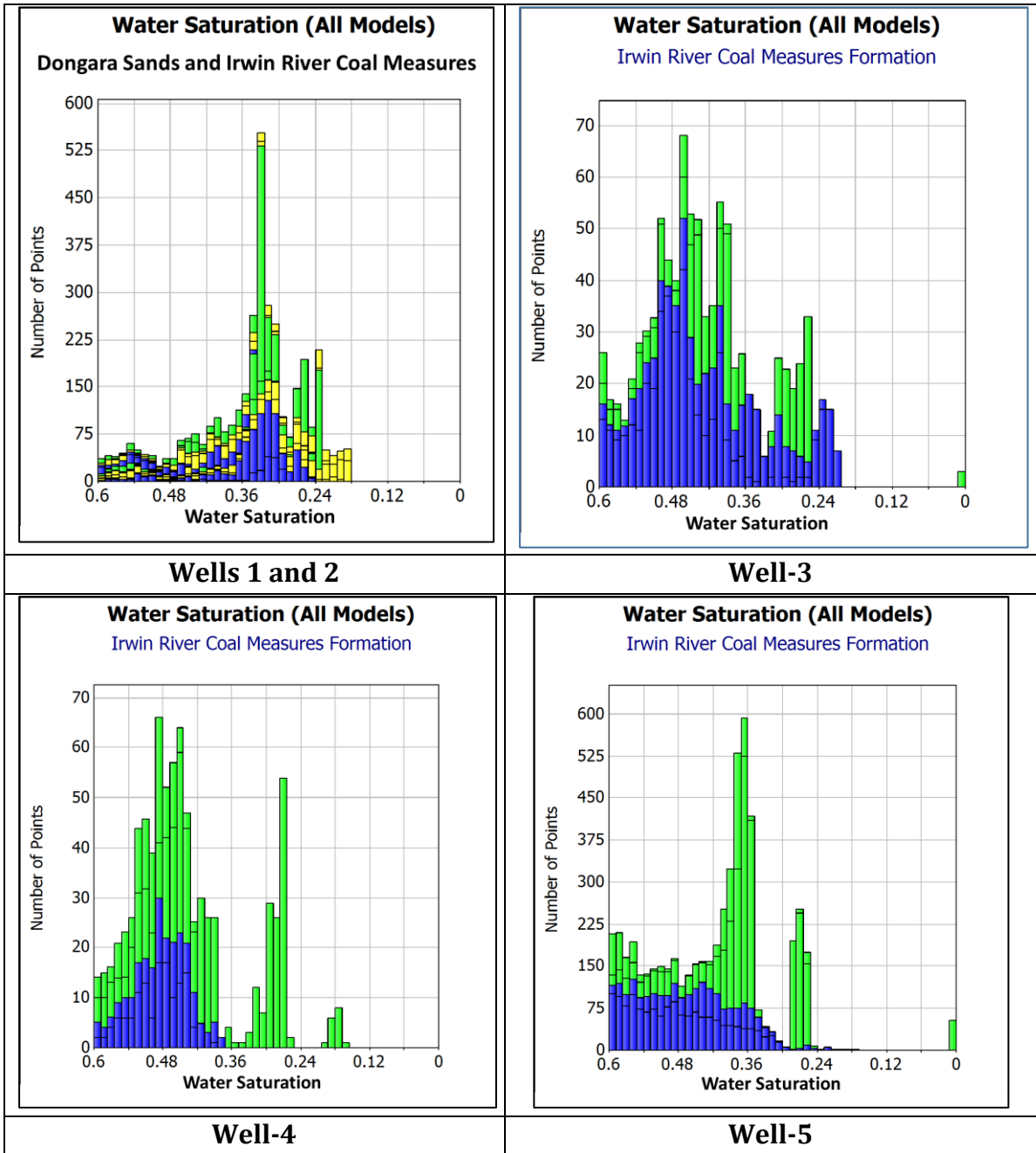
Figure 57: *Water saturation in Cliff Head Field wells from all models; The inversion mineralogical model (blue), the Swi from NMR interpretation (yellow) and the saturation height modeling (green)*

6.1.2.   Core Analysis Results

In the evaluation of Wells 1 and 3, the routine core measurements were used as a reference to calibrate the log interpretation. The mineralogical inversion seems to achieve very good results matching the core porosity. **Figure 58** shows Well-1 porosity match through the shaly sands of the Dongara and the clean sands of the Irwin River Coal Measures. A correlation coefficient of 0.85 could be achieved. On the other hand, in Well-3 the correlation coefficient for analysis achieved a 0.81 value as per **Figure 59**. This reflects that upon good selection for the minerals used in the modeling, a very good match can be achieved to the core porosity in shaly sands of high heterogeneity.

For the permeability comparison, the EFZI permeability was plotted versus the stressed core permeability in Well-1 (**Figure 60**) and Well-3 (**Figure 61**). A very good correlation coefficient can be observed with the core permeability of 0.71 and 0.83 for Wells 1 and 3 respectively.
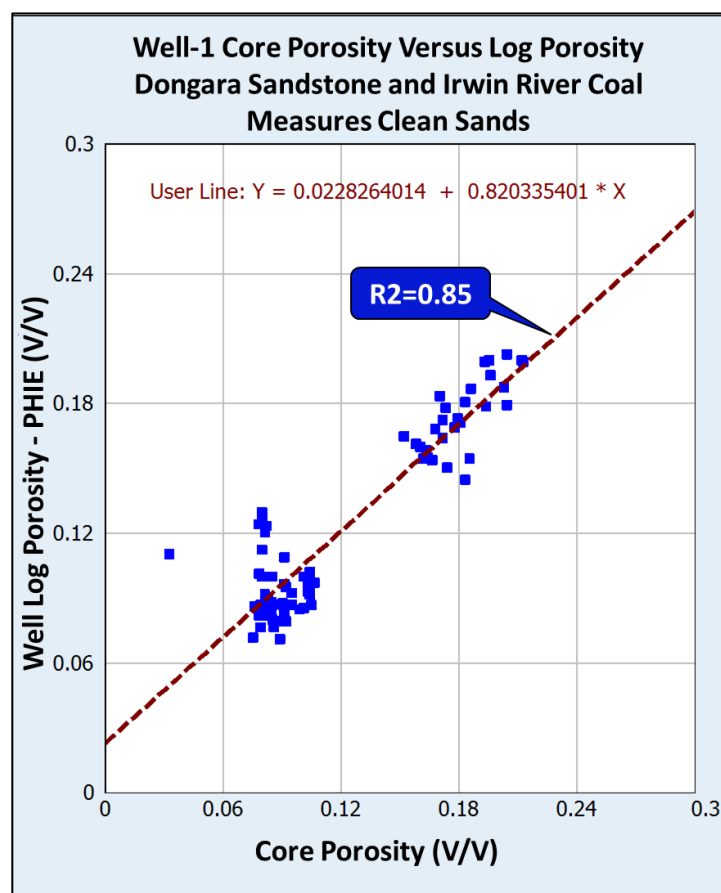
Figure 58: Well-1 core porosity versus total log porosity from the inversion analysis
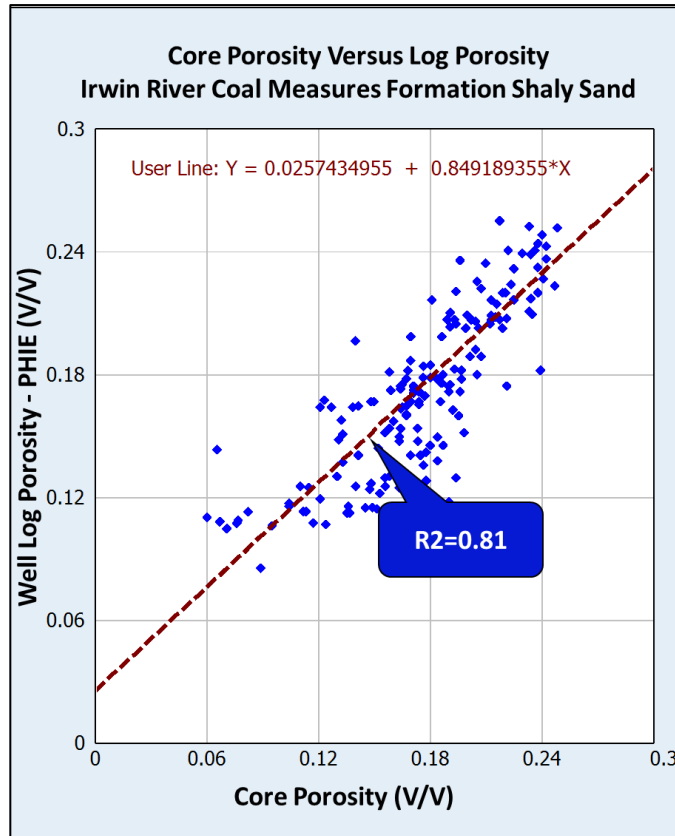
Figure 59: Well-3 shaly sands core porosity versus total log porosity from the inversion analysis
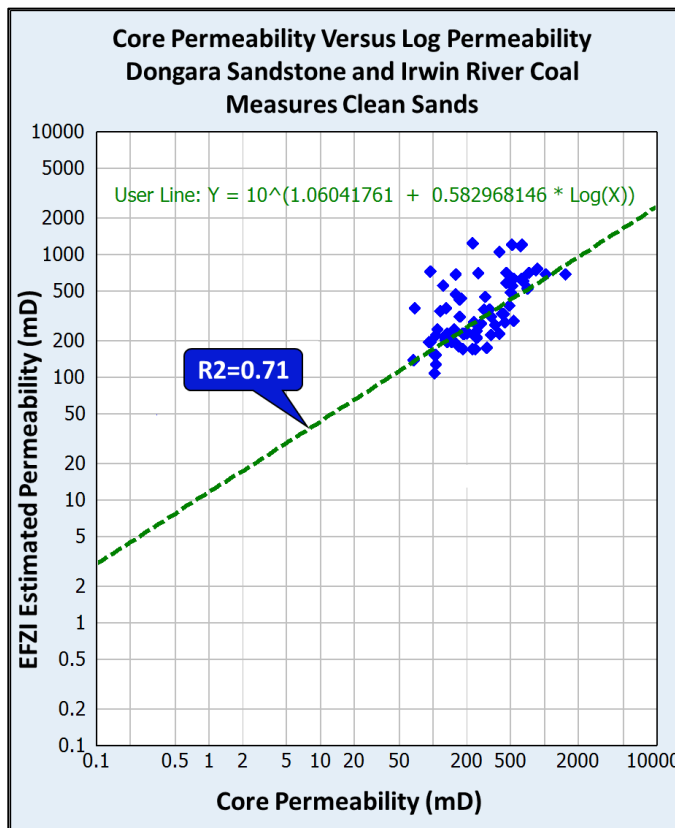
Figure 60: Well-1 core permeability versus EFZI permeability
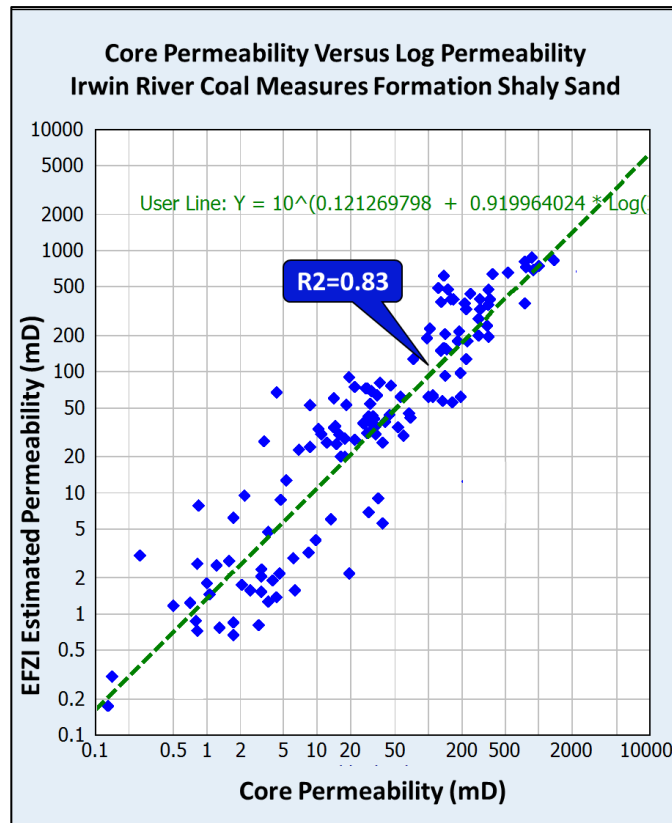
Figure 61: *Well-3 core permeability versus EFZI permeability*

6.2. Modeling Possible Problems

In the techniques applied through the research project, different datasets logged and analysed by different vendors were used to achieve the consistent formation characterisation study. Accordingly, with very high confidence the techniques used are very efficient in characterising complicated reservoirs. Nevertheless, there are possible issues that may result in compromised analysis for the high resolution facies, upon which the permeability and the saturation calculated depending on the electrofacies would include uncertainty. Below is a possible list of problems that may lead to compromised results:

- Enlarged boreholes that may lead to high washouts in the pad tools, including density and neutron
- High washed out intervals and boreholes will significantly affect the NMR tools, regardless of the vendor, and will lead to very wrong estimation for the free fluid index and or the total porosity
- Lack of valid density and neutron logs in any well will affect the results severely. If the density only is not logged in a well, the sonic or the neutron can be used to generate the EFZI facies. Nevertheless, the lithology confidence will be lower than normal, and uncertainty will exist in the results.

- Lack of density and neutron logs will lead to deficit in the subsequent distribution for the EFZI facies in the uncored wells, or the wells to which the modeling will be applied.
- Lack of high resolution density log will reduce the resolution of the classified electrofacies. Different vendors can log the density tools on slower speeds, as low as 900 ft/hour. If the speed of the tool exceeded this limit, lower resolution densities will be logged, which will certainly affect the subsequent electrofacies resolution.
- In the workflow that is dependent on logs, mobilities are very uncertain measurements that depends on the build-up trends of the pressure measurements from the Repeat Formation Tester logging tools. The mobilities need to be converted to permeability using the reservoir fluid viscosity. If the viscosity value for the reservoir fluid is not present, assumptions may lead to high uncertainty in the source of calibration for the permeability trends. An introduced correction factor for the RFT mobilities driven from the core measurements is a possible solution, in case they are present, which can be applied to all the uncored wells.

For future considerations, the techniques used were applied on clastics reservoir section of high heterogeneity. It is believed the EFZI method would achieve great results in carbonates, but it has not been tested in the data used in this project. Testing the methodology in carbonates would help significantly the industry, as such reservoirs have the typical signature of poor correlations between the porosity and permeability, where high permeability zones may be found in lower porosities and vice versa. Core measurements need to be available for such exercise, with valid special core measurements for Archie parameters, wettability and capillary pressure data.

6.3. Research Conclusions

Different new integrated workflows have been generated and discussed in detail with the aim to produce high resolution facies for complicated reservoirs. The shaly sands of the Early Permian Irwin River Coal Measures Formation in Cliff Head Field has been chosen to test the methodology utilising 5 wells that have different challenges. The different suite of conventional and advanced logging tools have been integrated with which a high resolution electrofacies modeling was obtained. The classified electrofacies were tested using different datasets between conventional core measurements, core thin sections and capillary pressure measurements. Nine electrofacies were classified for Cliff Head field clastics that were all related perfectly to the geological lithofacies, with an aim to ensure an existing consistency between petrophysics and geology. The reservoir permeability variation is found to be complicated in the reservoir section, with which 9 permeability models were generated and matched to the core measurements where a very good match was achieved.

Studying the water saturation in complicated reservoirs requires integration between petrophysics and reservoir engineering well test analysis. Higher or lower water production that is opposite to the log interpretation means high uncertainty in the water

saturation calculation. Hence, high uncertainty in the subsequent volumetric estimation. On the other hand, understanding the existing reservoir facies allows good prediction and understanding for the productivity of those rock types, where the nearest contacts are for each defined facies and any possibility of high or low flow from certain formation layers. As a result, quantitative production profiles can be well established at the early stages of the fields' reservoir management. Accordingly, three different models were calculated using the inversion mineralogical interpretation, NMR irreducible saturation and saturation height modeling dependent on the classified electrofacies. The accuracy of the calculated saturation was tested against a conducted well test in Well-1, during which the reservoir produced 3000 barrels of oil per day with negligible to no water cut. High consistency between the models was found that supported the petrophysical analysis and the saturation characterisation.

The methodologies established based on the two cored wells in the field were applied to the other three uncored wells used this study. A significant improvement was observed in the calculated permeability and saturation dependent on the electrofacies. Furthermore, the workflow can confidently be used on real time basis in any well trajectory, particularly in horizontalization activities to predict and design geosteering operations in complex formation environments.

Nomenclature

BVW	Bulk volume of water
BFE	Effective Bound Fluid
CBFT2cut	Clay bound water cutoff
COPO_ob	Overburden core porosity
$DPHI$	Density porosity
DRHO	Density log correction
DRT	Discrete Rock Type
EFZI	Equivalent Flow Zone Indicator
FFI	Free fluid index
FZI	The Flow Zone Indicator
FWL	Free Water Level
$HAFWL$	Height above free water level
HDRA	Density log correction
HFU	Hydraulic Flow Unit
J	Leveret-J Function
k	Plug permeability
K	Kaolinite
POTA-Feldspars	Potassium Feldspar
IRCM	Irwin River Coal Measures
K	Kaolin
KF	Potassium Feldspar
Kkl_ob	Overburden core permeability
MLR	Multi-Linear Regression
mD	Millidarcy
mSS	Meters below Subsea Level
(m)	Archie cementation Exponent
NMR	Nuclear Magnetic Resonance
nmrPhiB	NMR porosity bins
nmrFF	NMR free fluid
nmrPhie	NMR effective porosity
nmrT2M	NMR T2 logarithmic mean
nmrFacies_mlr	The nmr facies from the multi-liner regression, equivalent to the EFZI log
(n)	Archie saturation exponent
NMR	Nuclear Magnetic Resonance
NPHI	Neutron porosity
$NPHI_{fl}$	Neutron porosity log reading in 100% water
$NPHI_{ma}$	Matrix Neutorn porosity
$NPHI_{sh}$	Shale Neutron porosity
Pc	Capillary pressure
PHIE	Effective porosity
$PHIE_{NMR}$	Effective porosity from NMR interpretation
PHIT	Total porosity
PEF	Photoelectric factor
PHIE	Effective porosity
PHIT	Total porosity
PP	Primary porosity
PP	Primary porosity
p.u.	Porosity Units

QO	Quartz overgrowth
SP	Secondary porosity
RESD	Deep resistivity
RESM	Shallow resistivity
RESS	Micro-resistivity
RRT	Reservoir Rock Type
RESD	Deep resistivity
RESM	Shallow resistivity
RESS	Micro-resistivity
RHOB	Bulk density
SP	Secondary porosity
SCAL	Special Core Analysis
SHM	Saturation Height Modeling
s.u.	Saturation Units
Swi	Irreducible Water Saturation
Swi_{NMR}	Irreducible Water Saturation calculated from NMR interpretation
SW_Ht	Saturation height modeled water saturation
T2CUTOFF	Free fluid cutoff
T2-Dist	T2 Distribution log from the nuclear magnetic resonance tool
VClay	Volume of clay
Vsh	Volume of Shale
T2-Dist	T2 Distribution log from the nuclear magnetic resonance tool
φ	The formation porosity
φ_z	The normalized core porosity
ρ_{ma}	Matrix density
ρ_{fl}	Fluid density
ρ_b	Bulk density log
ρ_{oil}	Oil density
ρ_{sh}	Shale density
ρ_{Water}	Water density
σ	Interfacial Tension
θ	Contact angle
QO	Quartz overgrowth
$\emptyset$	The porosity
φ_z	The normalized core porosity
ρ_{ma}	Matrix density
ρ_{fl}	Fluid density
ρ_b	Bulk density log

References

Abbaszadeh, M., Fujii, H., and Fujimoto, F., 1996, Permeability Prediction by Hydraulic Flow Units - Theory and Applications, SPE-30158-PA, *Society of Petroleum Engineers Journal*, **11** (4), https://doi.org/10.2118/30158-PA

Amaefule, J.O., Kersey, D.G., Marschall, D.M., Powell, J.D., Valencia, D.K., and Keelan, D.K., 1988, Reservoir Description: A Practical Synergetic Engineering and Geological Approach Based on Analysis of Core Data, Paper SPE-18167, Presented at 63rd Annual Technical Conference and Exhibition of Society of Petroleum Engineers, Houston, Texas, 2-5 October.

Amaefule, J.O., Altunbay, M., Tiab, D., Kersy, D.G., and Keelan, D.K., 1993, Enhanced Reservoir Description: Using Core and Log Data to Identify Hydraulic (Flow) Units and Predict Permeability in Uncored Intervals/Wells, Paper SPE-26436, Presented at 68th Annual Technical Conference and Exhibition of the Society of Petroleum Engineers, Houston, Texas, 3-6 October.

Al-Ajmi, F.A., and Holditch, S.A., 2000, Permeability Estimation Using Hydraulic Flow Units in a Central Arabia Reservoir, Paper SPE-63254, Presented at the Annual Technical Conference and Exhibition of the Society of Petroleum Engineers, Dallas, Texas, 1-4 October.

Ahmed, T., 2001, Reservoir Engineering Handbook, Second Edition, Chapter 4, Fundamentals of Rock Properties, pp. 183 – 279 Gulf Professional Publishing Company, Houston, Texas, 2001, ISBN 0-88415-770-9, Published by Gulf Professional Publishing, Imprint of Butterworth-Heinemann. 225 Wildwood Avenue, Woburn, MA 01801–2041

Al Hinai, A., Rezaee, R., Saeedi, A., and Lenormand, R., 2013, Permeability Prediction from Mercury Injection Capillary Pressure: An Example from The Perth Basin, Western Australia, *APPEA Journal*, **53** (2013) 31 - 36. http://hdl.handle.net/20.500.11937/30149

Archbold, NW 1997, Studies on Western Australian Permian Brachiopods 14. The fauna of the Artinskian High Cliff Sandstone, Perth Basin: Proceedings of the Royal Society of Victoria v. 109, p. 199–231.

Archie, G., E., 1942, The Electrical Resistivity Log As an Aid in Determining Some Reservoir Characteristics, Trans. **146** (1942): pp. 54–62. doi: https://doi.org/10.2118/942054-G

Barson, D., Christensen, R., Decoster, E., Grau, J., Herron, M., Herron, S., Guru, U., K., Jordan, M., Maher, T. M., Rylander, E., and White, J., 2005 Spectroscopy: The Key to Rapid, Reliable Petrophysical Answers, Schlumberger Oilfield Review, Published in Summer 2005.

Bassiouni, Z., 1994, Theory, Measurements, and Interpretation of Well Logs, SPE Textbook Series Vol.4, Published by First Printing Henry L. Doherty Memorial Fund of AIME, Society of Petroleum Engineers, Richardson, Texas, 1994, 372 p.

Baker Hughes, 2018, MR Explorer Magnetic Resonance Service, https://www.scribd.com/document/462049565/mrex-bro

Bergmark, S. L. & Evans, P. R., 1987 - Geological controls on reservoir quality of the northern Perth Basin. *Australian Petroleum Exploration Journal*, 27(**1**), pp. 318-330

Bhatti, A., A., Ismail, A., Raza, A., Gholami, R., Rezaee, R., Nagarajan, R., and Saffou, E., 2020, Permeability Prediction Using Hydraulic Flow Units and Electrofacies Analysis, *Journal of Energy Geoscience*, **1** (2020) 81 – 91, https://doi.org/10.1016/j.engeos.2020.04.003

Bowen, D., G., 2003, Formation Evaluation and Petrophysics, Chapter-3. Section-1, Formation Evaluation and Log Analysis, pp. 170 – 175.

Cannon, S., 2016, Evaluation of Lithology, Porosity and Water Saturation, Chapter-6, Petrophysics: A Practical Guide, John Wiley & Sons, Incorporated, 2015. ProQuest eBook Central, https://ebookcentral.proquest.com/lib/curtin/detail.action?docID=4038302

Clarke, E., de, C., Prendergast, K., L., Teichert, C., and Fairbridge, R., W., 1951, Permian Succession and Structure in the Northern Part of the Irwin River Area, Western Australia, *Journal of The Royal Society of Western Australia*, **35** (1951) 31 – 84. https://www.biodiversitylibrary.org/part/299451

Claverie, M., Hansen, S., Daungkaew, S., Prickett, Z., Akinsanmi, O., and, Pillai, P., 2007, Applications of NMR Logs and Borehole Images to the Evaluation of Laminated Deepwater Reservoirs, Presented at the Society of Petroleum Engineers Asia Pacific Conference and Exhibition Held in Jakarta, Indonesia, October 30 – November 1, 2007, SPE-110223, pp. 1 - 15

Coates, R., G., Ziao, L., and, Prammer, M., G., 1999, NMR Logging Principles and Applications, Halliburton Energy Services Publication H02308, Houston, USA.

Coates, G., R., and, Dumanoir, J., L., 1973, A New Approach to Improve Log-Derived Permeability, Presented at the Society of Petrophysicists and Well Log Analysts 14th Annual Logging Symposium, May 6 – 9, 1973.

Darling, T., 2005, Well Logging and Formation Evaluation, Chapter-2: Quicklook Log Interpretation, pp. 29 – 48, Chapter-5: Advanced Log Interpretation Techniques, pp. 67 – 102, Gulf Professional Publishing; ISBN: 0-7506-7883-6, Imprint of Elsevier, 30 Corporate Drive, Suite 400, Burlington, MA 01803, USA, Linacre House, Jordan Hill, Oxford OX2 8DP, UK

Davis, G., Newbould, R. Lopez, A., Hadibeik, H., Guevara, Z., Engelman, B., Balliet, R., Ramakrishna, S., and Imrie, A., 2018, An Integrated Formation Evaluation Approach to Characterize a Turbidite Fan Complex: Case Study, Falkland Islands, presented at the 59th Annual Logging Symposium of the Society of Petrophysicists and Well Log Analysts, London, UK, June 2-6.

Desouky, S., 2003, Predicting Permeability in Un-Cored Intervals/Wells Using Hydraulic Flow Unit Approach, Paper OMC 2003-118, Presented at the Offshore Mediterranean Conference and Exhibition in Ravenna, Italy, 26-28 March.

Elkhateeb, A., Rezaee, R., and Kadkhodaie, A., 2019, Prediction of High-Resolution Facies and Permeability, An Integrated Approach in the Irwin River Coal Measures Formation, Perth Basin, Western Australia, *Journal of Petroleum Science and Engineering*, **181** (2019) 1-12. https://doi.org/10.1016/j.petrol.2019.106226

Elkhateeb, A., Rezaee, R., and Kadkhodaie, A., 2019, Log Dependent Approach to Predict Reservoir Facies and Permeability in a Complicated Shaly Sand Reservoir, Presented at the Australasian Exploration Geoscience Conference Held in Perth, Australia, September 2 – 5, 2019, https://doi.org/10.1080/22020586.2019.12072924

Elkhateeb A., Rezaee R., and Kadkhodaie A., 2021, A New Integrated Approach to Resolve the Saturation Profile Using High-Resolution Facies in Heterogeneous Reservoirs, *Journal of Petroleum*, 2021, pp. 1-12. https://doi.org/10.1016/j.petlm.2021.06.004

Freedman, R., 2006, Advances in NMR Logging, *Journal of Petroleum Technology*, **58** (1): 60 - 66, DOI:10.2118/89177-MS

Freedman, R., and Morriss, C., E., Processing od Data From NMR Logging Tool, Presented at the Society of Petroleum Engineers Annual Technical Conference and Exhibition Held in Dallas, United States, October 22 – 25, Paper SPE-30560, 1995, pp. 1 - 16

Harrison, B., and Jing, X., D., 2001, Saturation Height Methods and Their Impact on Volumetric Hydrocarbons in Place Estimates, Presented at the Society of Petroleum Engineers Annual Technical Conference and Exhibition Held in New Orleans, Louisiana, USA, September 30 – October 3rd ,2001

Hashim, N.S., Zakaria, A.F., and Ishak, N.A., 2017, An Innovative Approach Towards Improving the Relationship Between Flow Zone Indicators with Lithofacies: A Case Study in Carbonate Oil Field, Middle East, Paper SPE-186005-MS, Presented at the SPE Reservoir Characterization and Simulation Conference and Exhibition of the Society of Petroleum Engineers, Abu Dhabi, United Arab Emirates, 8 - 10 May, 2017.

Herric, D., C., and Kennedy, W., D., 2009, On the Quagmire of "Shaly Sand" Saturation Equations, Presented at the Petrophysicists and Well Log Analysts 50th Annual Logging Symposium Held in Texas, United States of America, June 21 – 24, 2009, pp. 1-16

Hilchie, D., W., 1978, Applied Openhole Log Interpretation (For Geologists and Petroleum Engineers),

Geoscience Australia, 2020, Perth Basin, Province and Sedimentary Basin Geology, Northern Perth Basin Stratigraphy, http://www.ga.gov.au/scientific-topics/energy/province-sedimentary-basin-geology/petroleum/offshore-southwest-australia/perth-basin#heading-2, (Last Accessed 11 November 2020)

Ghadami, N., Rasaei., M., R., Hejri, S., Sajedian, A., and Afsari, K., 2015, Consistent Porosity-Permeability Modeling, Reservoir Rock Typing and Hydraulic Flow Unitization in a Giant Carbonate Reservoir, *Journal of Petroleum Science and Engineering,* **131** (2015), 58 - 69. http://dx.doi.org/10.1016/j.petrol.2015.04.017

Government of Western Australia, Department of Mines, Industry Regulation and Safety, Australia, Public Domain of Western Australian Data website (WAPIMS), Data

retrieved from https://wapims.dmp.wa.gov.au/WAPIMS/Search/Wells (Last accessed 20 December 2018)

Guo, G., Diaz, M. A., Paz, F. J., Smalley, J., and Waninger, E. A. 2007, Rock Typing as an Effective Tool for Permeability and Water-Saturation Modeling: A Case Study in a Clastic Reservoir in the Oriente Basin, *Society of Petroleum Engineers Journal*, **10** (6), 2007, 730 – 739. **https://doi-org.dbgw.lis.curtin.edu.au/10.2118/97033-PA**

Garrouch, A., A., and Al-Sultan A., A., 2018, Exploring the Link Between the Flow Zone Indicator and Key Open-Hole Log Measurements: An Application of Dimensional Analysis, Journal of Petroleum Geoscience, **25** (2019) 219–234. https://doi.org/10.1144/petgeo2018-035

Juhasz, I., 1979. The Central Role Of Qv And Formation-Water Salinity In The Evaluation Of Shaly Formations. *The Log Analyst Journal*, **20** (1979), pp. 1 - 11

Kadkhodaie-Ilkhchi, A., Rezaee, R., and Moussavi-Harami, R., 2013, Analysis of the Reservoir Electrofacies in the Framework of Hydraulic Flow Units in the Whicher Range Field, Perth Basin, Western Australia, *Journal of Petroleum Science and Engineering*, **111** (2013), October 2013, 106 – 120. http://dx.doi.org/10.1016/j.petrol.2013.10.014

Kemp, E., M., Balme, B., E., Helby, R., J., Kyle, R., A., Playford, G., and, Price, P., L., 1977, Carboniferous and Permian palynostratigraphy in Australia and Antarctica - a review: BMR Journal of Australian Geology and Geophysics, **2** (1977) 177–208

Kennedy, Martin. (2015). Developments in Petroleum Science, Volume 62 - Practical Petrophysics, Chapter-6: Introduction to Log Analysis: Shale Volume and Parameter Picking, pp. 151 – 180, ISBN: 978-0-444-63270-8, Published by Elsevier, 2015, Redarweg 29, PO Box 211, 1000 AE Amsterdam, Netherlands

Mayer, C., and Sibbit, A., 1980, Global, A New Approach to Computer-Processed Log Interpretation, Paper Presented at the 55th Annual Fall Technical Conference and Exhibition of the Society of Petroleum Engineers of AIME, Held in Dallas, Texas, United States, September 21 – 24, 1980, SPE-9341.

McPhee, C., Reed, J., and Zubizarreta, I., 2015, Core Analysis: A Best Practice Guide, Chapter 1: Best Practice in Coring and Core Analysis, Chapter 6: Preparation for Special Core Analysis, and, Chapter 9: Capillary Pressure, pp. 1-3, pp. 297-298, pp. 452-511, in Cubitt, J., editor, Development in Petroleum Science Series, Holt, Wales.

Mcwhae, J. R. H., Playford, P. E., Linder, A. W., Glenister, B. F., and Balme, B. E., 1958, The stratigraphy of Western Australia: Journal of the Geological Society of Australia, V. **4** (2) 1–161. https://doi.org/10.1080/00167615608728471

Minh, C., C., and, Sundararaman, P., 2010, Nuclear-Magnetic-Resonance Petrophysics in Thin Sand/Shale Laminations. *Society of Petroleum Engineers Journal,* **16** (2011): 223–238, DOI: https://doi.org/10.2118/102435-PA

Mirzaei-Paiaman, A., Ostadhassan, M., Rezaee, R., Saboorian-Jooybari, H., and Chen, Z., 2018, A New Approach in Petrophysical Rock Typing, *Journal of Petroleum Science and*

Engineering, **166** (2018), 445 – 464, DOI: https://doi.org/10.1016/j.petrol.2018.03.075

Mory, A., J., Haig, D., W., Mcloughlin, S., and Hocking, R. M., 2005, Geology of the northern Perth Basin, Western Australia, a field guide: Western Australia Geological Survey, Record 2005/9, pp. 35-39.

Mory, A., J., and Haig, D., W., 2011, Permian-Carboniferous Geology of the Northern Perth and Southern Carnarvon Basins, Western Australia – A Field Guide, 2011, Publication of the Geological Survey of Western Australia, Record 2011/14, Department of Mines and Petroleum, pp. 14-15.

Mory, A., J., and Iasky, R., P., 1996, Stratigraphy and Structure of the Onshore Northern Perth Basin, Western Australia, Published by the Geological Survey of Western Australia, Report 46, ISSN 0508-4741, pp. 13-17.

Obeida, T., A., Al-Mehairi, Y., A., and, Suryanarayana, K., 2005, Calculations of Fluid Saturations from Log-Derived J-Functions in Giant Complex Middle-East Carbonate Reservoir, *E-Journal of Petrophysics*, 2005, ISSN: 1712-7866, DOI: https://doi.org/10.2523/IPTC-10057-MS.

Purcell, W. P., 1949, Capillary Pressures – Their Measurement Using Mercury and The Calculation of Permeability Therefrom, Society of Petroleum Engineers. https://doi:10.2118/949039-G.

Quirein, J., Kimminau, S., LaVigne, J., Singer, J., and, Wendel, F., 1986, A Coherent Framework for Developing And Applying Multiple Formation Evaluation Models, Presented at the Society of Petrophysicists and Well Log Analysts 27th Annual Logging Symposium, June 9 – 13, 1986.

Rasmussen, B., 1986, Petrology and Stratigraphy of Subsurface Sandstones Near the Permo-Triassic Boundary, Northern Perth Basin, Western Australia [thesis], University of Western Australia, 126 p.

Rezaee, M., R., Jafari, A., and Kazemzadeh, E., 2006, Relationships Between Permeability, Porosity and Pore Throat Size in Carbonate Rocks Using Regression Analysis and Neural Networks, *Journal of Geophysics and Engineering*, **3** (2006) 370 - 376. DOI: https://doi.org/10.1088/1742-2132/3/4/008.

Roc Oil Company, 2002, Cliff Head-1 Well Completion Report, Interpretation Volume, November 2002, An internal Report published on the Government of Western Australia, Department of Mines, Industry Regulations and Safety, WAPIMS, https://wapims.dmp.wa.gov.au/WAPIMS/Search/Wells .

Roc Oil Company, 2003, Routine Core Analysis, Well Cliff Head#3, Offshore Western Australia, File PRP-03001, May 2003, An internal Report published on the Government of Western Australia, Department of Mines, Industry Regulations and Safety, WAPIMS, https://wapims.dmp.wa.gov.au/WAPIMS/Search/Wells.

Roc Oil Company, 2003, Cliff Head-3 Incorporating Cliff Head-3 corehole-1 Well Completion Report, Part 2 - Interpretation, December 2003, An Internal Report

published on the Government of Western Australia, Department of Mines, Industry Regulations and Safety, WAPIMS Website.
https://wapims.dmp.wa.gov.au/WAPIMS/Search/Wells

Roc Oil Company, 2004, A Special Core Analyses Study of Selected Samples from Wells: Cliff Head-3 and Cliff Head-4, Australia, A Core Lab Report, April 2004, An internal Report published on the Government of Western Australia, Department of Mines, Industry Regulations and Safety, WAPIMS Website, https://wapims.dmp.wa.gov.au/WAPIMS/Search/Wells

Roc Oil Company, 2004, Petrographic Evaluation of Core Samples from Cliff Head-3CH-1, Cliff Head-4 and Mentelle-1 Wells, Offshore Western Australia, A Core Lab Report, July 2004, An internal Report published on the Government of Western Australia, Department of Mines, Industry Regulations and Safety, WAPIMS Website, https://wapims.dmp.wa.gov.au/WAPIMS/Search/Wells

Roc Oil Company, 2005, Routine Core Analysis Final Report of Cliff Head-6 for Roc Oil WA Pty Ltd., An ACS Laboratories Report, September 2005, An internal Report published on the Government of Western Australia, Department of Mines, Industry Regulations and Safety, WAPIMS, https://wapims.dmp.wa.gov.au/WAPIMS/Search/Wells

Roc Oil Company, 2005, Petrology of Cliff Head-6 Core and Rotary Sidewall Core Samples for Roc Oil WA Pty Ltd., , An ACS Laboratories Report, October 2005, An internal Report published on the Government of Western Australia, Department of Mines, Industry Regulations and Safety, WAPIMS Website, https://wapims.dmp.wa.gov.au/WAPIMS/Search/Wells

Roc Oil Company, 2006, Cliff Head-6 Well Completion Report, Part-2 Interpretation, February 2006, An internal Report published on the Government of Western Australia, Department of Mines, Industry Regulations and Safety, WAPIMS, https://wapims.dmp.wa.gov.au/WAPIMS/Search/Wells .

Romero, P., A., 2012, NMR Fluid Typing, pp. 1-7

Schlumberger, 2019, Techlog Manual 2019, Published Manual for Techlog Software Users.

Segroves, K., L., 1971, The sequence of palynological assemblages in the Permian of the Perth Basin, Western Australia: Proceedings and Papers of the Second International Gondwana Symposium, Johannesburg, South Africa, 1970, pp. 511–529.

Schlumberger, 1989, Log Interpretation Principles/ Application, Published by Schlumberger Wireline and Testing, 225 Schlumberger Drive, Sugar Land, Texas, 77478. 241 p.

Schlumberger, 2013, Log Interpretation Charts, 2013 Edition, Published by Schlumberger, 3750 Briarpark Drive, Houston, Texas 77042, 2013 www.slb.com

Simandoux, P., 1963, Dielectric measurements on porous media application to the measurement of water saturations: study of the behaviour of argillaceous formations, Revue de l'Institut Français du Petrole, 18, pp. 193–215

Spooner, P., 2014, Lifting the Fog of Confusion Surrounding Clay and Shale in Petrophysics, Presented at the Society of Petrophysicists and Well Log Analysts 55th Annual Logging Symposium Held in Abu Dhabi, United Arab Emirates, May 18-22, 2014, pp. 1 – 14

Spooner, P., 2018, Lifting the Fog of Confusion Surrounding Total and Effective Porosity in Petrophysics, Presented at the Society of Petrophysicists and Well Log Analysts 59th Annual Logging Symposium Held in London, United Kingdom, June 2 – 6, 2018, pp. 1-12

Sokhal, A., Benmalik, S., and Quadfuel, S., 2016, Rock Typing and Permeability Prediction Usign Flow Zone Indicator with an Application to Berkine Basin (Algerian Sahara), Paper SEG-2016-13943527, Presented at the Society of Exploration Geophysicists International Exposition and 86th Annual Meeting, pp. 3068 - 3072. DOI: https://doi.org/10.1190/segam2016-13943527.1

Soleymanzadeh, A., Jamialahmadi, M., Helalizadeh., A., and Soulgani, B., S., 2018, A New Technique for Electrical Rock Typing and Estimation of Cementation Factor in Carbonate Rocks, *Journal of Petroleum Science and Engineering,* **166** (2018), March 2018, 381 – 388. DOI: https://doi.org/10.1016/j.petrol.2018.03.045

Svirsky, D., Ryazanov, A., Pankov, M., Corbett, P.W.M., and Posysoev, A., 2004, Hydraulic Flow Units Resolve Reservoir Description Challenges in a Siberian Oil Field, Paper SPE-87056, Presented at the Society of Petroleum Engineers Asia Pacific Conference on Integrated Modelling for Asset Management, Kuala Lumpur, Malaysia, 29-30 March. 2004.

Steen M. V., Vallega,, V., Shaaban, S., Ghadiry, Sh., Hadda, E., and, Bassim, E., 2012, Application of New Techniques for Characterisation of an Eocene Carbonate Reservoir in the Gulf of Suez, Egypt, Presented at the North Africa Technical Conference and Exhibition for the Society of Petroleum Engineers Held in Cairo, Egypt, February 20 – 22, SPE-150845, 2012, pp. 1-17.

Thomas, E., C., 2018, Capillary Pressure Tutorial: Part 2 – The Path Out of the Jungle, *Petrophysics Journal*, **59** (2018): 557 - 563, DOI: https://doi.org/10.30632/PJV59N5-2018t1

Tiab, D., and Donaldson, E., C., Petrophysics: Theory and Practice of Measuring Reservoir Rock and Fluid Transport Properties, Chapter-4: Formation Resistivity and Waater Saturation, Well Log Analysis, pp. 285 – 300, Published by Gulf Professional Publishing, Imprint of Elsevier, 2nd Edition, ISBN: 0-7506-771 1-2.

Timur, A., 1968, An Investigation of Permeability, Porosity, and Residual Water Saturation Relationships for Sandstone Reservoirs, *The Log Analyst Journal*, **9** (4), 1968, pp. 8-17, SPWLA-1968-vIXn4a2, https://www.onepetro.org/journal-paper/SPWLA-1968-vIXn4a2

Timur, A., 1969, Producible Porosity and Permeability of Sandstones Investigated Through Nuclear Magnetic Resonance Principles, *The Log Analyst Journal,* **10** (1969), Paper SPWLA-1969-vXn1a1, pp. 3 – 11.

Triangle Energy, 2021, Cliff Head Oil Field, An Open Access Website for Triangle Energy, http://triangleenergy.com.au/projects/cliff-head-wa/, (Last Access, 28 July 2021)

Wyllie, M.R.J., Gregory, A.R., and Gardner, L.W. 1956. Elastic Wave Velocities in Heterogeneous and Porous Media. Geophysics **21** (1): 41–70. http://dx.doi.org/10.1190/1.1438217

Appendix

Paper: Prediction of high-resolution reservoir facies and permeability, an integrated approach in the Irwin River Coal Measures Formation, Perth Basin, Western Australia, *Journal of Petroleum Science and Engineering*, **181** (2019) 1-12

Abdelrahman Elkhateeb[1], Reza Rezaee[1], Ali Kadkhodaie[2]

[1]Department of Petroleum Engineering, Curtin University, Perth, Australia

[2]Earth Sciences Department, Faculty of Natural Sciences, University of Tabriz, Tabriz, Iran

Name	conception and design	Acquisition of data & method	Analysis & statistical method	Interpretation &discussion	Final approval
Reza Rezaee	✓		✓	✓	✓
I acknowledge that these represent my contribution to the above research output.					
Ali Kadkhodaie	✓		✓	✓	✓
I acknowledge that these represent my contribution to the above research output.					

Paper: Log Dependent Approach to Predict Reservoir Facies and Permeability in a Complicated Shaly Sand Reservoir, Presented in the Australasian Exploration Geoscience (ASEG) Conference, 2019:1, 1-5

Abdelrahman Elkhateeb[1], Reza Rezaee[1], Ali Kadkhodaie[2]

[1]Department of Petroleum Engineering, Curtin University, Perth, Australia

[2]Earth Sciences Department, Faculty of Natural Sciences, University of Tabriz, Tabriz, Iran

Name	conception and design	Acquisition of data & method	Analysis & statistical method	Interpretation &discussion	Final approval
Reza Rezaee	✓		✓	✓	✓
I acknowledge that these represent my contribution to the above research output.					
Ali Kadkhodaie	✓		✓	✓	✓
I acknowledge that these represent my contribution to the above research output.					

Paper: A New Integrated Approach to Resolve the Saturation Profile Using High-Resolution Facies in Heterogeneous Reservoirs, *Journal of Petroleum*, 2021, pp. 1-12

Abdelrahman Elkhateeb[1], Reza Rezaee[1], Ali Kadkhodaie[2]

[1]Department of Petroleum Engineering, Curtin University, Perth, Australia

[2]Earth Sciences Department, Faculty of Natural Sciences, University of Tabriz, Tabriz, Iran
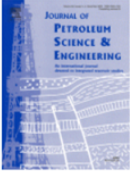
Name	conception and design	Acquisition of data & method	Analysis & statistical method	Interpretation &discussion	Final approval
Reza Rezaee	✓		✓	✓	✓
I acknowledge that these represent my contribution to the above research output.					
Ali Kadkhodaie	✓		✓	✓	✓
I acknowledge that these represent my contribution to the above research output.					

Copyright Agreements

The Copyright Agreements between the journals and author to reuse the published papers in this thesis are listed as following:

Paper-1

Paper-2:

From: Academic UK Non Rightslink <permissionrequest@tandf.co.uk>
Sent: Thursday, 7 October 2021 7:18 PM
To: Abdelrahman Elkhateeb <a.elkhateeb@postgrad.curtin.edu.au>
Subject: RE: texg19:Log dependent approach to predict reservoir facies and permeability in a complicated shaly sand reservoir

Dear Abdelrahman Elkhateeb,

Abdelrahman Elkhateeb, Reza Rezaee & Ali Kadkhodaie (2019) Log dependent approach to predict reservoir facies and permeability in a complicated shaly sand reservoir, ASEG Extended Abstracts, 2019:1, 1-5, DOI: 10.1080/22020586.2019.12072924

Thank you for your correspondence requesting permission to reproduce the above content from our Journal in your online thesis / dissertation and to be posted in the university's repository – Curtin University.
https://www.curtin.edu.au/?gclid=EAIaIQobChMIqffsktyC8wIVlBsrCh02YQimEAAYASAAEgJJpfD_BwE

We will be pleased to grant permission to reproduce your '**Accepted Manuscript'** on the sole condition that you acknowledge the original source of publication.

This is an '**Accepted Manuscript'** of an article published by Taylor & Francis Group in **ASEG Extended Abstracts** on **11 Nov2019** available online:
https://doi.org/10.1080/22020586.2019.12072924

Please note: This **does not allow** the use of the **Version of Record (VoR)** to be posted online, however you may include the VoR as an Appendix to the printed version of your thesis / dissertation. (The VoR is the final, definitive, citable version of your paper, which has been copyedited, typeset, had metadata applied, and has been allocated a DOI; the PDF version on Taylor & Francis Online)

Using a DOI to link to the VoR on Taylor & Francis Online means that downloads, Altmetric data, and citations can be tracked and collated – data you can use to assess the impact of your work.

This permission does not cover any third party copyrighted work which may appear in the material requested.

Thank you for your interest in our journals.

Yours Sincerely,

Sue McCarthy

Susan McCarthy | Permissions Administrator

Journals, Taylor & Francis Group

Permissions e-mail: permissionrequest@tandf.co.uk

Web: www.tandfonline.com

✉ 4 Park Square, Milton Park, Abingdon, OX14 4RN

☎ +44 (0) 20 80520600

Disclaimer: T&F publish Open Access articles in our subscription priced journals, please check if the article you are interested in is an OA article and if so which licence was it published under.

🌲 Before printing, think about the environment

Paper-3: The link presents the following permission for all Elsevier Publications. This paper has not issued yet a final issue number. A confirmation by a chat from Elsevier Team has confirmed the permission, which is available upon request.

https://www.elsevier.com/about/policies/copyright

ELSEVIER

About Elsevier   Products & Solutions   Services   Shop & Discover

Overview   Author rights   Institution rights   Government rights   Find out more

Author rights

The below table explains the rights that authors have when they publish with Elsevier, for authors who choose to publish either open access or subscription. These apply to the corresponding author and all co-authors.

Author rights in Elsevier's proprietary journals	Published open access	Published subscription
Retain patent and trademark rights	√	√
Retain the rights to use their research data freely without any restriction	√	√
Receive proper attribution and credit for their published work	√	√
Re-use their own material in new works without permission or payment (with full acknowledgement of the original article): 1. Extend an article to book length 2. Include an article in a subsequent compilation of their own work 3. Re-use portions, excerpts, and their own figures or tables in other works.	√	√
Use and share their works for scholarly purposes (with full acknowledgement of the original article): 1. In their own classroom teaching. Electronic and physical distribution of copies is permitted 2. If an author is speaking at a conference, they can present the article and distribute copies to the attendees 3. Distribute the article, including by email, to their students and to research colleagues who they know for their personal use 4. Share and publicize the article via Share Links, which offers 50 days' free access for anyone, without signup or registration 5. Include in a thesis or dissertation (provided this is not published commercially) 6. Share copies of their article privately as part of an invitation-only work group on commercial sites with which the publisher has a hosting agreement	√	√